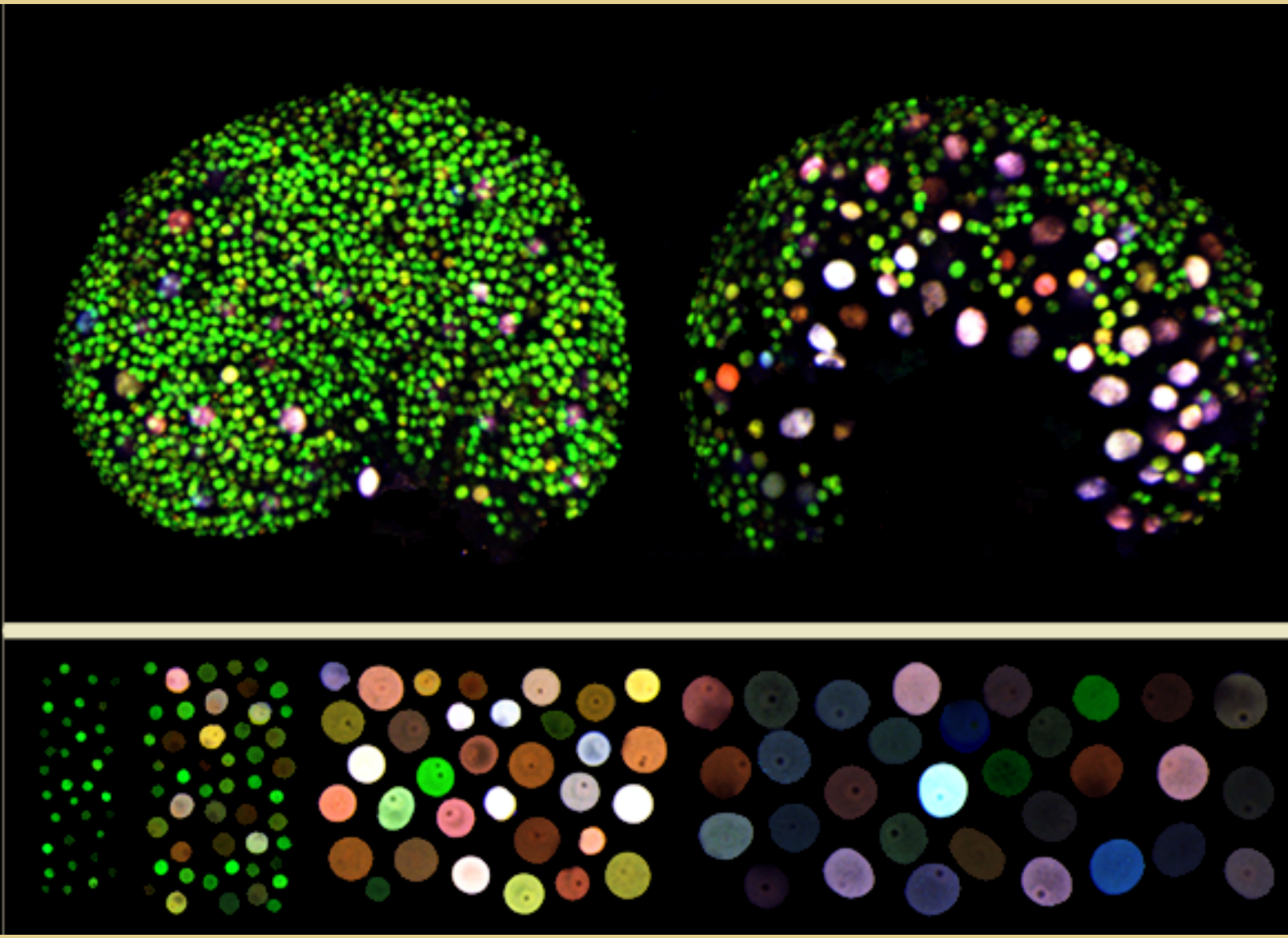

Marília Henriques Cordeiro

Generation of a VASA/GDF-9/ZP3-promoter driven triple transgenic reporter mouse line as a tool to study ovarian dynamics

Tese de Doutoramento em Biociências, especialização em Biologia Celular e Molecular, Orientada pela Professora Doutora Teresa Woodruff (Universidade de Northwestern, EUA) e pelo Professor Doutor João Ramalho-Santos (Departamento de Ciência da Vida, FCTUC) e apresentada ao Departamento de Ciência da Vida, Faculdade de Ciências e Tecnologia da Universidade de Coimbra

Setembro 2014

· U C ·

UNIVERSIDADE DE COIMBRA

• U C • FCTUC FACULDADE DE CIÊNCIAS E TECNOLOGIA
UNIVERSIDADE DE COIMBRA

Generation of a VASA/GDF-9/ZP3-promoter driven triple transgenic reporter mouse line as a tool to study ovarian dynamics

Marília Henriques Cordeiro

Tese de Doutoramento em Biociências, especialização em Biologia Celular e Molecular, orientada pela Professora Doutora Teresa Woodruff (Universidade de Northwestern, EUA) e pelo Professor Doutor João Ramalho-Santos (Departamento de Ciência da Vida, FCTUC) e apresentada ao Departamento de Ciência da Vida, Faculdade de Ciências e Tecnologia da Universidade de Coimbra

Setembro 2014

.

"Only those who dare to fail greatly can ever achieve greatly."

Robert F. Kennedy

Aos meus Pais

To my parents

Acknowledgments

Agradecimentos

I would like to thank my PhD advisor Dr. Teresa Woodruff for believing in me and giving me the opportunity of working in her laboratory. Working in a risky project taught me more that I could ever imagine about motivation, challenge and friendship. The experience of working in the Woodruff laboratory has been extremely complete and made me discover so much about science, life and myself. I would like to also thank the opportunity of going to international conferences and meeting some important scientists in the field. A special thanks to my advisor Dr. João Ramalho-Santos for always being so patient and especially for helping, caring and knowing what to say in the moments I needed the most.

A big thanks to So-Youn Kim for the invaluable friendship, smile and energy. So-Youn you are the kindest person I know and one of the most brilliant and critical scientists I had the pleasure to meet. Science with you is always fun and what I learn from you will always inspire the way I think and work in the future. Thanks for always having time for me, you made my PhD experience memorable.

I would like to acknowledge Katy Ebbert for the friendship, positive energy and precise hands in very critical moments. Thanks to Francesca Duncan for all the help especially in the begining of the project, starting from the project proposal through e-mail to teaching basic molecular biology techniques. A special thanks to Kelly Whelan, Megan Romero and Keisha Barreto for animal care assistance and sectioning of the samples.

Acknowledgement to Jie Zhu for advice during cloning of the DNA constructs and other moments of the project, and for 4 years of friendship. Thanks to Ru Yu for your sweet mind and strength, it has been a lot of fun to work with you. I would like to acknowledge Jessica Hornick for your help at distinct stages of my PhD project. A special thanks to Yuanming Xu for the friendship and lab companion until late hours. Thanks to all current members of the Woodruff laboratory for making the experience of working in the lab so enjoyable. A special thanks also to all the past lab members which have positively marked my life and the work present in this thesis. A big thanks to all the members of the Northwestern University Center for Reproductive Science for impacting so positively my scientific carreer.

I would like to acknowledge the Northwestern University (NU) Transgenic and Targeted Mutagenesis Laboratory and the NU Genomics Core Facility for generation of the transgenic mouse line and traditional sequencing services, respectively. A

.

special thanks to Dr. Lynn Doglio for crucial advice during mouse design. Thanks to Sheila Heilman and Justin Meyer for important help with sperm cryopreservation and IVF protocols. Thanks to NU Cell Imaging Facility and Dr. Leong Chew for imaging assistance. I would like to acknowledge to Dr. Richard M. Schultz, Dr. Austin J. Cooney and Dr. Diego Castrillon for generously providing the plasmids containing the promoters, and GenScript for performing subcloning of the VASA promoter.

Um obrigada muito especial aos meus pais e irmão pelo amor e apoio incondicional, por acreditarem sempre em mim e me darem colo quando mais precisei, mas também por aturarem o meu mau feitio e aceitarem a minha ausência em momentos bem complicados. Um agradecimento muito especial também ao resto da minha família por me apoiarem sempre e serem elementos muito importantes na minha vida. Às minhas maninhas Vi, Nokas e Leninha por estarem sempre comigo e me oferecerem a mais pura amizade 'que nem um oceano separa'.

Um agradecimento especial à Gabriela e Ana Rita por estarem tão perto, apesar de estarem tão longe. Um grande obrigada à Daniela e Vera pelo carinho, preocupação e me proporcionarem momentos bem divertidos sempre que venho a Portugal, a vossa força e alegria são inspiradoras. À Gisela e à Andrea um agradecimento do fundo do coração por me darem sempre força e carinho.Um agradecimento muito especial à Rute e ao João por me darem uma mão amiga numa das alturas mais incertas da minha vida. E por fim queria agradecer aos restantes amigos de curso, do grupo de reprodução, de mestrado, do programa doutoral e da Batalha pelos bons momentos que passámos juntos e por se lembrarem de mandar um e-mail de vez em quando a perguntar como anda a vida.

.

Resumo

Neste estudo foi criada, caracterizada uma nova linha de ratinhos transgénicos, posteriormente usada como ferramenta para explicar o papel da anatomia do ovário no estabelecimento da primeira onda de activação folicular. Neste ratinho, promotores exclusivamente expressos no oócito (*Vasa*, *Gdf9* e *Zp3*) foram usados para controlar a expressão de três proteínas fluorescentes (EGFP, mCherry e AmCyan, respectivamente), criando uma linha reporter que permite seguir de forma dinâmica a activação e crescimento foliculares. Para criar a linha transgénica, três construções de DNA independentes foram co-injectadas em embriões de ratinho. A linha 5570 foi selecionada para estudo pormenorizado, revelando uma expressão de proteínas fluorescentes dependente da classe folicular e apresentando também heterogeneidade dentro da mesma classe folicular, sugerindo uma estratificação de actividade não previamente descrita. A expressão de proteínas fluorescentes revelou também que os primeiros folículos a serem activados encontram-se restritos à região anterior-dorsal do ovário, levando a explorar a relação anatómica entre meiose, formação e activação folicular. Foram observadas diferenças dorso-ventrais, com células germinais na região ventral do ovário a entrar mais cedo em meiose. Em contraste, os primeiros folículos formados aparecem na região dorsal do ovário. Foi também observado que diferenças geográficas no momento de formação de folículos resultam em capacidades distintas para iniciar crescimento folicular, como revelado por diferenças na expressão de proteínas fluorescentes nas regiões dorsais e ventrais do ovário, mantidas durante todo o período pré-pubertal. Em resumo, este estudo sugere que a especificação do ovário em córtex e medula influencia a localização da primeira onda de activação folicular, permitindo um desenvolvimento distinto em zonas diferentes do ovário o que determina uma hierarquia de recrutamento de folículos primordiais.

.

Abstract

In this study a triple transgenic mouse line was generated, characterized and used as a tool to explain the role of ovarian anatomy in the establishment of the first wave of follicle activation. In this mouse, oocyte-specific promoters (VASA, GDF-9 and ZP3), active at distinct stages of oocyte and follicle development, were used to drive the expression of exogenous fluorescent proteins (EGFP, mCherry and AmCyan, respectively), creating a reporter line to dynamically follow follicle activation and growth. The mice were generated by co-injection of three independent DNA constructs, resulting in nine independent transgenic founder lines. Line 5570 was then selected for further study, revealing a follicle-class dependent expression of fluorescent protein. Interestingly, the fluorescent profile of the oocytes differed even within follicle classes, suggesting an underlying activity or intrinsic stratification of function not previously appreciated. In addition, the expression of fluorescent protein revealed that the first growing follicles were restricted to the anterior-dorsal ovarian region, which led an exploration of the anatomical relationship between meiosis, follicle formation and activation. Dorsal-ventral differences in the onset of meiosis were observed, with an early entry in the ventral region. In contrast, the first germ cells encapsulated into were present in the dorsal region. Furthermore, the geographic differences in the timing of follicle formation resulted in distinct ability to initiate growth, as revealed by different fluorescent profiles in dorsal and ventral regions maintained throughout the prepubertal period. Altogether, this study suggested that the specification of cortical and medullar regions impacts where the first follicular activation occurs, with an asynchronous germ cell development in different regions of the ovary determining the order of primordial follicle recruitment.

.

Abbreviations

AMH – Anti-Mullerian Hormone
BDNF – Brain-derived neurotrophic factor
BMP4 – Bone morphogenetic protein 4
BMP7 – Bone morphogenetic protein 7
BSA – Bovine serum albumin
CMV – Cytomegalovirus
COC – Cumulus-oocyte complex
DNA – Deoxyribonucleic acid
dpc – Days *post coitum*
ECM – Extracellular matrix
EGFP – Enhanced green fluorescent protein
FBS – Fetal bovine serum
Foxl2 – Forkhead box protein L2
Foxo3 – Forkhead box O3
FSH – Follicle-stimulating hormone
GDF-9 – Growth differentiation factor-9
GDNF – Glial cell-derived neurotrophic factor
GFP – Green fluorescent protein
GnRH – Gonadotropin-releasing hormone
H&E – Hematoxylin and eosin stain
hCG – Human chorionic gonadotropin
IVF – *in vitro* fertilization
LH – Luteinizing hormone
MII – Metaphase II
MIS – Mullerian Inhibitory Substance
MVH – Mouse vasa homologue protein
NGF – Nerve growth factor
NU – Northwestern University
Oct4 – Octamer-binding transcription factor 4, also known as POU5F1
PBS – Phosphate buffered saline
PCOS – polycystic ovarian syndrome
PCR – polymerase chain reaction
PDK1 – 3-phosphoinositide dependent protein kinase-1

.

PGCs – Primordial Germ Cells

PI3K – Phosphoinositide 3-kinase

PMSG – Pregnant mare's serum gonadotropin

POF – Premature ovarian failure

POI – Primary ovarian insufficiency

PTEN – Phosphatase and tensin homolog

PVP – Polyvinylpyrrolidone

RA – Retinoic acid

SD – Standard deviation

Sry – Sex-determining region on the Y chromosome

Stra8 – Stimulated by retinoic acid gene 8

TBS – Tris-buffered saline

TBS-T – Tris-buffered saline with Tween 20

TSA – Tyramide Signal Amplification

Tsc1/Tsc2 – Tuberous sclerosis 1/ tuberous sclerosis 2

YFP – Yellow fluorescent protein

ZP3 – Zona pellucida glycoprotein 3

.

Table of Contents

.

.

CHAPTER 1

State of Art

1. Introduction

1.1. Synopsis

Although the structure of the ovary was described several hundred years ago, there are still many questions regarding the functionality of this organ. For example, the mechanisms underlying selective follicular activation over decades of life, namely why certain primordial follicles enter the growth phase whereas others remain quiescent, is still largely unknown; although new data are emerging regarding global activation [1]. The mammalian ovary contains follicles and corpora lutea at various stages of development supporting the endocrine health of the individual and the development of the oocyte, the female germ cell, which contributes with half of the genetic complement of the new organism, plus mitochondrial DNA. Since the number of ovarian follicles is fixed by birth, the mechanisms permitting a regulated recruitment of primordial follicles over time are a critical part of ovarian biology. However, as posited above, these mechanisms are not well understood. Thus the purpose of this thesis was to develop a new model to explore follicle activation by creating a transgenic animal wherein gene activation profiles can be monitored in vivo and in vitro. This animal model represents a major contribution to the field and this thesis will outline the developing and initial testing of the mouse line. This introduction will limit its scope to what is known about follicle development in the mouse in order to contextualize the new work presented in later chapters.

1.2. Sex Determination and Ovarian Development

The mammalian gonad is formed during embryonic development through a complex and tightly regulated process (Figure 1.1). Primordial germ cells (PGCs) migrate from the hindgut into the genital ridge between 9 to 10.5 dpc (days post coitum) in mouse and 7 weeks of gestation in human [2, 3]. At this stage the gonad is bipotent, and in the presence of a Y chromosome, the expression of the *Sry* gene

.

(Sex-determining region on the Y chromosome) directs male development, through a process called sex determination [4]. In contrast, sex determination in females has been seen as a default program, due to lack of knowledge of a gene equivalent to *Sry* able to induce female development by repressing male development (also called as 'Z factor') [5]. Although no definitive 'Z factor' has been found, several genes have been reported to repress testis development, such as *Wnt4*, *Foxl2* and *Rspo1,* as their loss causes partial sex reversal [6]. After sex determination the early ovary, starts to present distinct structural features, characteristic of the female gonad, including the formation of germ cell clusters through multiple mitotic divisions of a

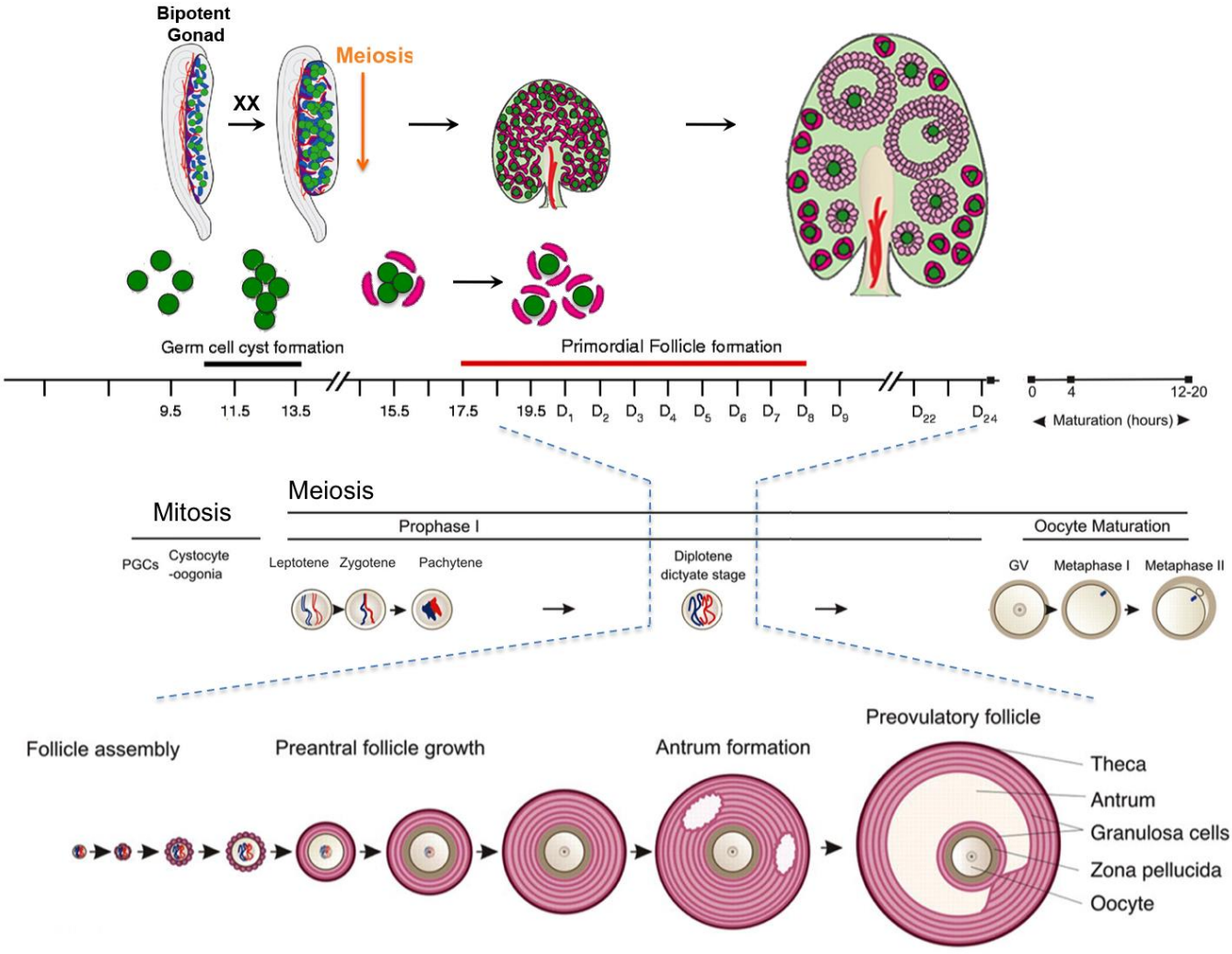

Figure 1.1 – Timeline of major ovarian developmental events in the mouse. Oogenesis from PGC migration into the genital ridge until first folliculogenesis and meiotic maturation is depicted. Onset of meiosis is also represented. The timeline is represented in dpc, with 19.5 being the day of birth in mouse (D_0). Schematic representation based on [7-11].

.

single progenitor [12]. These germ cell clusters interact with somatic cells forming ovigerous cords, enclosed by pregranulosa cells and delimitated by a basement membrane [13, 14]. After mitotic division, female germ cells remain connected by cytoplasmic bridges, forming cysts, which were suggested to be important for germ cell development [15, 16].

1.3. Meiosis Onset

Around 13.5 dpc germ cells enter meiosis in an anterior to posterior gradient driven by retinoic acid (RA) [17-20]. Meiosis, crucial to originate haploid gametes, starts during embryonic development in the female gonad, while in the male gonad it occurs postnatally before puberty. Although the developing testis is also exposed to RA during the same time window, the production of CYP26B1 allows degradation of RA and the male germ cells remain arrested in G_1/G_0 [19, 21]. Retinoic acid induces *Stra8* (Stimulated by Retinoic Acid gene 8), while suppressing the pluripotency gene *Oct4* [17, 22]. Oogonia enter the first stages of meiosis and begin to arrest in diplotene of Prophase I by 17.5 dpc, and at this time are referred as oocytes. Importantly, the newly formed oocytes remain arrested in this stage for days or years, with the final stages of meiotic division completed after fertilization (Figure 1.1). The source of RA has been discussed over the years, being initially proposed to be produced by the developing adrenal gland or mesonephros [20]. Experimental evidence showed RA-induced gene expression in the mesonephric duct and tubules [19], supported by the fact that germ cells do not undergo meiosis in the absence of the rete ovarii (tubular region connecting the mesonephros with the ovary) [23]. Recently the ovary itself was sugsted as the main the source of RA [24], which seems to be the case of the human ovary as well [25]. Future studies are required to clarify the source and production trigger of RA in the embryonic ovary.

.

1.4 Primordial Follicle Formation

The newly formed oocytes are next individually encapsulated in a single layer of somatic cells and described as 'primordial follicles' (Figure 1.1). In contrast to humans and other large mammals, in rodents most primordial follicles are formed a few days after birth with some activating soon after formation [26]. This process of primordial follicle formation is also called nest breakdown because the pre-granulosa cells invade and degrade the cytoplasmic bridges, which is associated with germ cell loss by apoptosis [16]. During nest breakdown a subset of oocytes within the individual cyst die, and similarly to what occurs in *Drosophila* ovary [27], it has been suggested that mitochondria and endoplasmic reticulum can reorganize and be transferred to the surviving germ cells [16]. Based on this hypothesis germ cell loss may work as a mechanism to ensure oocyte quality, allowing to eliminate germ cells with damaged nuclei or organelles and ensuring high genomic integrity. However, a recent study challenged this notion by suggesting that the cytoplasmic bridges between germ cells are dispensable for female fertility [28]. Another common explanation for germ cell loss during this developmental period is to ensure an appropriate ration between germ cells and supporting cells [29]. Several molecules have been identified as modifiers of the process of nest breakdown by controlling its timing and extent, such as *Foxl2*, *Notch* and *Nobox* (for review see [30]). Thus, the molecular mechanisms controlling germ cell survival and loss at the time of primordial follicle formation are of intense interest to the reproductive biology field and the mouse line described in this thesis may have value in the study of this stage in future years.

1.5 Folliculogenesis

To produce mature oocytes, follicles from the ovarian reserve (pool of dormant primordial follicles) are activated and undergo several changes in

.

morphology and size, developing through primary and secondary stages before acquiring an antral cavity, through a process called folliculogenesis (Figure 1.2). The fate of each follicle is controlled by endocrine, paracrine and autocrine factors, with bidirectional communication between oocytes and somatic cells playing an important role in follicular development [31-33]. Many follicles are lost by atresia at the antral stage, while few of them grow further and reach the preovulatory stage under the cyclic gonadotropin stimulation, controlled by the hypothalamus-pituitary-ovary axis [26, 34, 35]. During each reproductive cycle, in response to the preovulatory surge of gonadotropins, the dominant Graffian follicle ovulates to release the mature oocyte for fertilization, whereas the residual follicle (the remaining theca and granulosa cells) undergo a transformation to become the corpus luteum. The hormone-regulated

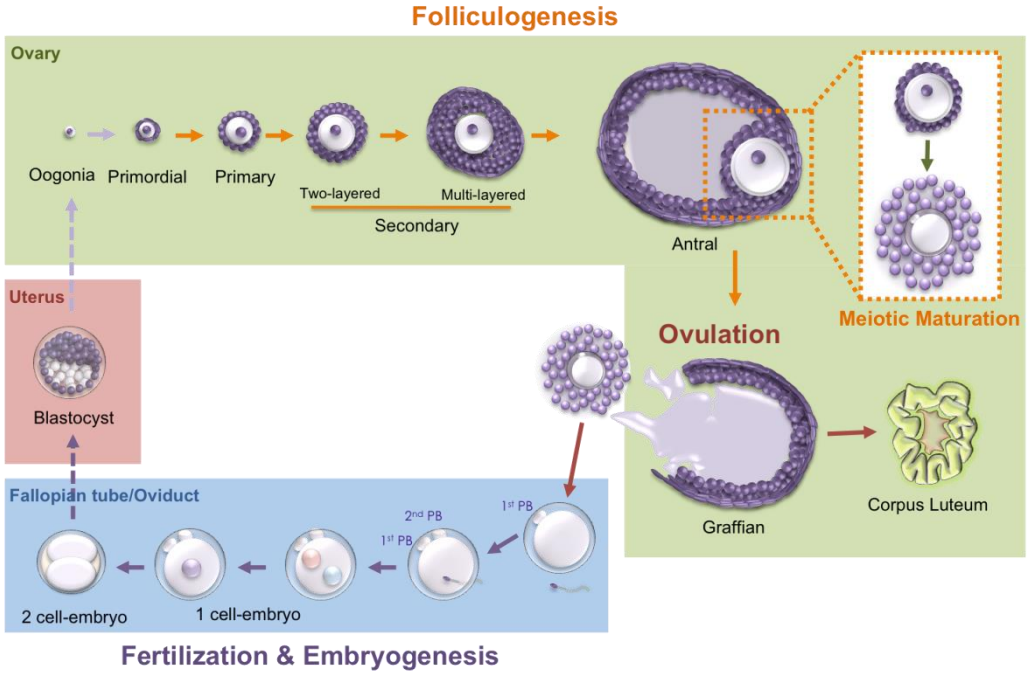

Figure 1.2 – The oocyte life cycle. At each cycle a subset of primordial oocytes is recruited to grow and produce mature oocytes through the process of folliculogenesis. The oocyte increases in size as the number and complexity of the granulosa cell layers expands. When the follicle reaches the antral stage, it forms a liquid filled cavity, the antrum, causing differentiation of the granulosa cell layers into mural and cumulus cells. Following the LH surge, the oocyte resumes meiosis becoming arrested at metaphase II (MII), while cumulus cells expand and the follicle wall is prepared for ovulation. The MII oocyte is then released from the follicle cavity, ovulated, and if fertilized by available sperm becomes a zygote and initiates embryogenesis. The embryo then travels through the fallopian tube and arrives at the uterus where implantation takes place. During embryogenesis, the presumptive germ cells are established and ultimately move to the developing bipotent gonad where the oogonia life cycle begins again.

.

follicular development is relatively well-characterized and involves the integration of feedback loops between the ovarian secreted estrogen, progesterone, inhibin A and inhibin B, pituitary FSH (Follicle-stimulating hormone) and LH (Luteinizing hormone) and hypothalamic GnRH (Gonadotropin-releasing hormone) [26, 36, 37]. However, the intrinsic ovarian factors that regulate oocyte and follicular development before the follicles can respond to FSH are less well understood [34, 38] and are the focus of this thesis.

1.6. Mechanisms controlling Primordial Follicle Activation

The primordial follicles are the first follicles formed in mammalian ovaries and consist of an oocyte surrounded by a single layer of flattened granulosa cells [35, 39]. Each primordial follicle has three possible fates: to remain quiescent, to begin development but later undergo atresia, or to develop, mature, and be ovulated. Primordial follicles can also die directly from their dormant stage [40-42]. When a primordial follicle is activated/recruited (a process independent of gonadotropin stimulation), the oocyte increases in size dramatically and the surrounding pregranulosa cells proliferate and differentiate [26, 35]. The molecular mechanisms underlying primordial follicle activation have been a high interest topic for many scientists in the reproductive field, since it represents a key event to regulate normal ovarian function and reproductive lifespan. A number of factors have been found to be important for primordial follicle growth, including kit ligand, vascular growth factor, BMP4, BMP7, leukemia inhibitor factor, neurotrophins (NGF, BDNF, GDNF), and others (for reviews see [1, 38]). Multiple studies demonstrated the importance of PI3K-PTEN-AKT-mTOR signaling pathway to control primordial follicle dormancy, including several genetic mouse models and inhibitors (for reviews [1, 38, 43]). Transgenic animals in which Foxo3a [44], Tsc1 and Tsc2 [45, 46], PTEN [47]and p27 [48] have been genetically removed resulted in premature ovarian failure (POF) due to global follicle activation. On other hand, genetic depletion of PDK1

.

(phosphoinositide dependent kinase 1) and RpS6 (ribosomal protein 6) can also cause POF, but through accelerated clearance and atresia [49]. These studies indicated that PI3K signaling pathway is critical to control primordial follicle recruitment and survival. In addition, it has been suggested that AMH (Anti-Mullerian Hormone, also called MIS, Mullerian Inhibitory Substance) produced by growing follicles inhibit primordial follicle recruitment, as mice lacking AMH have an elevated number of growing follicles and becoming depleted of primordial oocytes earlier than wild-type littermates [50]. Moreover, the *in vitro* culture of follicles or cortical ovarian pieces has been another useful approach to answer this question. For instance, in culture of whole newborn mouse ovaries and ovarian cortical pieces from bovine and baboon, primordial follicles spontaneously activate in serum-free medium without exogenous gonadotropins. These experiments suggest that primordial follicles quiescence is based on inhibitory pathways, which are lost *in vitro.* In contrast, it is also possible that an increase in stimulatory factors occurs when follicles are cultured *in vitro* [51-55].

Although the studies described above have identified some of the molecular players involved in primordial follicle activation, the trigger(s) for selective follicle activation is still unknown. A popular proposition to explain the order of follicle activation is the 'production line' hypothesis. This hypothesis was originally proposed to justify the high incidence of aneuploidy in reproductively aged females and suggests that the first oogonia to undergo meiotic arrest are the first to become activated after puberty, implying that the order of follicle activation is established during embryonic development [56]. Importantly, any insults during ovarian embryonic development may impact negatively the adult ovarian function; such as poor nutrition, exposure to environmental pollutants, drugs, etc. Interestingly, the origin of adult ovarian diseases, as polycystic ovarian syndrome (PCOS) has been linked to gonad developmental defects, by exposure to androgens during gestation

.

and abnormal expression of the ECM protein fibrillin 3 [7]. Thus, the ovarian development represents a critical window to regulate normal gonadal function in the adult animal.

1.7. Significance to Human Reproduction

The use of mice as animal models has been extremely useful to study the physiology of the ovary, especially due to possibility of creating genetically modified animals, as the one generated in this thesis. Over the years the mouse ovary has been extensively studied and the number of follicles present at different ages is very well described [41, 57]. Similarly to the mouse ovary, the human ovary also contains a finite number of primordial oocytes, which serve as a source of developing follicles and oocytes that declines with age [26, 58-60]. When the available primordial follicle pool is depleted, the reproductive capacity of a woman ceases and she enters menopause. In the human, from a peak of 6–7 million at 20 weeks of gestation, the total number of primordial follicles falls drastically to approximately 300,000 to 400,000 remaining per ovary at birth [26, 61]. The loss of primordial follicles remains steady at about 1000 follicles per month and accelerates after the age of 37 years, causing ovarian aging. At the time of menopause, the number of follicles remaining drops below 1000. Due to an exhaustion of the ovarian follicle reserve, menopause occurs at about 51 years of age, a time point that has been constant for centuries [26, 58]. Premature ovarian

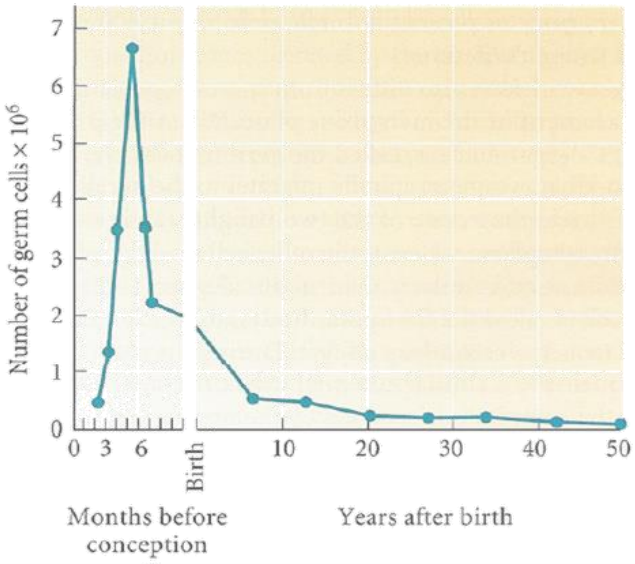

Figure 1.3 – The finite ovarian reserve. Number of germ cells in the human ovary decreases as a women advance in age. Graph from [60] based on original data from [61].

.

failure (POF), also known as POI (primary ovarian insufficiency) or premature menopause, refers to cessation of ovarian function before the age of 40. This condition affects 1% of the female population and in the majority of the cases is idiopathic since the underlying cause is unknown (chromosomal, genetic, metabolic, autoimmune, iatrogenic and infections causes explain the remain cases) [62]. Understanding the molecular mechanisms involved in primordial follicle activation will be crucial to intervene in some of these patients and maintain their fertility and endocrine system function until later in age.

Although the contribution of both gametes is required to generate a new individual, the oocyte developmental competence dictates the fate of the embryo. Curiously, during IVF (*in vitro* fertilization) only a small fraction of the retrieved oocytes originates good quality embryos able to result in life births, with the use of artificial hormones and non-ideal *in vitro* culture conditions explaining some of the failure. To avoid transference of several embryos, which can cause risky multiple pregnancies, oocytes and embryos are selected based on morphologic criteria, frequently inefficient to predict developmental ability [63]. The development of non-invasive methods to access oocyte quality is vital to improve the success and cost of infertility treatments. On other hand, the rapid decline of fertility in aging women has important implications in view of the current socioeconomic trend to postpone childbearing. Reproductive

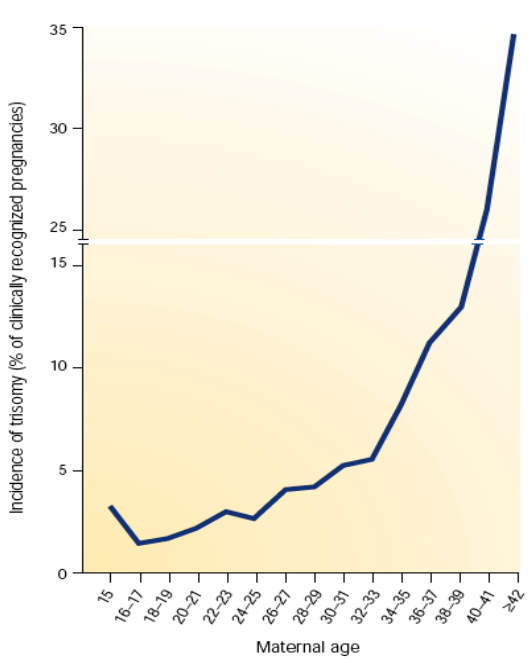

Figure 1.4 – The decrease in oocyte quality with maternal age is associated with a higher rate of oocyte aneuploidy, which can originate chromosomal abnormalities. The graph from [59] represents the increased incidence of trisomy as women advance in age.

.

aging is associated with a gradual decrease in quantity and quality of the oocytes, as well as, altered reproductive endocrinology, and increased incidence of reproductive tract defects, leading to lower pregnancy rates and increased risk of miscarriage and fetal chromosomal anomalies [64]. However, the success rate in oocyte donor programs indicated that the decline in fertility is primarily caused by poor oocyte quality, rather than changes in endometrial receptivity [65, 66]. Oocyte aneuploidy is likely to be the main mechanism responsible for increased infertility in women over the age of 35 [67-70]. Several authors have suggested that the long period of arrest of the primordial follicle might negatively impact oocyte integrity and lead to the production of poorer quality oocytes over time [71, 72].

Further studies of the basic mechanisms involved in ovarian development, primordial oocyte activation, follicle selection and oocyte quality are vital to understand normal ovarian function and allow the development of new therapies for infertility. Thus, the objective of this study was to create a reporter line to non-invasively follow follicular development, by taking advantage of important oocyte-specific promoters, whose activity was shown to be essential for oocyte development. Therefore, the fluorescent profile of the oocytes from this mouse line promises to be a valuable tool to expand fundamental knowledge about the female gonad.

.

CHAPTER 2

Material and Methods

2.1. Cloning of *Vasa/Gdf-9/Zp3* DNA constructs

The three DNA linear fragments used to generate transgenic mice were built into the *Zp3* cassette plasmid [73] by engineering the promoter and fluorescent protein regions. EGFP, mCherry and AmCyan were amplified from the plasmids *Zp3* cassete, pIVT+NtermCherry (both generously provided by Dr. Richard M. Schultz, University of Pennsylvania, PA) and pAmCyan1-N1 (Clontech, CA), respectively. New restriction sites and epitope tags - HA, His and T7 tags, to ensure reporter detection - were engineered into the 5'ends of the primers (P1-P6, see Table 2.1 for complete list of primers). PCR products were inserted into TA cloning vector (Life Technologies, NY), digested with *Sma*I and *Xba*I restriction enzymes and cloned into the basis backbone, creating the plasmids *Zp3*-EGFP-T7, *Zp3*-AmCyan-HA and *Zp3*-mCherry-His. When required *Zp3* promoter was excised from the resulting plasmid using *Bgl*II/*BspM*I or *Bgl*II/*Pst*I and replaced with a 500 bp fragment of DNA (from pAmcyan1-N1 vector - 685 to 1145bp) containing new restriction sites *Acc*65I/*Hind*III or *Asc*I/*Pac*I also added through the primers (P7-P10). *Gdf-9* promoter was obtained from the pGDF-9-Luc vector [74] (generously provided by Dr. Austin J. Cooney, Baylor College of Medicine, TX) by digesting with *Acc*65I and *Hind*III and then cloned into the backbone plasmid containing mCherry-His. *Vasa* promoter sequence was amplified from pVASA-creN vector [75] (provided by Dr. Diego H. Castrillon, University of Texas Southwestern Medical Center, TX; through Addgene, MA) into the intermediate vector pUC57 (subcloning was performed by GenScript, NJ) before insertion on the EGFP-T7 vector through *Asc*I and *Pac*I restriction sites. Schematic of the complete cloning strategy is represented in Figure 2.1. Sequencing was used to confirm correct construct building (Traditional sequencing performed by Northwestern University Genomics Core, Chicago, IL). The map and DNA sequence of the plasmids *Vasa*-EGFP-T7, *Gdf9*-mCherry-His and*Zp3*-Amcyan-HA can be found in Appendix I to III.

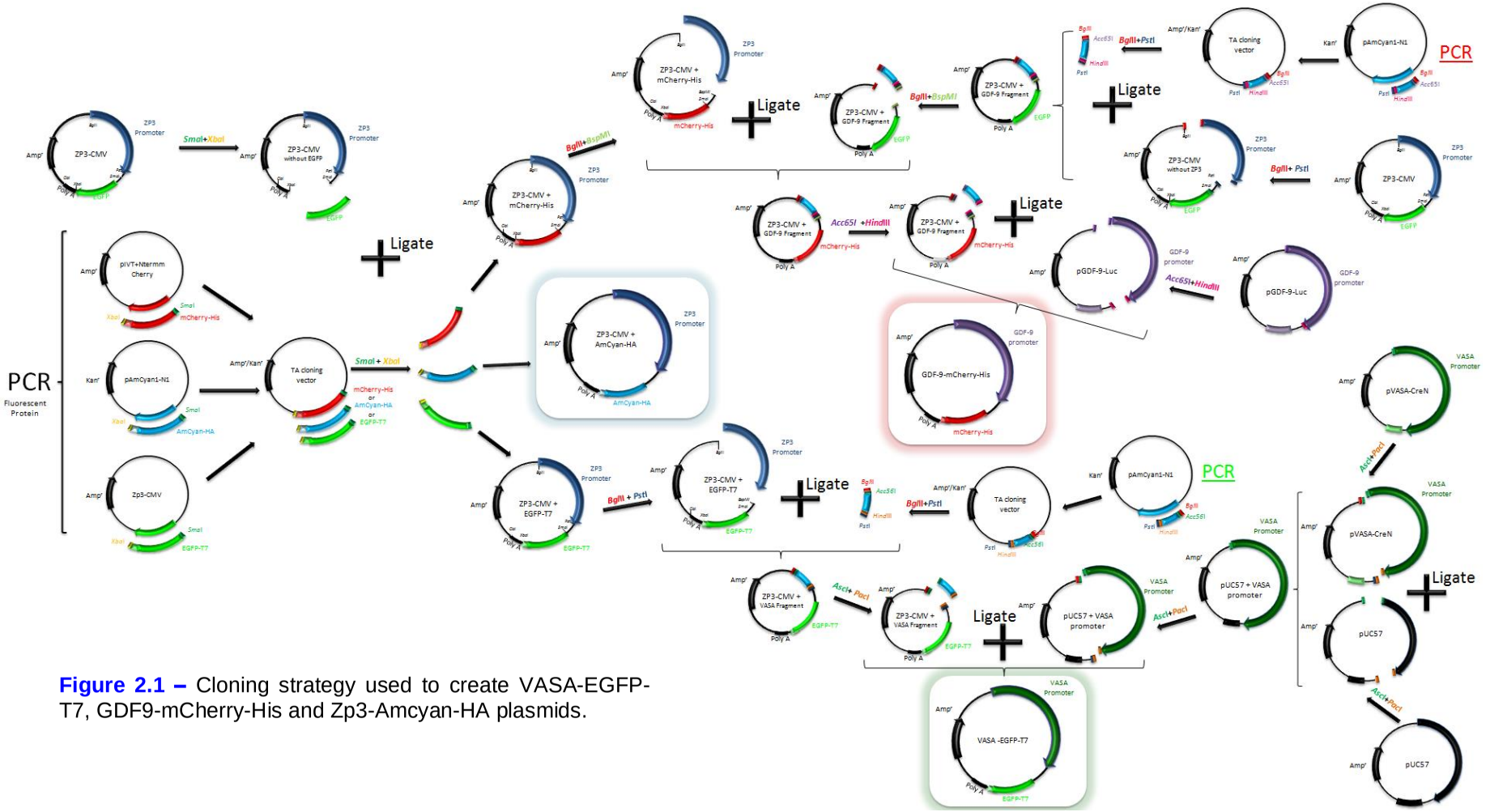

Figure 2.1 – Cloning strategy used to create VASA-EGFP-T7, GDF9-mCherry-His and Zp3-Amcyan-HA plasmids.

Table 2.1 – Primers used to generate the three linear fragments

Name	Type	Propose	Primer sequence
P1	Forward	Amplify AmCyan inserting *Sma*I restriction site	5'-TATATACCCGGGCGCCACCATGGCCCTGT CCAACAAGTTC-3'
P2	Reverse	Amplify AmCyan inserting *Xba*I restriction and HA tag	5'-CGATTCTAGATCAAGCGTAATCTGGAACAT CGTATGGGTAGAAGGGCACCACGGAGGTGAT GTGG-3'
P3	Forward	Amplify mCherry inserting *Sma*I restriction site	5'-ATATATCCCGGGCGCCACCATGGTGAGCA AGGGCGAGG-3'
P4	Reverse	Amplify mCherry inserting *Xba*I restriction and His tag	5'-TATATCTAGACTAGTGATGGTGGTGATGGT GGTTTCCGGACTTGTACAGCTCGTCC-3'
P5	Forward	Amplify EGFP inserting *Sma*I restriction site	5'-ATATATCCCGGG CGCCACC ATG GTGAGCAAGGGCGAGGAGCTGTTC-3'
P6	Reverse	Amplify EGFP inserting *Xba*I restriction and T7 tag	5'-CGCGTCTAGATTAACCCATTTGCTGTCCAC CAGTCATGCTAGCCATCTTGTACAGCTCGTCC ATGCCGAGAGTGATCC-3'
P7	Forward	Insert *Bgl*II and *Asc*I restriction sites to replace *Zp3* with *Vasa* promoter	5'-ATATAGATCTTAAGGCGCGCCCTGTCCAA CAAGTTCATCGGCGACG-3'
P8	Reverse	Insert *Pst*I and *Pac*I restriction sites to replace *Zp3* with *Vasa* promoter	5'-CGCGCTGCAGCGCTTAATTAATCGCACAC GGTCATCTTCTCGAAGG-3'
P9	Forward	Insert *Bgl*II and *Acc65*I restriction sites to replace *Zp3* with *Gdf9* promoter	5'-ATATAGATCTATAGGTACCCTGTCCAACAA GTTCATCGGCGACG-3'
P10	Reverse	Insert *Pst*I and *Hind*III restriction sites to replace *Zp3* with *Gdf9* promoter	5'-CGCGCTGCAGCGCAAGCTTTCGCACACGG TCATCTTCTCGAAGG-3'

2.2. Transfection of Cell Line to Test Construct Functionality

The functionality of the fluorescent proteins was tested by transfection of HEK293T cells. To induce expression in the cell line, the oocyte specific promoters *Gdf-9*, *Zp3* and *Vasa* were replaced with CMV (cytomegalovirus) promoter. *Gdf9*-mCherry-His and *Zp3*-Amcyan-HA plasmids were digested with *Bgl*II/*Hind*III to replace *Gdf9* and *Zp3* promoters with CMV promoter from pcDNA3 vector. The *Zp3* promoter was excised from *Zp3*-EGFP-T7 plasmid with *Bgl*II/*Pst*I and replaced with CMV promoter from pcDNA4/myc-HisA vector. HEK293T cells were cultured in DMEM media containing 1% penicillin-streptomycin and 10% FBS (Life Technologies, NY). Cells were plated in circular glass coverslips coated with poly-L-lysine in a 24-well plate and cultured for 24-48h before transfection. Lipofectamine 2000 (11668-027, Life Technologies, NY) was used to transfect cells with 800 ng of

plasmidic DNA (CMV-EGFP-T7, CMV-mCherry-His or CMV-AmCyan-HA) in Opti-MEM media, according to manufacture instructions. Transfection of cells with pcDNA3 plasmid was used as negative control. 24h after transfection, coverslips were gently removed from the plate and mounted into a microscope slide to visualize fluorescent protein expression using Nikon Eclipse E600 microscope.

2.3. Generation of the Triple Transgenic Mice and Animal Care

Following linearization by *Bgl*II and *Cla*I or *BamH*I, the linear DNA fragments *Zp3*-AmCyan-HA (2886 bp), *Vasa*-EGFP-T7 (6694 bp) and *Gdf-9*-mCherry-His (4471 bp) were purified using Elutip-D columns (10462615, Whatman Schleicher and Schuell, Germany) and co-injected at equimolar ratios into CD-1 [Charles River Crl:CD1(ICR)] 1-cell embryos using standard protocols (pronuclear microinjection performed at Northwestern University Transgenic Facility, Chicago, IL, USA). Generation of transgenic mice through co-injection of the three independent promoter-fluorescent protein coding sequence constructs is expected to result in random insertion of exogenous DNA into the mouse genome [76]. All procedures involving mice were approved by the Northwestern University Animal Care and Use Committee. Mice were housed and bred in a barrier facility within Northwestern University's Center of Comparative Medicine (Chicago, IL, USA) and were provided with food and water *ad libitum*. Temperature, humidity, and photoperiod (14L : 10D) were kept constant.

2.4. Genotyping PCR

The genotype was assessed by PCR of tail and ear tissue using the following primers: *Gdf9*-mCherry (F1 5'-TCAAAATTATGTAGCTCTGACTGTCC-3', R1 – 5'-CCCTCCATGTGCACCTTGAAGCGCAT-3'), *Zp3*-Amcyan (F2 – 5'-AGAGTTACAC-TGAGAAATCCTGCCC, R2 – 5'-CCTCGCCCTTCACGGTGAAGTAGTG) and *Vasa*-EGFP (F3 – 5'-ACGTGCAGCCGTTTAAGCCG-3', R3 – 5'-TTGCCGTCGTCCTTGA AGAA-3'). The primers were designed to originate a PCR product that contains part

of the promoter sequence and part of the fluorescent protein, therefore detecting the functional unit of the transgenes (Figure 2.2). The different transgenes were distinguished by the size of the PCR product and detected as 943-bp, 695-bp and 610-bp products, respectively. To extract genomic DNA, tail or ear pieces were digested with 50 µl of 50 mM NaOH at 95ºC and neutralized with 25 µl of 1M Tris-HCl. Each 20 µl PCR reaction included 1 µl of genomic DNA, 2 µl of 10x reaction buffer, 0.6 µl 2.5 mM dNTP mix, 0.4 µl 50mM $MgCl_2$, 0.4 µl of forward primer, 0.4 µl of reverse primer, 0.1 µl Taq polymerase (10342-020, Life Technologies, NY) and 15.1 µl of molecular grade water (46-000-cv cellgro, VA). The PCR conditions were 94ºC 5 minutes, (94ºC 45 seconds, 56ºC (*Gdf-9* and *Zp3*) or 60ºC (*Vasa*) 45 seconds, 72ºC 1 minute) x 40 cycles, 72ºC 2 minutes. PCR products were run in 2% agarose gel containing ethidium bromide or GelRed™ (41003, Biotium, CA).

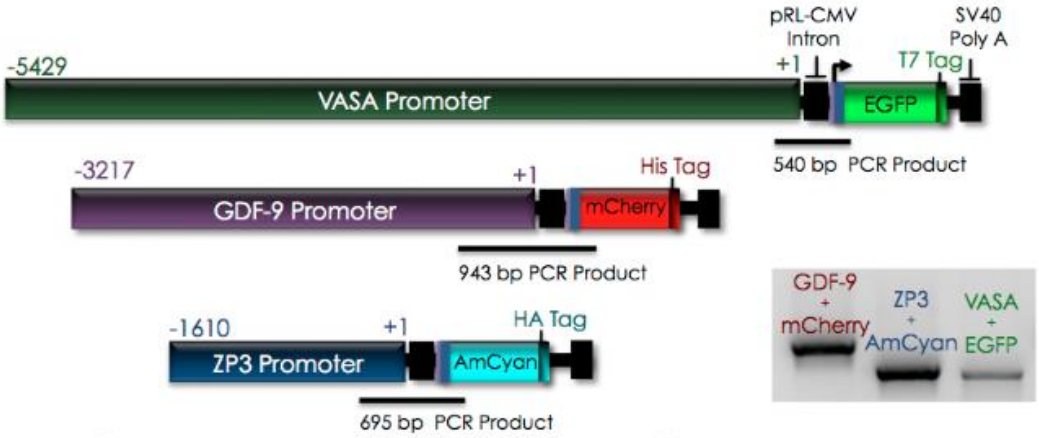

Figure 2.2 – Maps of the linear constructs, design of the genotyping primers and PCR products in agarose gel.

2.5. Initial Screening of the Founder Lines

Founder mice were bred with wild-type animals to determine germ line transmission and segregation pattern of the transgenes in F_1 generation. Mouse ovaries from the F_1 generation were analyzed to evaluate which line expressed the highest levels of the three fluorescent proteins in their oocytes. Ovaries were collected and dissected from the bursa in L15 medium containing penicillin-streptomycin and 10% FBS (Life Technologies, NY), and immediately imaged using

Nikon Eclipse E600 microscope. Cross-detection of EGFP and AmCyan is expected using this imaging system.

2.6. Generation of Homozygous Mice

Homozygous mice were generated by crossing F_2 heterozygous individuals (Figure 2.3). Although differences in the intensity of genotyping PCR product bands could be identified, due to the sensibility to error of this technique, breeding studies with wild-type animals were performed to confirm homozygosis.

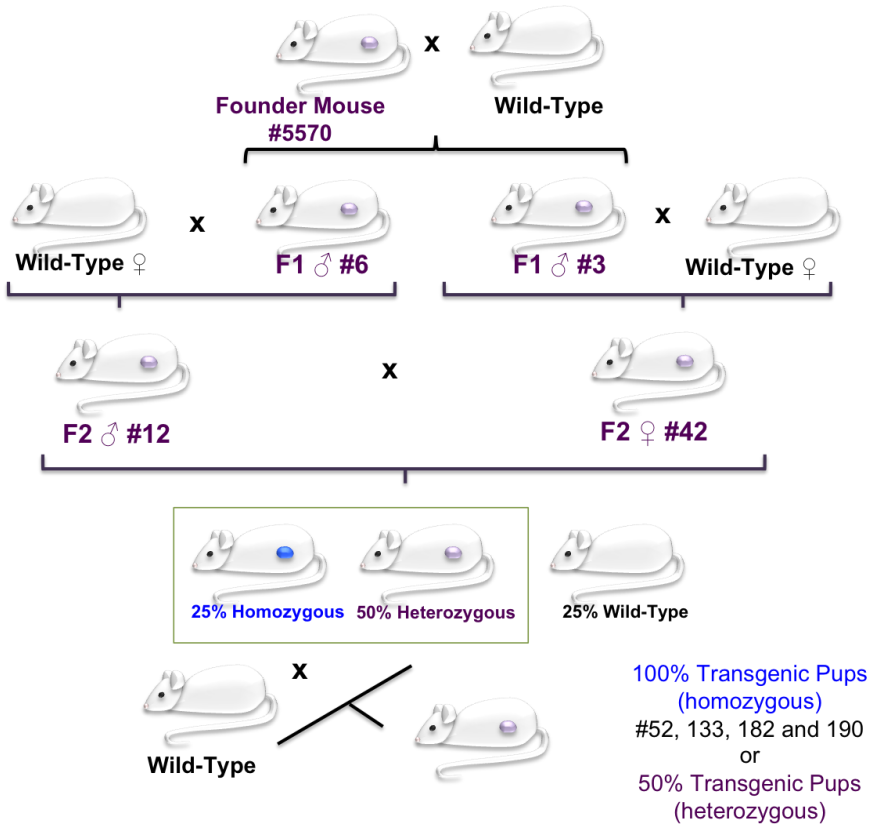

Figure 2.3 – Breeding scheme used to generate homozygous triple transgenic mice.

2.7. Fertility Study

Fertility data was collected over generations assessing the number of pups from male and female breeders crossed with wild-type individuals. Breeding cages were set up at 4 week of age and the animals were left together during the whole duration of the study. To determine the fertility of homozygous mice, 8 transgenic females and 2 transgenic males were used (similar litter size was generated independently of the gender).

2.8. Timed Pregnancy and Embryo Collection

Vaginal cytology was used to follow estrous cycle, as described by [77]. Wild-type CD1 females on proestrus were housed overnight with a transgenic male and separated in the next morning independently if a sperm plug was observed or not to ensure accurate timing of pregnancy. Conception was estimated to occur at midnight prior to the morning of the vaginal plug. Noon of plug detection day was considered embryonic day 0.5. Embryos were collected in L15 medium containing 10% FBS (Life Technologies, NY) and dissected according to [76]. Briefly, embryos were removed from their extraembryonic membranes and the anterior half of the embryo was cut off just below the armpits. A cut was done along the ventral midline of the posterior half of the embryo, and the liver and intestine were removed with fine forceps, allowing visualization of the genital ridges lying on the dorsal wall of the embryos. To image the embryonic ovary in its native orientation, the embryos were placed ventrally against the dish and visualized using an inverted microscope as described below.

2.9. Ovary Collection and Imaging

The day of birth was counted as postnatal day 0. Ovaries were collected and dissected from the bursa in L15 medium containing penicillin-streptomycin and 10% FBS (Life Technologies, NY). Embryonic and postnatal ovaries were imaged immediately after collection on Nikon Eclipse Ti epifluorescent microscope using C-FL CFP 96341 (AmCyan), C-FL YFP BP HYQ 96345 (EGFP) and C-FL Y-2E/C Texas Red 96313 (mCherry) cubes from Nikon. Yellow fluorescent protein (YFP) cube was used to detect EGFP to minimize cross-detection of AmCyan, since the two fluorescent proteins have similar spectral properties. The detection of EGFP using the YFP cube is not optimal, since it filters away not just the cyan light but also some of the green signal, reason why EGFP appears relatively weak on the epifluorescence images. Confocal images were acquired on a Nikon A1R Laser

Resonant Scanning Confocal Microscope using the laser lines 457 (AmCyan), 488 (EGFP) and 561 (mCherry) (Northwestern University Cell Imaging Facility). Cross-detection of the distinct fluorescent proteins was minimized by the imaging settings but cannot be excluded in any of the imaging systems used (Figure 2.4) Z-stack images of the ovaries were collected from the first layer of cells on the surface of the ovary until no signal could be detected. 3D maximum projection reconstructs of the z-stacks were created on Nikon Elements NIS software.

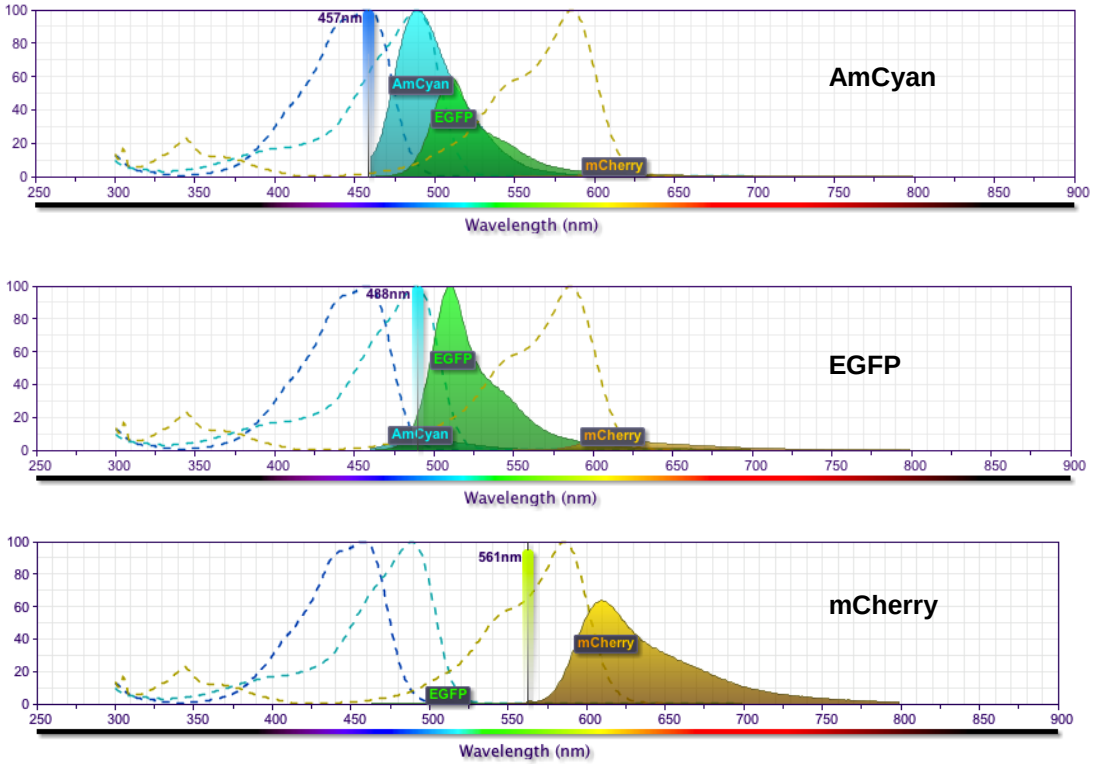

Figure 2.4 – Theoretical cross detection of fluorescent proteins when using the selected laser lines to excite the reporter proteins. AmCyan – 457 nm, EGFP – 488 nm and mCherry – 561 nm. While EGFP and mCherry signal detection is relatively specific, the use of 457 nm for AmCyan can collect some EGFP signal. These graphs only represent the crossdetection associated with the confocal microscopy. Simulated on BD Biosciences Fluorescence Spectrum Viewer.
http://www.bdbiosciences.com/research/multicolor/spectrum_viewer/index.jsp

The ovaries were kept intact during live imaging. Ventral and dorsal regions of the same ovary were imaged by rotating the ovary horizontally using a blunted pipette tip (Figure 2.5).

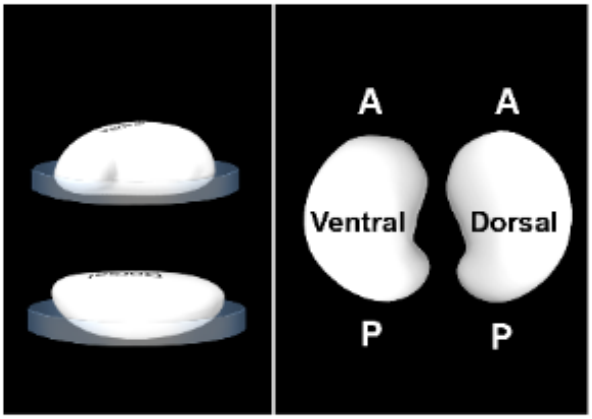

Figure 2.5 – Intact ovaries were imaged by epifluorescence or confocal microscopy as shown in this image on the right, with ventral or dorsal regions of the ovary facing the dish. On Chapter 4 the two faces of the same ovary were represented as shown here, with the anterior region of the ovary on the top (left image). A (anterior), P (Posterior).

2.10. Histological Analysis

Embryonic and postnatal mouse ovaries from transgenic mice and wild-type siblings were fixed with Modified Davison's fixative (Electron Microscopy Sciences, PA) overnight-24h at 4 °C. Tissue was then included in an alginate disk before processed and embedded in paraffin. The inclusion in alginate disks allowed sectioning of the tissue with a specific orientation. This protocol, developed by Min Xu for sectioning of ovarian follicles, was used with the propose of orientate the tissue for the first time on this thesis. Briefly, ovaries were washed with a gradient of ethanol (70%, 50% and MilliQ water) and rinsed with Ca^{2+}/Mg^{2+} free PBS (14190, Life Technologies, NY), before placing in top of a 0.4 µm pore MiilliCell insert (PICM01250, Millipore, Germany) and covered with 100 µl of 2% alginate (diluted in Ca^{2+}/Mg^{2+} free PBS). Ovaries were oriented, with the ventral ovarian region facing against the membrane, using insulin needles. Insert was placed in top of a 4%PFA-Ca^{2+}-Cacodylate Solution (2 ml of MilliQ water, 0.5 ml of 2M $CaCl_2$, 1.25 ml of 4x Cacodylate, and 1.25 ml of 16% PFA) and let crosslink overnight at 4ºC. In the next day fixative solution was removed and the alginate disk was rinsed with MilliQ water. 100 µl of Alcian Blue dye was added to the surface for 5 minutes and rinsed with 50% ethanol until all the excess of dye is removed. Alginate disk was carefully removed from the insert and placed in 70% ethanol until embedding in paraffin. Ovarian tissue was serially sectioned with 5 µm thickness from the ventral to the

dorsal face of the ovary (Figure 2.6). H&E staining was performed using standard methods. Megan Romero and Keisha Barreto from the Northwestern University Ovarian Histology Core performed almost all sectioning and staining.

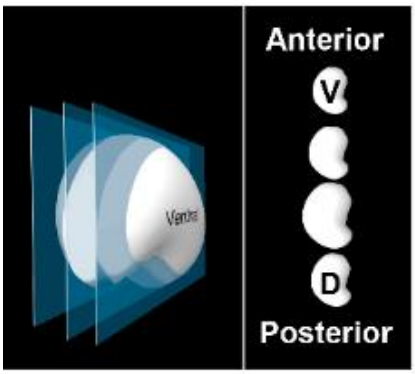

Figure 2.6 – Ovaries were serially sectioned from ventral to dorsal regions. In Chapter 4, embryonic and postnatal ovaries were represented as shown on this figure, with the anterior region of the ovary in the top of the image. V (Ventral), D (Dorsal)

2.11. Immunohistochemistry

Immunofluorescence assay was performed as previously described [57, 78] with some modifications. Briefly, after deparaffinization and rehydration of the ovarian sections, antigen retrieval was performed using fresh made Sodium Citrate buffer (10mM Sodium Citrate, 0.05% Tween-20, pH 6) in a pressure cooker for 40 min. After cooling down, slides were rinsed three times with tap water and incubated with 3% hydrogen peroxide in TBS (Tris-buffered saline) for 15 min. Ovarian tissue was then washed with TBS before incubation with Avidin-Biotin Blocking kit according to manufacture instructions (SP-2001, Vector Laboratories, CA) and blocked with blocking solution (2% donkey serum, 1% BSA, 0.1% cold fish skin gelatin, 0.1% Triton, 0.05% Tween-20, 0.05% sodium azide in 0.01M PBS) for 1 hour at room temperature. Sections were incubated overnight at 4ºC with EGFP (1:100, GFP (FL), sc-8334, Santa Cruz, TX), HA tag (1:200, H6908, Sigma, MO), VASA (1:50, DDX4/MVH antibody, ab138440, Abcam, Cambridge, UK), Oct4 (1:50, P0056, Sigma, MO), Stra8 (1:50, ab49602, Abcam, Cambridge, UK), Foxl2 (1:50, ab5096, Abcam, Cambridge, UK), Laminin (1:100, L9393, Sigma, MO) and TAp63 (1:100, sc-8431, Santa Cruz, TX) primary antibodies. Three TBS-T (TBS with 1ml/L Tween 20) washes of 15 minutes were performed to remove the excess of antibodies. Signals

were amplified using biotinylated secondary antibodies against rabbit (711-065-152, Jackson ImmunoResearch, PA) and goat (BA-5000, Vector Laboratories, CA), followed by ABC kit (PK-6100, Vector Laboratories, CA) and TSA Plus Fluorescein System (1:400 dilution for 1 minute, NEL741001KT, PerkinElmer, MA). Sections were washed with TBS-T after each kit (5 times for 5 minutes). Laminin and TAp63 antibodies did not require amplification, thus, fluorophore-conjugated secondary antibody was used instead (711-546-152 anti-rabbit AlexaFluor 488 and 715-586-150 anti-mouse AlexaFluor 594, both from Jackson ImmunoResearch, PA), followed by 3 washes of 15 minutes with TBS-T. Slides were mounted with Vectashield containing DAPI (H-1200, Vector Laboratories, CA) and sealed with nail polish. Slides were imaged using Nikon Eclipse E600 microscope. The specificity of signals was confirmed with a negative control in which the primary antibody was omitted. Additionally, a second negative control with wild-type ovary was performed to test the specificity of the antibodies against reporter proteins. GFP antibody showed unspecific binding to the outline of the oocytes from wild-type ovaries, however cytoplasmic signal was only observed in transgenic ovaries. Three to five animals from 3 independent litters (total 9 to 15 independent ovaries) were analyzed per each developmental timepoint represented in this thesis.

2.12. Oocyte Isolation and Fluorescent Protein Quantification

Oocyte collection from primordial, primary, secondary, antral and Graffian follicles was performed using 0, 3, 6, 8, 12, 17 and 22 days old mice, as described [79] with some modifications. Cumulus-oocyte complexes were isolated from 17 and 22-days-old mice by puncturing the antral follicles with syringe needles. Oocytes were then denuded by repeated pipetting using a thin stripping tip and washed with αMEM medium supplemented with 10% FBS and 1µl/ml Milrinone (Life technologies, NY). Oocytes from primary and secondary follicles were isolated from day 12 mice by digesting the ovaries using Ca^{2+}/Mg^{2+} free CZB media with 0.1% collagenase and

0.02% DNAse-I [80]. Oocytes were rinsed with L15 medium with 0.05% PVP (polyvinylpyrrolidone) and kept in drops of αMEM under embryo culture oil until imaging. Primordial and primary oocytes were obtained by digesting day 3, 6 and 8 mouse ovaries with 0.05% trypsin-EDTA (Life technologies, NY) supplemented with 0.02% DNAse-I at 37ºC for 20 min with constant agitation [32]. Gentle pipetting was done until a single cell suspension was obtained. Isolated oocytes were cultured overnight to allow somatic cells to attach to the bottom of the dish and allow collection of a purified sample of primordial and primary oocytes. All the isolated oocytes were kept at 37 °C under 5% CO_2 until and during imaging. Confocal images were acquired using Nikon A1 confocal microscope, as described before in Section 2.9. NIS software was used to quantify the fluorescent signal. The diameter of the oocyte was used to determine follicle class: Primordial <15 µm; Primary 15-30 µm; Secondary 30-60 µm; Antral 60-70 µm; Graffian >70 µm [81, 82].

2.13. Follicle Isolation and Fluorescent Protein Quantification

Follicles from Day 8 to 3 months old mice were mechanically isolated using insulin needles, in phenol-red free L15 media supplemented with penicillin-streptomycin and 10% FBS (Life Technologies, NY). Follicles were incubated with the DNA probe Hoechst 33342 (H1399, 10µg/ml, Life Technologies, NY) for 5 minutes at 37ºC to allow identification of granulosa cell shape and number of layers. Follicles were classified according to their morphologic features [81]. Ovarian follicles were then rinsed with fresh media before imaging in a teflon printed slide (63422-06, Electron Microscopy Sciences). Nikon Eclipse Ti epifluorescent microscope using the same cubes described in Section 2.9 was used to determine the intensity of the fluorescent signal. Quantification of the number of gray pixels on the follicle images was done using ImageJ. A square of 70,000 pixels (size of a primordial oocyte) was used to quantify all the follicles. The size of the oocyte and follicle was calculated by measuring the area of the structure, to allow accurate dimension of elongated

follicles. All the follicles presenting morphological damage including dark granulosa layer, misshapen oocytes and disrupted basement membrane were excluded.

2.14. *In vitro* Fertilization (IVF)

Female mice at 21 and 42 days of age were injected intraperitoneally with 5 IU of PMSG (pregnant mare's serum gonadotropin, 367222, EMD Millipore, MA) followed by 5 IU of hCG (human chorionic gonadotropin, C1063, Sigma, MO) 48 hours later. PMSG was used to mimic the oocyte maturation effect of endogenous follicle-stimulation hormone (FSH) and hCG was used to mimic the ovulation induction effect of luteinizing hormone (LH) [76]. The IVF and sperm cryopreservation protocols were based on Justin Meyer personal communications (from Northwestern Transgenic Facility, Chicago, IL). Cryopreserved sperm from wild-type CD-1 mice was used for IVF. Sperm was cryopreserved on CPM media (18% raffinose, 3% skim milk, 0.04 µl/ml of 97% 1-thioglycerol in distillated water) as described by [83]. Sperm straw was thaw for 10 seconds at room temperature, followed by 30 seconds in water bath and left to equilibrate for 1 hour in a 5% CO_2 incubator at 37 ºC. Equilibration was performed in 400 µl drops of HTF media (K-RVFE-50, Cook Medical, IN) under oil where COCs (cumulus-oocyte complexes) were added later.

Oviducts were excised from female mice in PBS-BSA media (MR-006C, EMD Millipore, MA), 14-16 hours after hCG administration, and dissected under a microscope to collect COCs at Metaphase II stage (MII), on HTF media. COCs were individualized from the cluster using insulin needles and then place in 8 µl drops of media under oil. After imaging the oocytes using Nikon Eclipse Ti epifluorescent microscope oocytes were classified and grouped based on the intensity of AmCyan signal as high, medium and low. Grouped COCs were added to the equilibrated sperm and let together for 5 hours, before transferring to drops of KSOM supplemented with 0.4g/ml of BSA. 24 hours after IVF the embryos were scored and

all the 2-cell embryos were transferred to a new drop of KSOM. Embryos were only scored again at 96 and 120 hours after IVF to determine the number of embryos that reach blastocyst stage. All the culture media used for IVF were allowed to equilibrate overnight in a 5% CO_2 incubator at 37 °C. The embryo oil was mixed aggressively with embryo culture water and let set for at least 1 hour before use, to wash away any possible contaminants.

2.15. Statistical Analysis

All statistical analyses were performed using the software Prism 4.0 (GraphPad Software, San Diego, CA). Shapiro-Wilk test was used to access normality of the data. One-way ANOVA was used to determine differences between breeders in the fertility study. Kruskal-Wallis test (non-parametric) followed by Dunn's test was used to evaluate differences between follicular classes and different ages. A difference was considered to be significant when $p<0.05$. Statistical significance was marked with ** ($p<0.01$) and *** ($p<0.001$).

CHAPTER 3

Generation and Characterization of the Triple Transgenic Mouse Line

3.1. Introduction

The discovery and development of GFP (Green Fluorescent Protein) revolutionized biological research, awarding Martin Chalfie, Osamu Shimomura, and Roger Y. Tsien the 2008 Nobel Prize in Chemistry (http://www.nobelprize.org/nobel_prizes/chemistry/laureates/2008/). The intrinsic fluorescence of this protein, without the addition of co-factors, allows non-invasive visualization of promoter expression without fixation of the tissue, making it an excellent reporter *in vivo* and *in vitro*. Several GFP variants with different spectral properties were created by amino acid manipulation of the recombinant protein, allowing multiple reporter detection in the same biological system [84]. Currently, many fluorescent proteins with unique spectral properties and derived from different aquatic organisms are available for research use. Over the years, innumerous transgenic lines have been created to express one or multiple fluorescent proteins, under the control of constitutive or cell-restricted promoters, for instance [85-87].

Live imaging using fluorescent proteins driven by specific promoters has been useful to visualize and study germ cell development; including primordial germ cell migration [2, 3, 88, 89], spermatogonial renewal and proliferation [90], Sertoli cell development [91], as well as functional analysis of promoter elements [92] and cellular localization of endogenous proteins [93, 94]. Although several mouse lines have been generated to label the germ cells at a specific time of ovarian development and/or stages of the follicle [74, 95], we lack a reporter line able to represent dynamically the developmental progression of the ovarian follicle. In order to generate a reporter line to dynamically follow follicle activation and growth, the oocyte-specific promoters *Vasa*, *Gdf-9* and *Zp3* were used to drive the expression of the fluorescent proteins EGFP, mCherry and AmCyan, respectively. These well-characterized promoters are active at distinct stages of follicle development and have been used routinely to create oocyte-specific knockouts (such as [47, 74, 75, 96-98]).

In the mouse, VASA (MVH, Mouse Vasa Homolog, DDX4) expression begins at the time of gonad colonization by primordial germ cells, localizing strongly in the cytoplasm of primordial oocytes and decreasing during follicle development until it is undetectable in antral follicles [99, 100]. GDF-9 (Growth Differentiation Factor 9) is critical for both early and late follicle growth and cumulus cell functions. Although the onset of GDF-9 expression is somewhat controversial, it appears that the promoter begins to be active at the primordial follicle stage and continues at later developmental stages as well [74, 101, 102]. ZP3 (Zona Pellucida Glycoprotein 3), one of the glycoproteins that comprise the zona pellucida and serves as a primary sperm receptor, is the last of these three proteins to be expressed in primary follicles, reaching its maximal expression in growing follicles, and decreases in fully-grown oocytes [103, 104]. Therefore, we expected that the temporal difference in activity of these promoters would result in an oocyte fluorescent signature able to provide readout of follicular function (Figure 3.1).

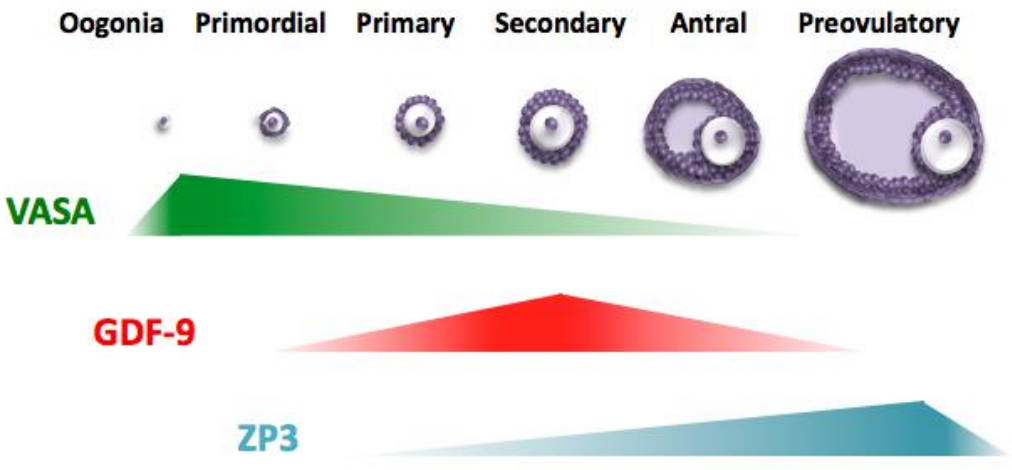

Figure 3.1 – Expected temporal expression pattern of VASA, GDF-9 and ZP3 promoters.

The selection of EGFP and mCherry took in account their spectral properties and the availability of plasmids containing their DNA sequence. AmCyan was selected to match the confocal laser lines available in the Woodruff laboratory and ensure detection of specific and bright signal. However, the spectral properties of

EGFP and AmCyan are relatively similar (Figure 3.2), requiring caution when setting up the laser power in confocal microscopy and the use of specific light cubes in epifluorescence microscopy (the green fluorescence light cube in most fluorescent microscopes does not allow differentiation of the two reporter proteins). At the time, no transgenic mice were produced using AmCyan protein, which represented a risk of unpredictable toxicity, reported for other fluorescent proteins such as DsRed [105]. The selected fluorescent proteins are derived from distinct organisms (EGFP – *Aequorea victoria*, mCherry – *Discosoma* sp. and AmCyan – *Anemonia majano*) allowing specific detection with antibodies.

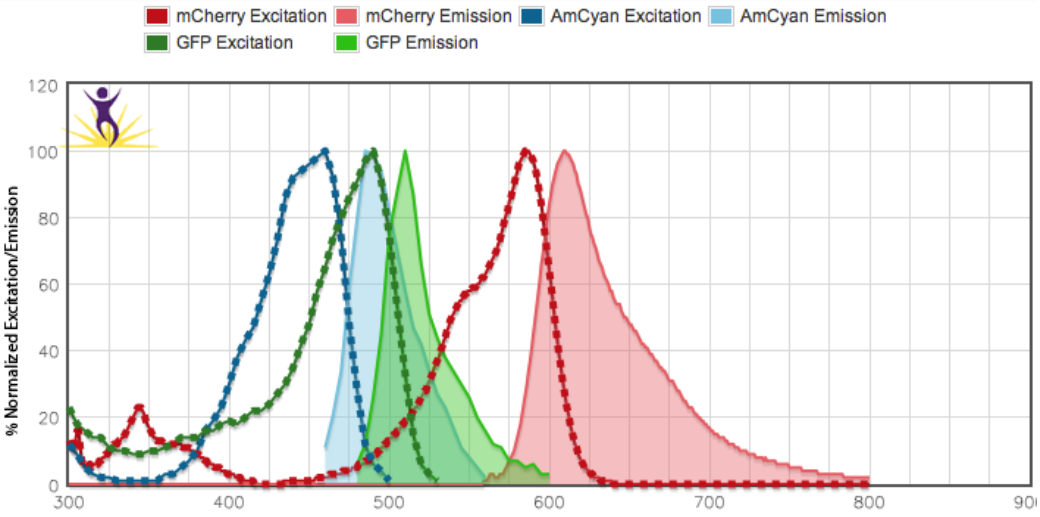

Figure 3.2 – Spectral properties of the three fluorescent proteins simulated using BioLegend's Fluorescence Spectra Analyzer. The close excitation and emission spectra of AmCyan and EGFP can cause crossdetection of fluorescent proteins, represented in Figure 2.4. (http://www.biolegend.com/spectraanalyzer)

3.2. Results

In order to verify the functionality of the three fluorescent proteins, manipulated by addition of epitope tags, transient transfection of HEK293T cells was performed. Replacement of the oocyte-specific promoters with the CMV promoter enabled the expression of the reporter proteins in this immortalized cell line. As expected, all fluorescent proteins could be detected 24 h after transfection (Figure 3.3). Due to the difficulty in testing promoter functionality in mature oocytes, caused by their low ability to transcribe protein [80], *Vasa*, *Gdf9* and *Zp3* promoters were just checked by sequencing.

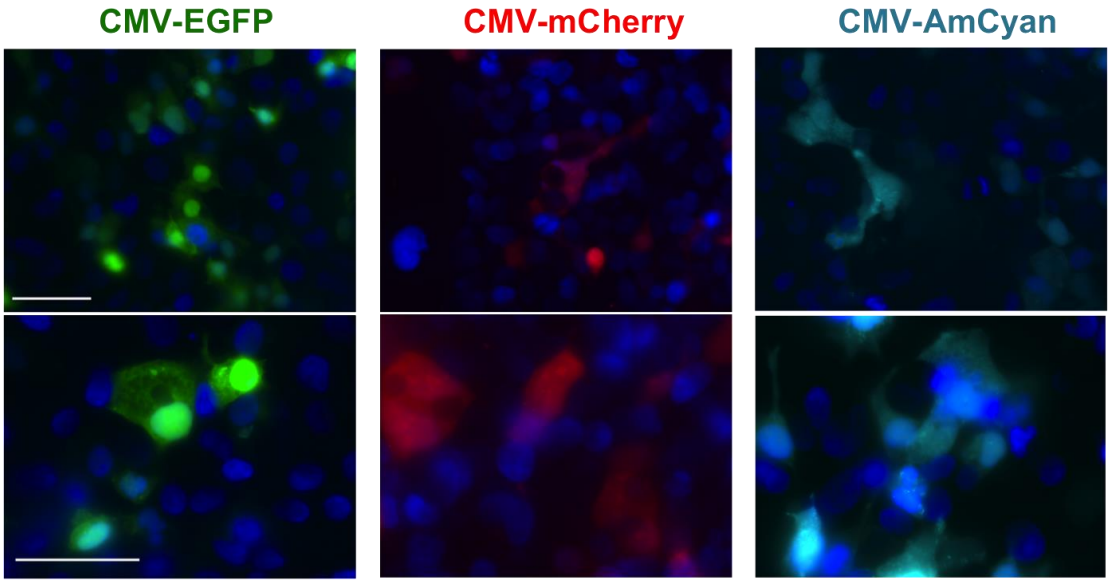

Figure 3.3 – Functionality of the fluorescent protein sequence validated using CMV promoter in transfected HEK2973T cells. Scale bars = 50 μm.

Two rounds of pronuclear injection resulted in the generation of 57 founder mice, from which nine carried the transgenes – one double transgenic and eight triple transgenic founder animals (Figure 3.4 and 3.5). Each founder line had a unique segregation pattern and expression level (Figure 3.6 and Table 3.1), likely related to differences in integration site and copy number of the transgenes [76]. Promoter specificity was observed with fluorescent protein expression restricted to the germ cells, being present in both the cytoplasm and nucleus.

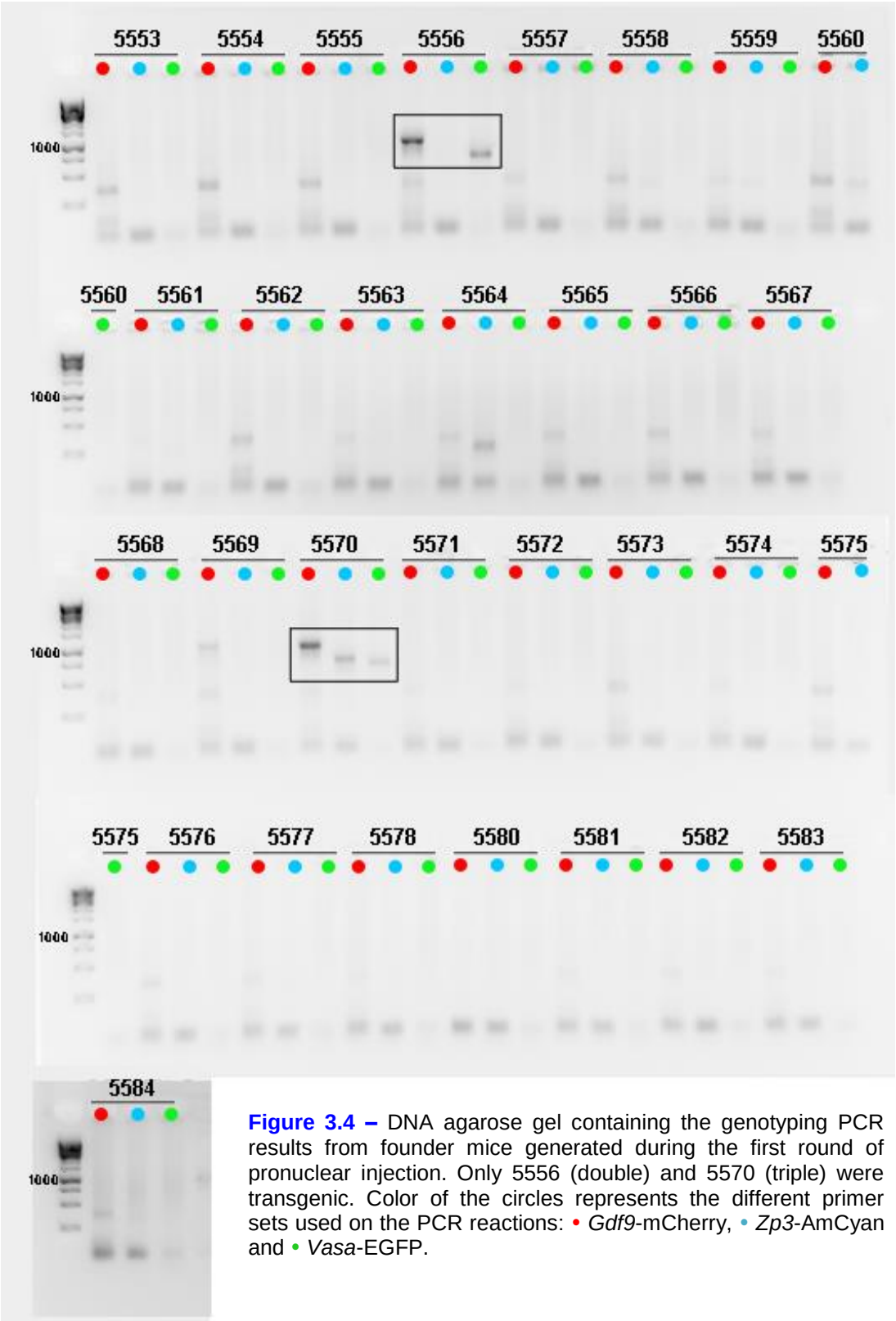

Figure 3.4 – DNA agarose gel containing the genotyping PCR results from founder mice generated during the first round of pronuclear injection. Only 5556 (double) and 5570 (triple) were transgenic. Color of the circles represents the different primer sets used on the PCR reactions: • *Gdf9*-mCherry, • *Zp3*-AmCyan and • *Vasa*-EGFP.

-

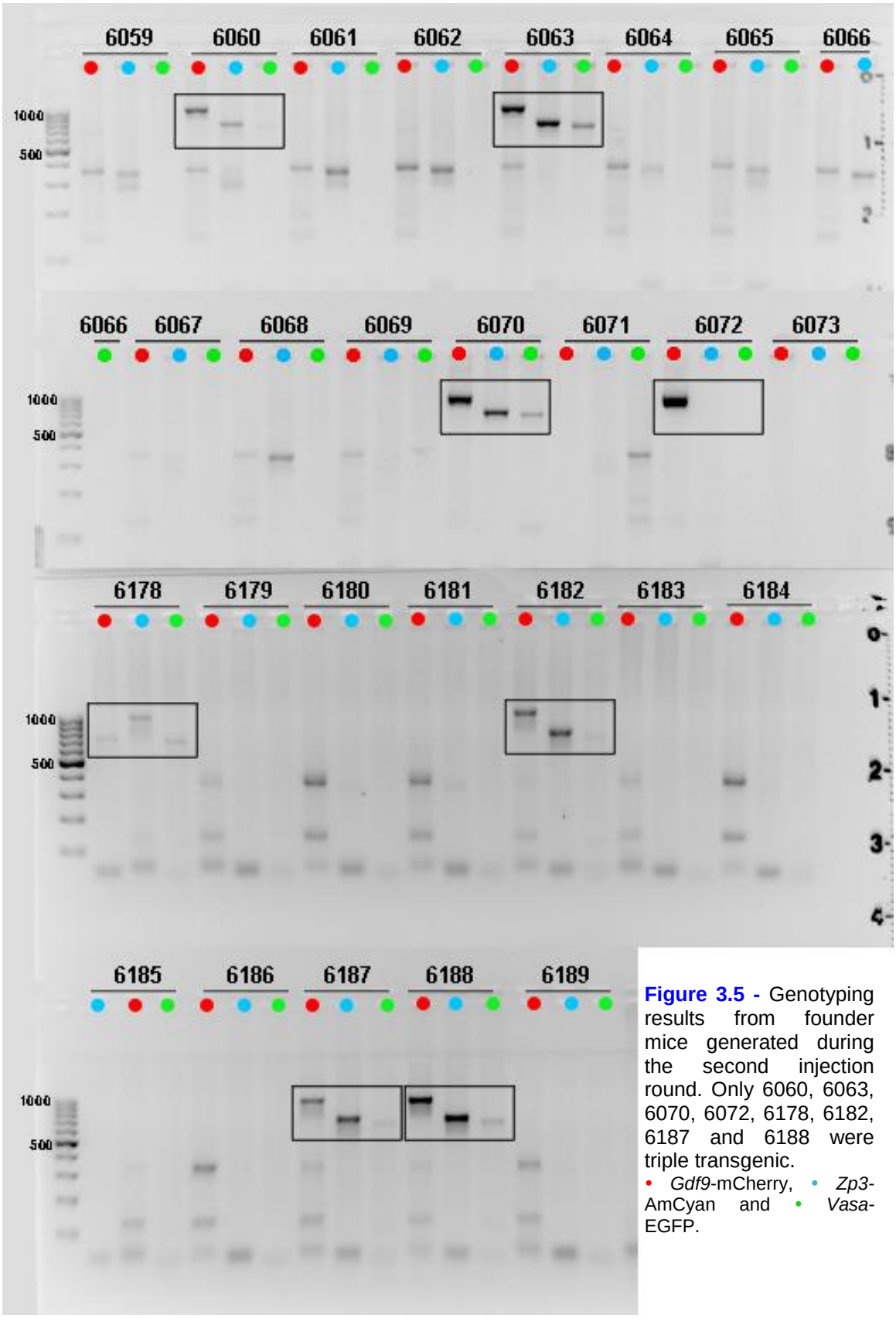

Figure 3.5 - Genotyping results from founder mice generated during the second injection round. Only 6060, 6063, 6070, 6072, 6178, 6182, 6187 and 6188 were triple transgenic. • *Gdf9*-mCherry, • *Zp3*-AmCyan and • *Vasa*-EGFP.

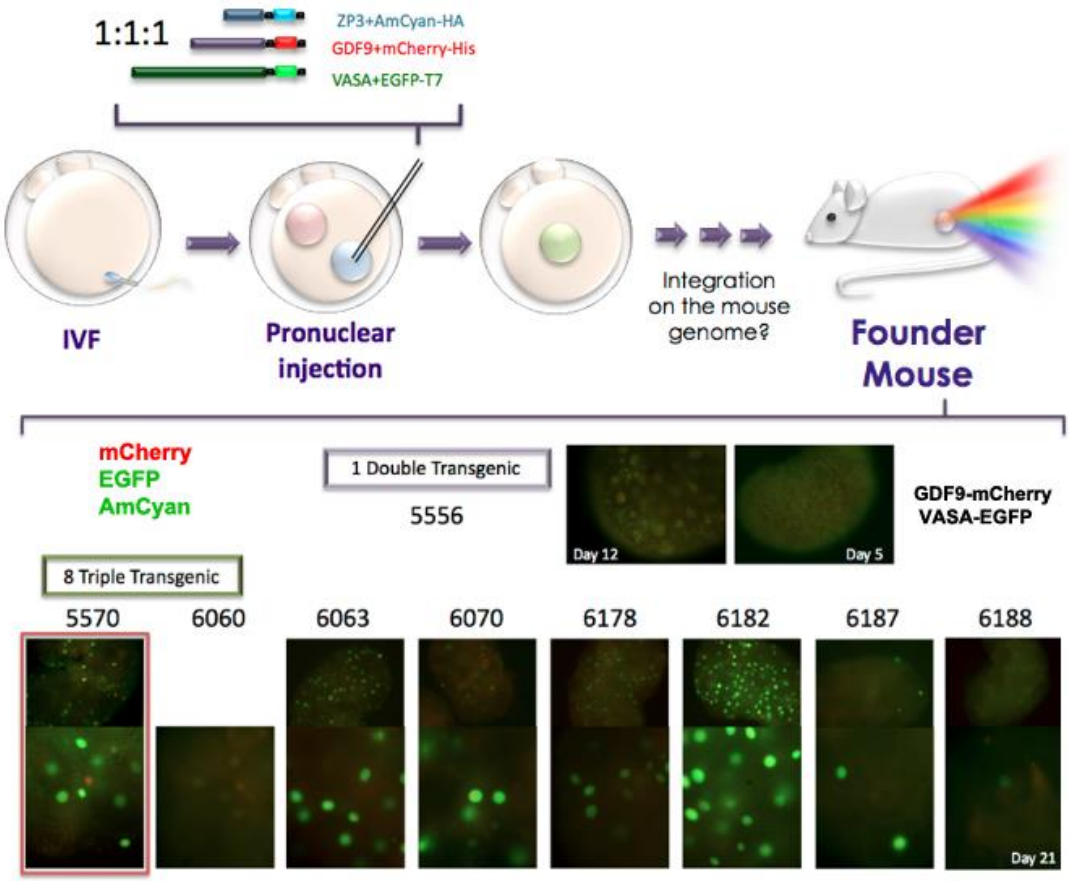

Figure 3.6 – Approach used to generate the triple transgenic line and expression level on the ovaries of F_1 mice from different founder lines.

Summary of the expression levels of the different transgenic lines can be found in Figure 3.6 and Table 3.1. Due to the cost associated with mouse maintenance, only one mouse line could be used for further studies, therefore comparison of the expression level and segregation pattern of at least three F_1 litters were performed. Lines 6060, 6182 and 6187 were excluded because of independent segregation of the transgenes, originating both double and triple transgenic pups (for percentages see Table 3.2). On other hand, lines 6063, 6070, 6178, 6187 and 6188 were excluded due to low expression level of one or several fluorescent proteins. Thus, founder line 5570 was selected for further study, because of high expression levels and co-segregation of the transgenes over 4 generations.

Table 3.1 – Transgene segregation pattern and expression level in the different transgenic lines generated

1º Injection Round – Positive 2/32

Founder Line	Genotype	Expression Level	Segregation patter	Genotype of the Offspring (F1)
5556	Double Transgenic VASA-EGFP GDF-9-mCherry	Low expression level of all transgenes	Transgenes linked	All Double
5570	Triple Transgenic VASA-EGFP GDF-9-mCherry ZP3-AmCyan	High expression level of the three transgenes	Transgenes linked	All Triple

2º Injection Round – Positive 7/25

Founder Line	Genotype	Expression Level	Segregation patter	Genotype of the Offspring (F1)
6060	Triple Transgenic VASA-EGFP GDF-9-mCherry ZP3-AmCyan	Very low expression levels	Independent segregation	Triple and Double Transgenic (VASA-EGFP GDF-9-mCherry)
6063	Triple Transgenic VASA-EGFP GDF-9-mCherry ZP3-AmCyan	High expression level of AmCyan and mCherry; lower expression of EGFP than line 5570	Transgenes linked	All Triple
6070	Triple Transgenic VASA-EGFP GDF-9-mCherry ZP3-AmCyan	Low expression levels	Transgenes linked	All Triple
6178	Triple Transgenic VASA-EGFP GDF-9-mCherry ZP3-AmCyan	Low expression level of mCherry	Transgenes linked	All Triple
6182	Triple Transgenic VASA-EGFP GDF-9-mCherry ZP3-AmCyan	Very high expression levels on the triple transgenic; low expression on the double transgenic	Independent segregation	Triple and Double Transgenic (VASA-EGFP ZP3-AmCyan)
6187	Triple Transgenic VASA-EGFP GDF-9-mCherry ZP3-AmCyan	Very low expression levels	Independent segregation	Triple and Double Transgenic (GDF-9-mCherry ZP3-AmCyan)
6188	Triple Transgenic VASA-EGFP GDF-9-mCherry ZP3-AmCyan	Very low expression levels	Transgenes linked	All Triple

Founder line 5570 showed normal gonad histology and fertility, confirming that the transgenes did not interfere with reproductive function (Figure 3.7). Curiously a lower number of pups (average 6 pups) were observed when breeding the #5570 founder and its F1 generation (Table 3.2). In contrast, homozygous mice for the transgenes produced similar number of pups to wild-type individuals (average 15 pups), suggesting that the lower fertility was not caused by the presence of the transgenic DNA. Despite the reduced number of pups observed while breeding heterozygous mice from F1, the percentage of transgenic mice generated was 50%. Interestingly, when F2 wild-type animals derived from F1 heterozygous transgenic

mice were breed with non-related wild-type individuals the number of pups originated was also low (6-8 pups). These results suggest that the decreased number of pups observed in the first 2 generations of the #5570 line might be caused by a genetic characteristic of the founder mouse rather than the presence of the transgenes.

Table 3.2 – Percentage of transgenic mice and average litter size of the different founder lines and 5570 generations

.

Mouse Line	Generation	Number of litters analyzed	Percentage of transgenic mice	Average litter size
# 5570 50% (269/499)	Founder	11	50% (34/69)	6
	F1	27	50%	7
	F4	32	50%	8
#6060	Founder	2	58% (17/29) Double: 3, Triple: 14	15
#6063	Founder	6	30% (32/98)	16
#6070	Founder	3	57% (19/33)	11
#6178	Founder	3	65% (21/32) Double: 4, Triple: 17	11
#6182	Founder	3	44% (19/43) Double: 16, Triple: 3	14
#6188	Founder	3	25% (10/41)	14

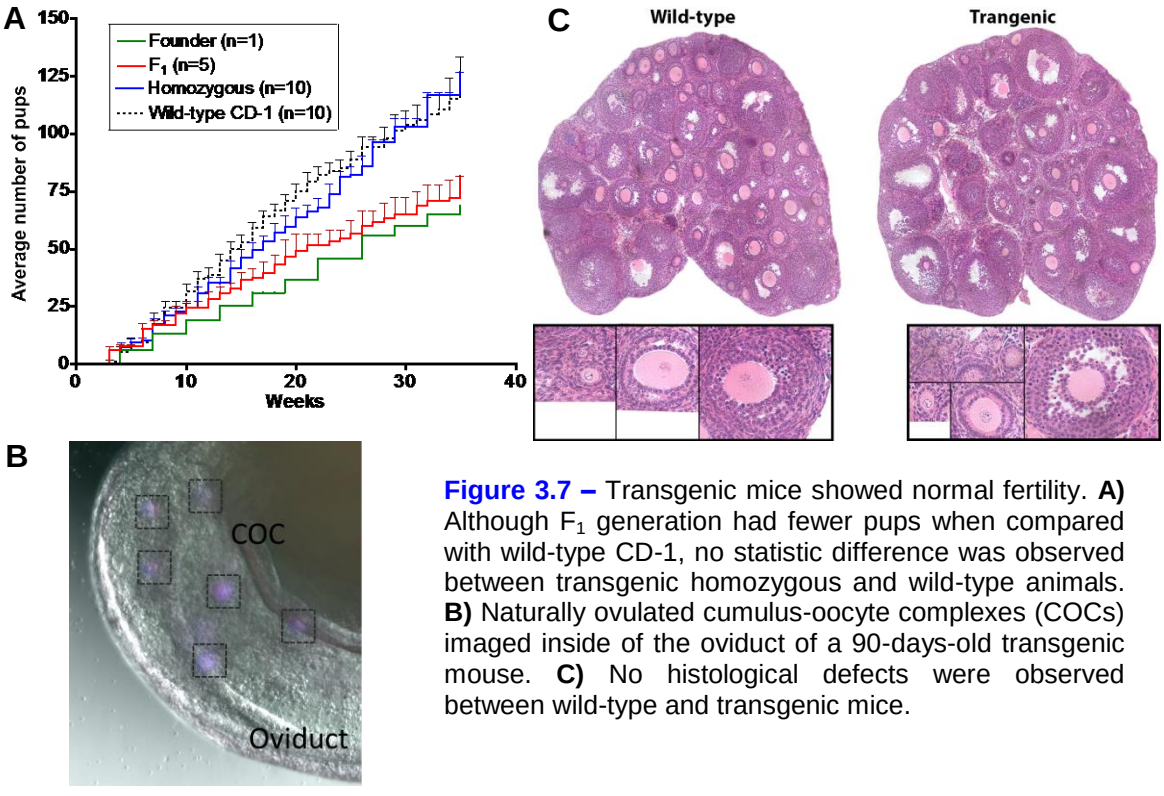

Figure 3.7 – Transgenic mice showed normal fertility. **A)** Although F_1 generation had fewer pups when compared with wild-type CD-1, no statistic difference was observed between transgenic homozygous and wild-type animals. **B)** Naturally ovulated cumulus-oocyte complexes (COCs) imaged inside of the oviduct of a 90-days-old transgenic mouse. **C)** No histological defects were observed between wild-type and transgenic mice.

To determine if the fluorescent protein expression in the transgenic mice reflected follicle development and ovarian physiology, whole ovary live imaging was performed at different ages (Figure 3.8). As expected, based on the timing of expression described for the promoters, EGFP was the only fluorescent protein detected on the germ cells during the embryonic period (Figure 3.8A, 16.5 and 18.5 dpc). The first appearance of mCherry occurred at birth (Figure 3.8A, Day 0), while AmCyan was only observed at day 4 for the majority of the animals (Figure 3.8A, Day 4). Interestingly, the first appearance of these fluorescent proteins was always restricted to a few oocytes located in the medullar region of the ovary (Figure 3.8A, Day 4, arrow). For separate channels see Appendix IV. Since ZP3 promoter expression is associated with transition to primary follicle stage [74, 103], this data indicated that the first wave of follicle activation occurs in a specific region of the mouse ovary, which will be further explored on Chapter 5 of this thesis.

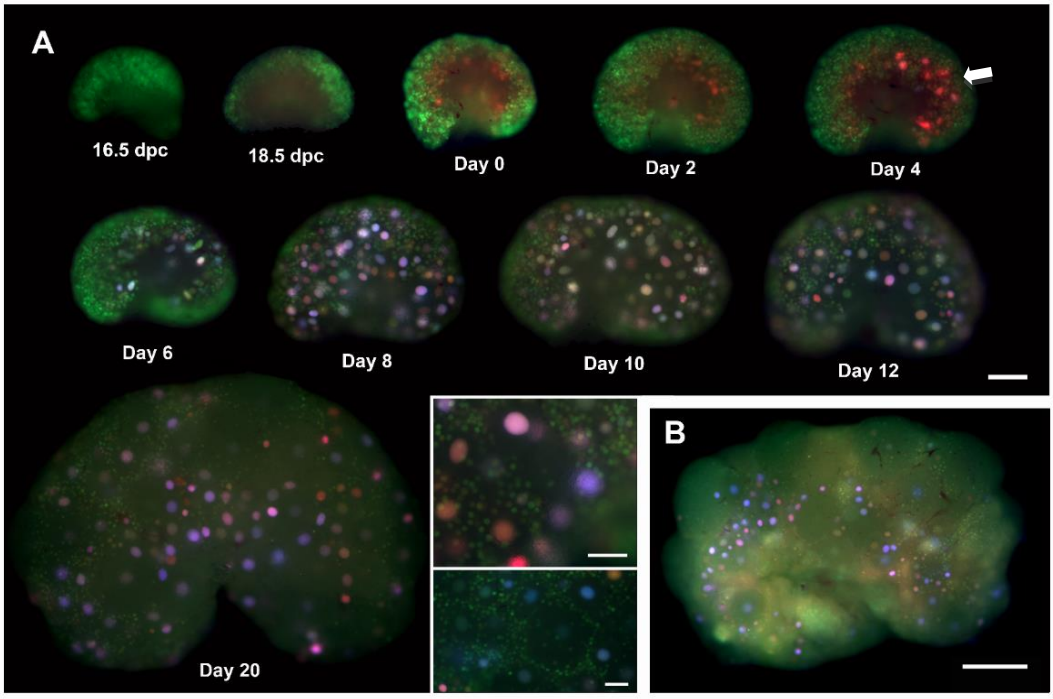

Figure 3.8 – The fluorescent profile reflects the developmental stage of the germ cell. Epifluorescent live imaging of ovaries from different age mice. **A)** As primary and secondary follicles are formed, the mCherry and AmCyan signal increased (day 0 to 20), validating the follicle-class dependent expression pattern expected. Scale bar=200 µm. Detail of day 16 ovarian surface is represented in the inserts. Scale bar=100 µm **B)** Fluorescent protein expression was also observed in the adult ovary, however the large size of the gonad and the presence of autofluorescence challenge accurate detection of the reporter proteins. Scale bar= 1mm:

In addition to localized patterns of follicle activation, follicle class dependent expression patterns were observed. In primordial oocytes, easily identified due to their small size and localization to the periphery, EGFP and mCherry were the only fluorescent proteins detected (Figure 3.9, white arrows). In contrast, growing follicles had larger sizes and elevated levels of the reporter proteins (Figure 3.9, red arrows). This indicates that the fluorescent signal changed according to the developmental stage of the oocyte, consistent with documented promoter activity [74, 75].

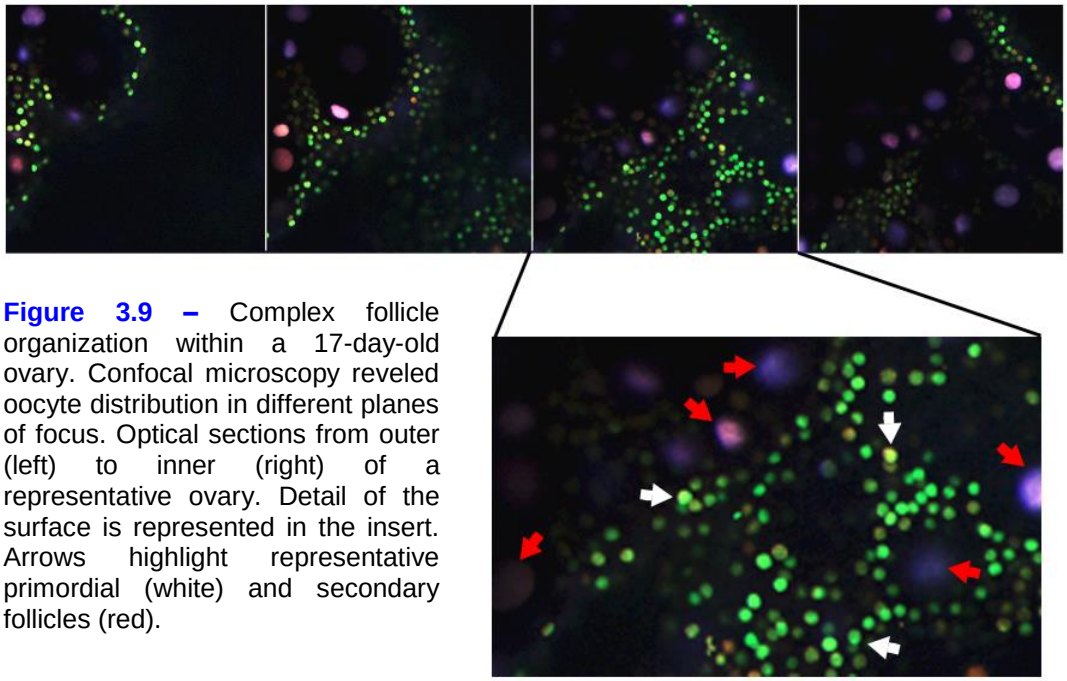

Figure 3.9 – Complex follicle organization within a 17-day-old ovary. Confocal microscopy reveled oocyte distribution in different planes of focus. Optical sections from outer (left) to inner (right) of a representative ovary. Detail of the surface is represented in the insert. Arrows highlight representative primordial (white) and secondary follicles (red).

Since the expression profile of this outbred mouse line is sensitive to the transcriptional activity of three key promoters during oocyte development, differences between individual animals and litters were recognized (Figure 3.10). Interestingly, a complex and heterogeneous pattern of color was observed within the same ovary, caused by the overlay of the different reporter proteins at distinct expression levels, even among oocytes at the same follicular stage, suggesting that each oocyte had its own fluorescent signal identity. The fluorescent profile of the mouse line will be further explored in Chapter 4.

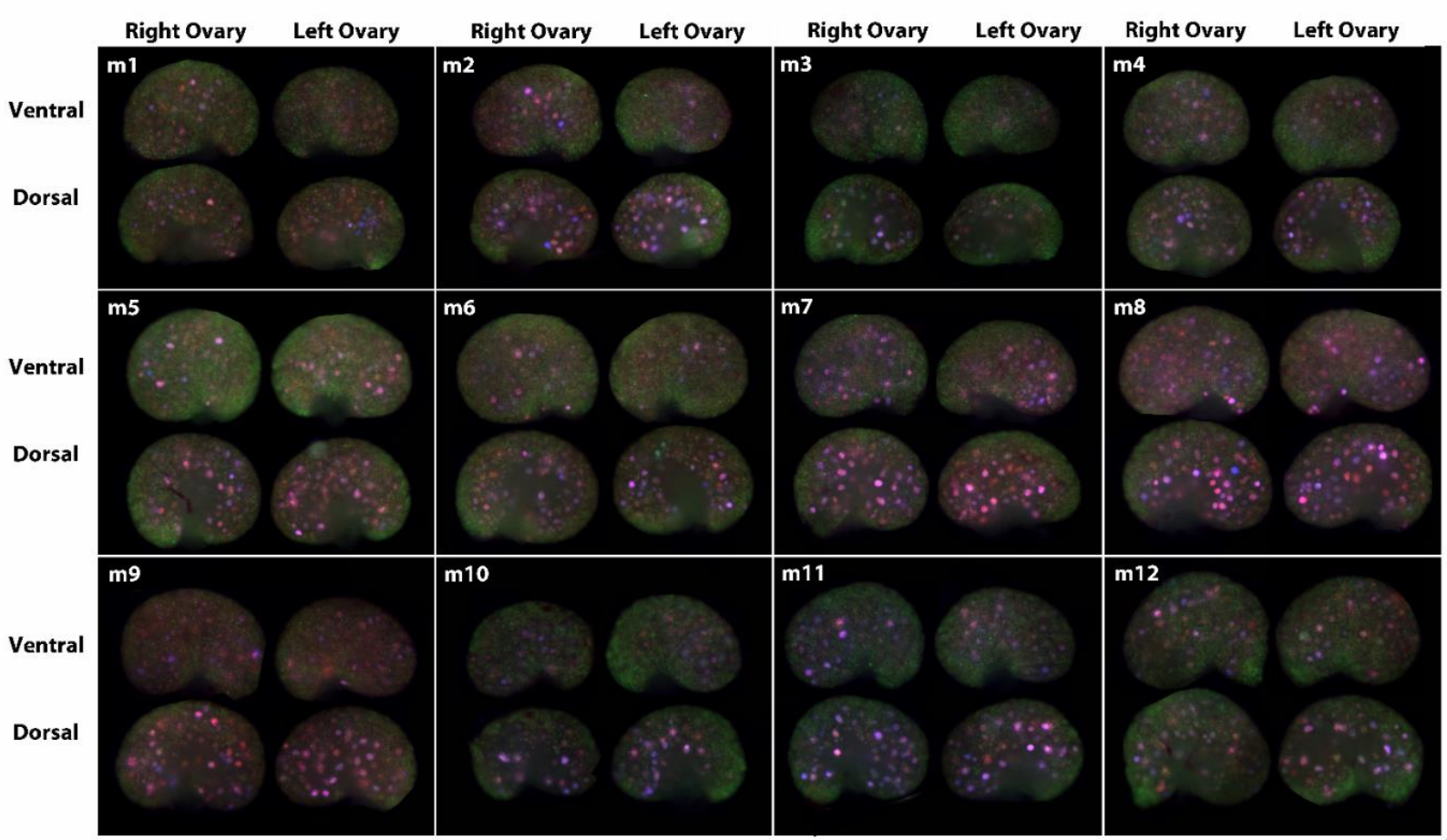

Figure 3.10 – Variability between animals of the same age. Ovaries from twelve different day-8-old animals are represented, including pups from 3 independent litters. Animals were weighted before imaging. No clear association between the size of the ovary and the weight of the mouse was observed. Slight differences between right and left ovaries could be observed, but differences between individuals were more accentuated.

Dramatic changes in the intensity of the fluorescent signal occurred during the neonatal period (Figure 3.11). Specifically, while EGFP levels in the surface of the ovary gradually decreased through day 8; mCherry and AmCyan levels increased and were associated with the appearance of growing follicles, requiring the use of different imaging settings for different ages.

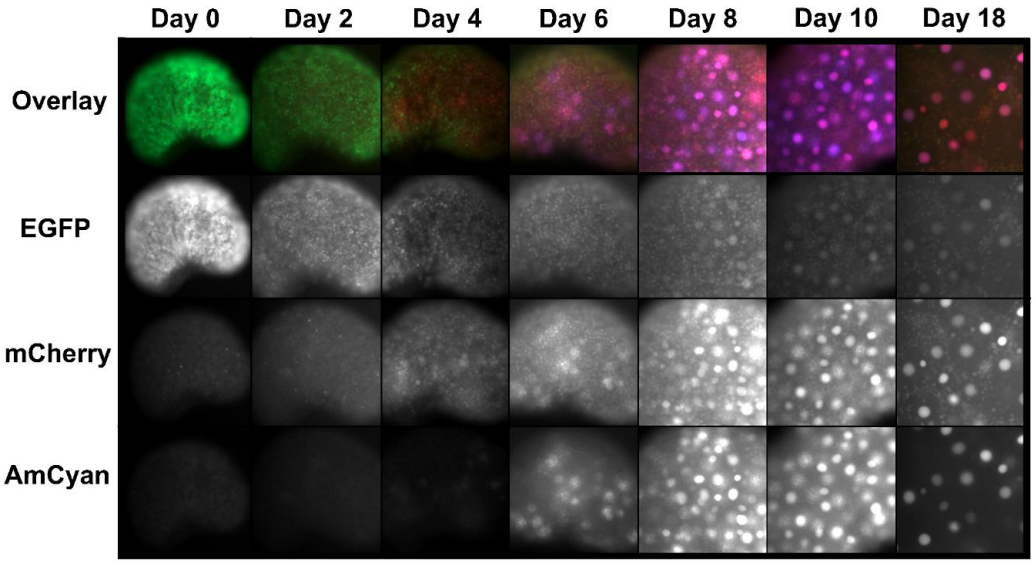

Figure 3.11 – Dramatic changes in fluorescent signal as mice advances in age. Images were acquired using the same imaging settings. Note the presence of saturated pixels in the images from Day 8 and 10, but not at day 18-old mouse ovaries.

During the first week of life, a gradual decrease in EGFP expression was observed in superficial oocytes, which was associated with a slight increase in germ cell size and in the level of mCherry. However, discrete ovarian areas contained oocytes still in cysts (or ovarian nests) expressing high levels of EGFP (Figure 3.12, top panels, inserts). To confirm that the change in EGFP expression was associated with ovarian follicle formation (nest breakdown), immunofluorescence assay with EGFP and VASA antibodies was performed and higher expression levels in oocytes within the germ cell clusters was observed (Figure 3.12, arrows). Together these data indicated that there is a decrease in VASA expression levels as individual primordial oocytes are formed.

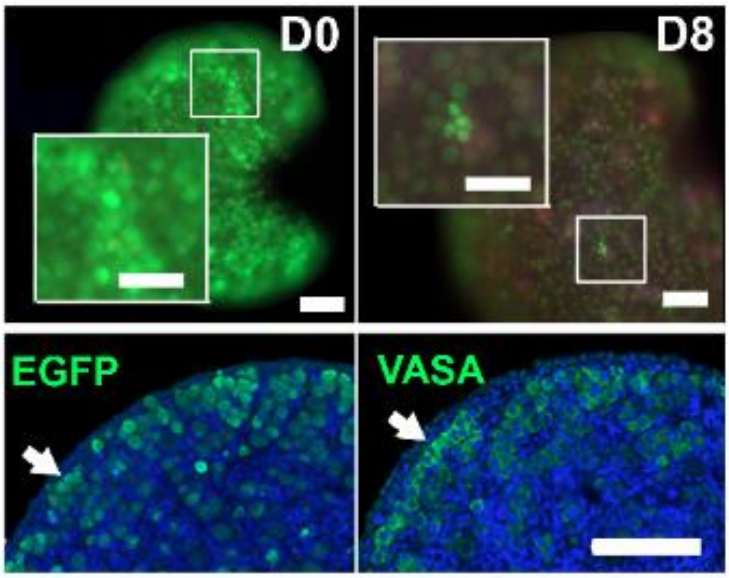

Figure 3.12 – Expression of EGFP at the surface of the ventral side before (day 0) and after nest breakdown (day 8) *(top panels)*. Immunofluorescence assay with EGFP and VASA antibodies at day 0 *(bottom panels)*. Areas with residual nest (insert and arrows). Same imaging settings used. Scale bars = 100 µm; scale bar of the insert on day 8 = 50 µm.

Morphologic features of the follicles, including the oocyte and follicular diameters have been commonly used to assess the stage of development of the germ cell [79, 81, 82], thus it was expected that the fluorescent profile of the oocyte would change in a predictable way according to its size. Therefore, oocyte isolation and quantification of the reporter protein was performed to determine if a certain range of fluorescence was associated with a specific follicular class. (Figure 3.13). Surprisingly, quantification of the reporter proteins revealed a high degree of heterogeneity of fluorescent signal on the same size range (Figure 3.14A) and follicular class (Figure 3.14B). In fact, heterogeneity of fluorescent signal was also observed in the intact ovary (Figure 3.15).

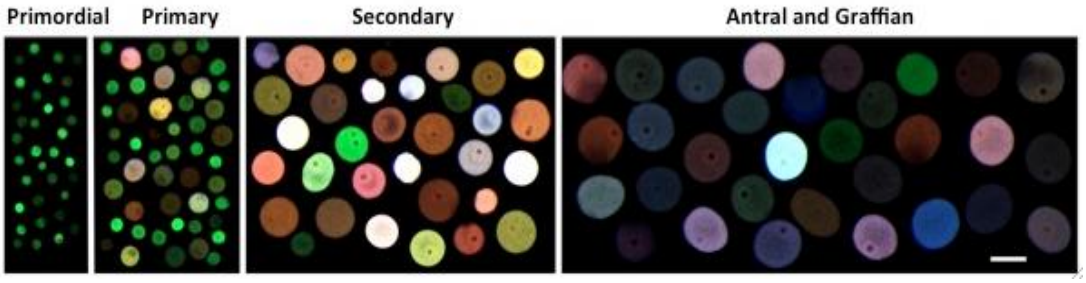

Figure 3.13 – Representative oocytes from different follicle classes imaged with confocal microscopy. Scale bar = 50 µm. Follicle class was determined based on the oocyte diameter: Primordial <15 µm; Primary 15-30 µm; Secondary 30-60 µm; Antral 60-70 µm; Graffian >70 µm. Oocytes isolated from day 3, 6, 8, 12, 17 and 22-old mice.

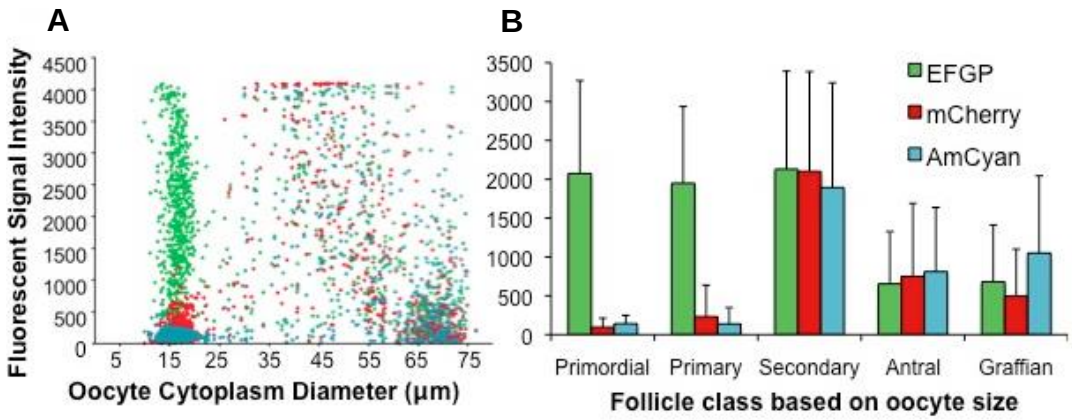

Figure 3.14 – Quantification of the fluorescent proteins shows signal variability on same size range (A) and follicle class (B). Despite the variability, statistic differences were found between all the groups present in graph B, with $p<0.001$. Error bars represent SD.

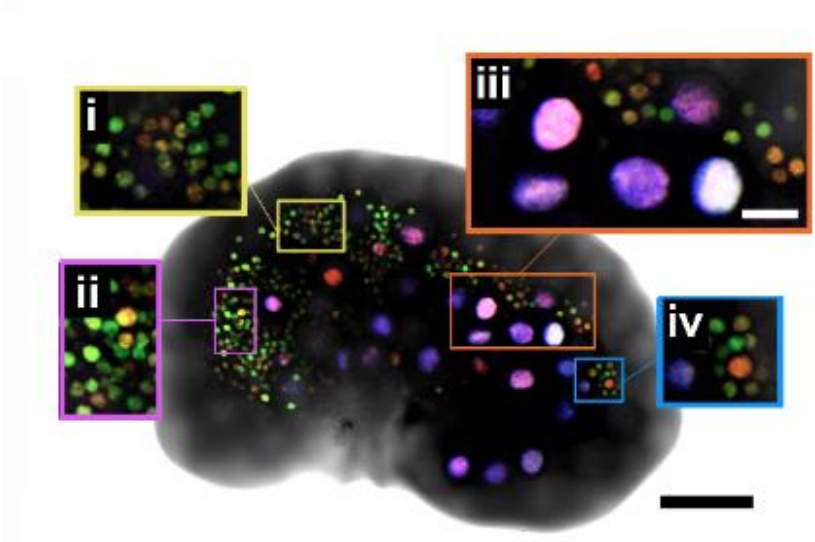

Figure 3.15 – Variability of fluorescent signal in an intact day 12 ovary. Primordial oocytes, i and ii; secondary oocytes, iii. A primary follicle oocyte surrounded by primordial oocytes is shown in iv. Scale bar = 200 µm; scale bar of the insert = 50 µm.

Despite the variability associated with the data, when oocytes were grouped by follicular class (based on their diameter), statistically significant differences between follicle classes could be recognized, suggesting that the fluorescent profile of the germ cell changed as the follicle develops (Figure 3.14). Primordial and primary follicles had lower levels of mCherry and AmCyan, increasing dramatically at secondary stage, and decreasing when the follicle reached antral stage. EGFP levels were high until the secondary stage and also decreased in antral follicles. However, the experimental design used on this experiment may lead to several interpretation

problems, including the assessment of the follicle stage based on the diameter of the oocyte instead of the number of layer of granulosa cells, and the fact that oocytes derived from different animals were combined to overcome the low yield associated with some of the isolation protocols. In addition, mice of different ages were used to collect oocytes from a specific follicle class, making it impossible to evaluate if the age of the animals could influence the intensity of the fluorescent signal. Thus, follicle isolation and quantification was done to further explore the value of the mouse line to predict follicle development and to determine if the age of the animal could explain some of the heterogeneity observed. Differences between follicular classes as a population were observed, despite the inter-individual and inter-follicle variability in the level of fluorescent protein, also observed in isolated follicles (Figure 3.16). Importantly, mCherry and Amcyan signals were higher in transitional and primary when compared with primordial follicles, suggesting that the signal of these fluorescent proteins could be used as a follicle activation marker. Moreover, we observed that the majority of the follicles with elevated mCherry and AmCyan signal (higher that 2000 gray pixels) had a size range of 50-150 µm, corresponding to primary and small secondary follicles (Figure 3.17). However, 62% of the follicles on

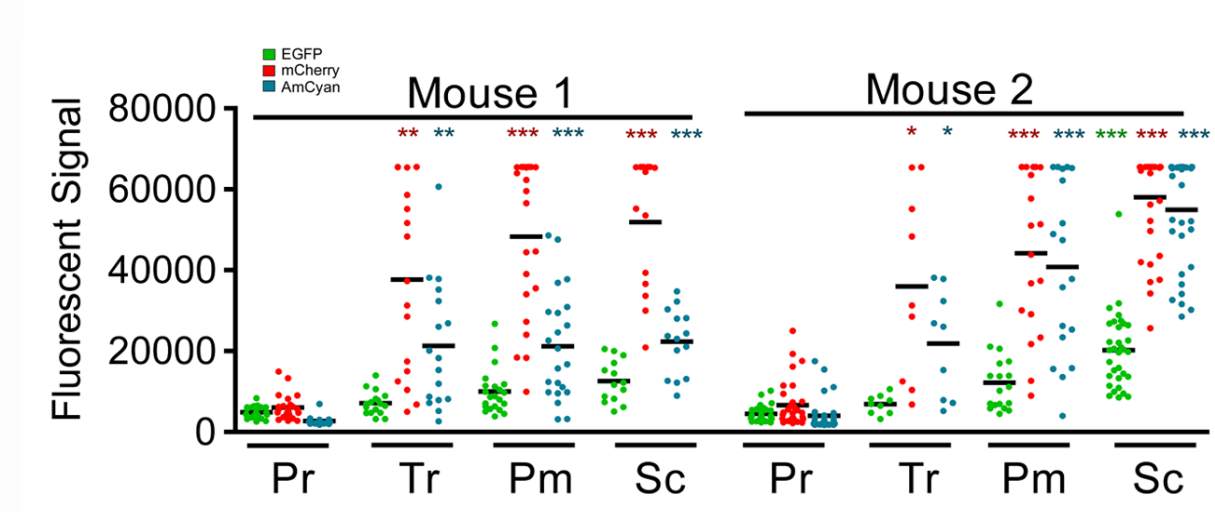

Figure 3.16 – Differences in fluorescent signal between follicular classes independently of the high heterogeneity. Mouse 1 and 2 are two 8-day-old mice from the same litter. Pr, primordial; Tr, transitional; Pm, primary; Sc, Secondary. * ($p<0.05$), ** ($p<0.01$) and *** ($p<0.001$).

this size range had reduced fluorescent signal (lower that 2000 gray pixels), revealing again high heterogeneity in the level of reporter protein between cells.

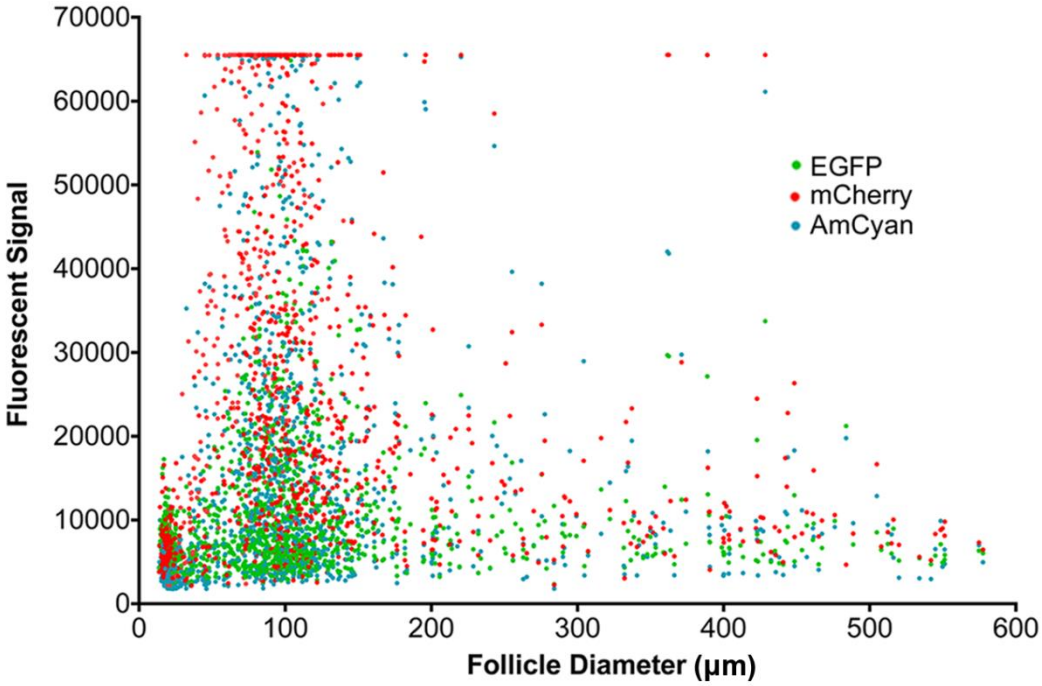

Figure 3.17 – Fluorescent profile of the triple transgenic line by follicle diameter. Whole follicular population isolated from 8, 18, 28 and 90-day-old mice.

Additionally, when follicles were analyzed by age, differences in fluorescence between follicles of the same class could be observed (Figure 3.18). While no differences were observed on primordial follicles; primary and secondary follicles from 8-day-old mouse had significantly higher levels of all reporter proteins when compared to follicles of the same classes in older animals. This data suggested that the first growing follicles had increased expression levels when compared to the follicles that grow in the consequent follicular waves. In accordance with this observation, antral follicles present in 18-day-old mice also had higher expression levels when compared with 28 and 90-day-old. Importantly, no differences in follicular size were observed between ages, except the secondary follicles from day 8, which were significantly smaller. Similar expression pattern was also observed in Fig 3.11 with lower expression level at 18-day-old mouse ovaries. Furthermore, the variability between follicles, as represented by the error bars, decreased as the mouse reaches

sexual maturity (day 28 and 90). Altogether, the expression profile of this transgenic line showed differences between follicular class and age; and revealed an unexpected but important heterogeneity in the fluorescent signal, which suggests an underlying activity or intrinsic stratification of function not previously appreciated.

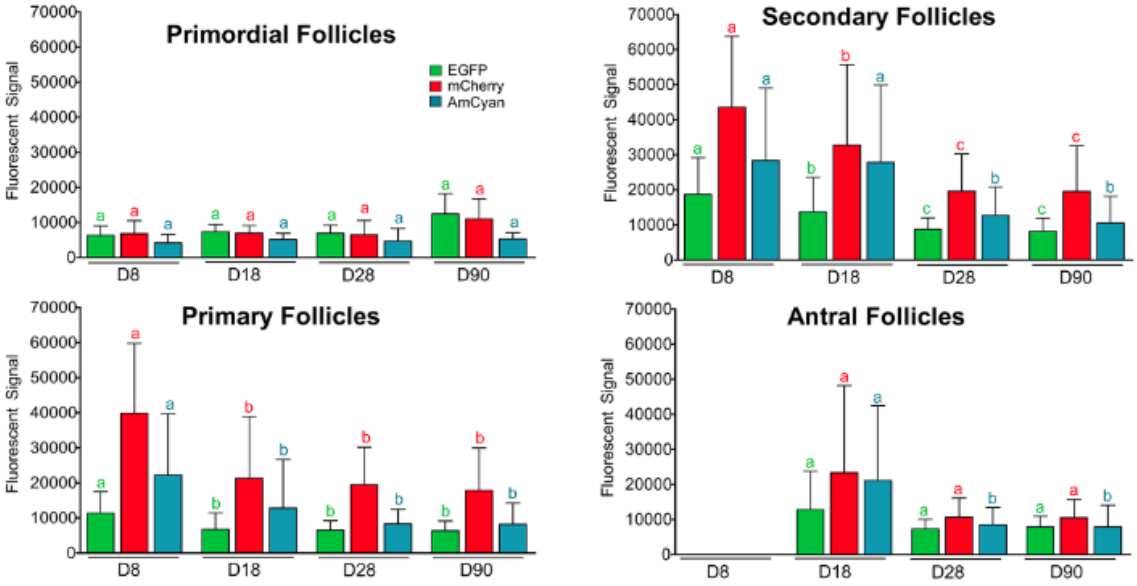

Figure 3.18 – Age differences between follicles from the same class. Error bars indicate SD. Same letter represents groups with no statistical differences. D8, D18, D28 and D90 represent the age of the animal in days.

The overall differences in signal between the isolated oocytes and isolated follicles are associated with the use of different imaging systems with distinct properties and settings. In particular, the lower EGFP signal is likely associated with the use of YFP cube to detect green fluorescent protein during follicle quantification. Another factor to take into consideration is the use of animals of younger age in the oocyte isolation (day 3 and 6), which may have an impact on the intensity of the fluorescent protein signal, as suggested by Figure 3.11, Figure 3.12 and Figure 3.18.

Finally, *in vitro* fertilization (IVF) was performed to explore if the fluorescent profile of the oocyte could be associated with its developmental potential. The first round of IVF was performed with 42-day-old female mice, resulting in 80% and 86% blastocyst rate for MII oocytes of high and low intensity of AmCyan, respectively. A

similar blastocyst rate was obtained with wild-type animals (82%). After analyzing these results it became clear that if a lower blastocyst rate was observed for any of the oocyte groups it would mean that the mice were subfertile, since at day 42 a 100% blastocyst rate can be obtain under ideal IVF conditions. Thus, for the next 3 round of IVF 21-day-old mice were used, assuming that at this younger age a lower yield of embryos progressing until blastocyst would be obtain. Interestingly, cumulative data from these rounds of IVF showed a similar rate of 2-cell embryos (Table 3.3) and blastocysts (Table 3.4), suggesting that the developmental potential of the MII oocyte could not be predicted by the intensity of the AmCyan signal.

Table 3.3 – Percentage of 2-cells embryos 24 hours after in vitro fertilization

Fluorescent Signal	2 cells	Total	% 2-cells
High	19	23	82.6
Medium	11	18	61.1
Low	33	39	84.6

Figure 3.4 – Percentage of blastocysts 120 hours after in vitro fertilization

Fluorescent Signal	Blastocyst	Morula	Degenerated	Total	% Blastocyst
High	13	0	6	19	68.4
Medium	7	1	3	11	63.6
Low	22	6	5	33	66.6

Importantly, the expression of EGFP and mCherry could also be observed in testis from transgenic males with a distinct pattern of expression according to the meiotic status (Figure 3.19). Only EGFP signal was detected in neonatal testis (day 0 to Day 16), while mCherry started to be expressed when germ cells undergo meiosis, as observed in day 21 and 10 weeks-old mouse testes, consistent with previous reports [100, 106]. ZP3-AmCyan driven expression is not expected in testis and it was not detected.

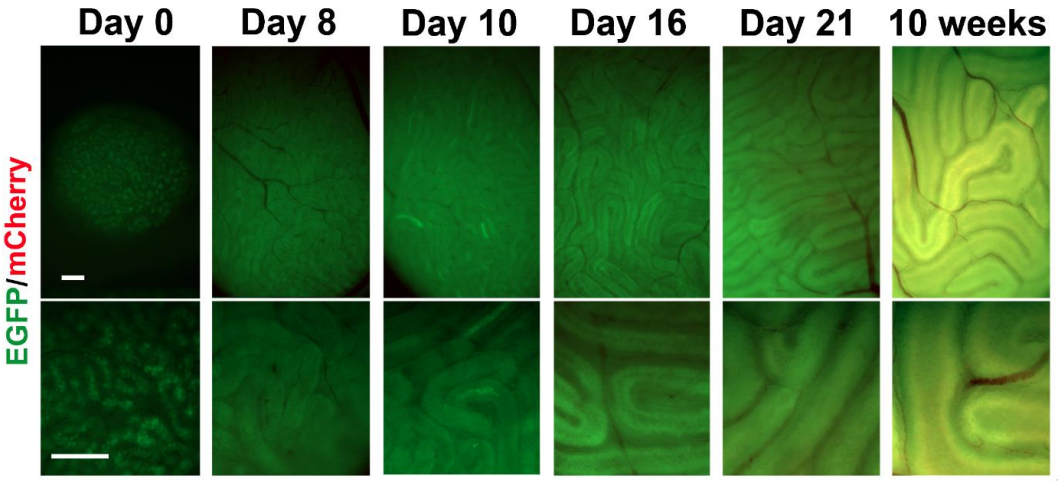

Figure 3.19 – Fluorescent protein expression in triple transgenic male testis from different age mice. Each age required specific imaging settings, since EGFP expression dramatically increased during the prepubertal period. Using the same imaging settings would result in saturation of all the pixels of the image.

3.3. Discussion

This study generated the first oocyte specific reporter linage in which three fluorescent proteins can be used to dynamically follow follicular development. As expected, these animals showed normal folliculogenesis and expressed the fluorescent proteins in a follicle-class dependent pattern, consistent with prior studies using the same promoter constructs. The complexity in terms of color combinations in individual follicles suggested that germ cells are regulated differently (momentarily and/or throughout development) and that each germ cell has a unique molecular signature, rather than being part of an amorphous homogeneous pool. In the mammalian ovary germ cell loss occurs at virtually at every stage of oocyte development, from primordial germ cell apoptosis to antral follicle atresia [26, 38, 42], resulting in selection of one or few ovulated oocytes, depending on the species. Although the amplitude of heterogeneity between oocytes was unexpected, this data is not completely surprising taking in account the complex mechanisms involved in follicle recruitment, communication and selection that occur normally in the female gonad. The variability in fluorescent signal may also be associated with a fast turnover of the reporter proteins, which needs to be explored in future studies. The heterogeneity associated with the data, challenges the use of the fluorescent signal to predict follicular class, although differences were observed when the whole follicle population was analyzed.

Furthermore, the quantification of individual follicles indicated that the first follicles recruited showed higher levels of fluorescent proteins when compared with follicles that started to grow around and after puberty – not expected based on the published literature for the promoters. However, follicles growing during the first wave of activation were reported to be morphologic and dynamically different, reaching antral stage faster [107, 108]; which is consistent with the elevated level of fluorescent protein observed. Interestingly, differences between the first and

consecutive waves of spermatogenesis have been also reported in mouse testis [109]. As follicles expanded and reached their terminal size, a decrease in intensity of fluorescent signal was observed, possibly explained by an increase in germ cell volume and/or a decrease in expression level due to transition to transcriptionally inactive state [110]. Additionally, the fluorescent profile of the oocytes changed with the developmental stage of the germ cells revealing new data regarding the region of first follicle activation and the change in expression of VASA before and after follicle formation. Although variability in fluorescent protein was observed between antral stage oocytes, the IVF study showed that their developmental potential is equivalent, with bright and dim oocytes having a similar ability to generate blastocysts. These data indicated that the differences in intensity of signal at this oocyte stage might reflect their developmental past, rather that differences in quality of the germ cell. However, only AmCyan signal was taking in account during the IVF study, which might not reflect the quality prediction potential of the other two fluorescent proteins. Further studies are required to prove that the heterogeneity associated with the fluorescent profile is correlated with differences in individual follicle function. This validation is very important taking in account that the integration site and inter-influence of the transgenes is unknown.

Altogether, the triple transgenic mouse line represents an important tool for expanding the basic understanding of the mechanisms controlling follicle activation, oocyte quality and ovarian developmental dynamics. Similar utility may be found in the male offspring.

CHAPTER 4

Ovarian Geography and Follicle Activation

4.1. Introduction

Normal ovarian function throughout the mammalian reproductive lifespan requires a tight control between germ cell arrest, differentiation and loss at the time of gonadal development and in each reproductive cycle. The size of the ovarian germ cell pool changes during development, achieving its maximum as the primordial germ cells (PGCs) colonize the gonad and undergo mitotic divisions [41, 61]. In mouse, the female gonad begins meiosis around 13 dpc, which occurs in an anterior to posterior wave driven by retinoic acid, while male gonad only undergo meiosis after birth [17-20]. Female germ cells arrest at prophase I included into cell clusters connected by intercellular bridges. These germ cell 'cysts' undergo a process of nest breakdown resulting in individual primordial follicle formation due to invasion of pregranulosa cells or germ cell loss [16]. In each cycle a small number of primordial follicles are activated to grow and under hormonal control, release a matured oocyte. Since follicle activation is irreversible, and the starting pool of follicles is finite, the size of the ovarian reserve is gradually reduced defining the female reproductive lifespan [41, 61].

The mechanism by which a particular follicle is selected to growth while others remain dormant is still not completely understood. Genetically modified animals have been extremely valuable to identify molecules and signaling pathways involved in global primordial follicle activation and survival (for reviews see [38, 43]) however the trigger for individual follicle activation at different times is still unknown. The 'production line' hypothesis is a popular proposition to explain the order of activation. This hypothesis, originally proposed to justify the high incidence of aneuploidy in reproductively aged females, suggests that the first oogonia to undergo meiotic arrest are the first to become activated after puberty, implying that the order of follicle activation is established during embryonic development [56]. However, this hypothesis has remained controversial, with evidence in favor [111-113] and against

[54, 114-117]. In support of the ‘production line’ hypothesis, follicle formation progresses gradually from the medulla to the cortex, with the germ cells closest to the medulla becoming the first formed and activated follicles [14, 118, 119]. It has been accepted that the first growing follicles, consisting on the first wave of follicle activation, reach the antral stage before puberty in the absence of gonadotropin regulation and therefore are lost by atresia [120]. However, a recent study showed that these first wave follicles not only induce the onset of puberty but are also ovulated, growing faster than follicles activated in the adult ovary [108]. On the other hand, pregranulosa cells rise from the surface epithelium in two waves; an initial fetal wave integrated into medullary follicles, which initiate growth shortly after birth, and a neonatal wave that surrounds cortical follicles, resulting in differences between follicles located in different regions of the ovary. Furthermore, at the time of individual follicle formation granulosa cells undergo mitotic arrest, which might impact the rate of follicle activation [112, 121]. As described above, major differences have been identified in germ and somatic cell dynamics between follicles from the first and consecutive waves of activation, however no studies have analyzed and integrated how the first wave of activation is established and its importance in the selective recruitment of primordial follicles.

4.2. Results

The initial characterization of the triple transgenic mouse revealed that follicle activation in the neonatal mouse ovary was restricted to a specific region of the gonad (Figure 3.8 arrow). Embryonic ovaries from transgenic mice were collected to study if the localization of the first wave of activation was related with the onset of meiosis, well-established to occur in an anterior to posterior wave [17-20]. The anatomic orientation of the ovary in relation to the body axis was studied, since the female gonad during the neonatal period was located almost perpendicularly to the anterior-posterior axis (Figure 4.1).

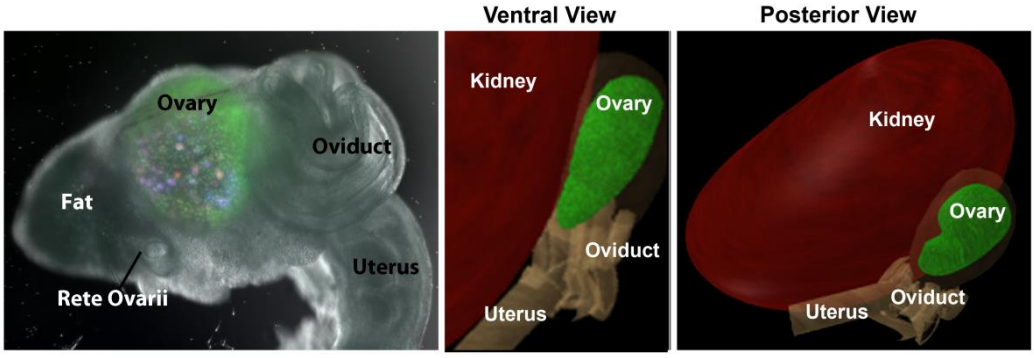

Figure 4.1 – Anatomic orientation of the ovary during the neonatal period. Left image shows a 6-day-old transgenic mouse ovary imaged inside of the bursa. First growing follicles appeared in the ovarian region closer to the rete ovarii and never on the ovarian region facing the oviduct. The 3D models represent two different views of the neonatal ovary anatomic position of the in relation to the body axis.

While imaging the ovaries inside of the animal in their native orientation, significant changes in the anatomical orientation of the gonad in relation to the body axis were observed, possibly caused by the C-shape curvature of the Müllerian duct and massive growth of the kidney observed during the embryonic period (Figure 4.2, and Figure 4.3). As observed in Figure 3.8, EGFP was the only fluorescent protein detected on the germ cells during this period (Figure 4.2), revealing key anatomical and cellular events during early development, including changes in gonadal shape and establishment of germ cell clusters organized in cord-like structures visible at 14.5 dpc (Figure 4.2, yellow arrow). By 16.5 dpc the specification on of a medullar

region was prominent in the dorsal side of the ovary, as evidenced by the absence of germ cells in this region (Figure 4.2, blue arrow). Despite the significant changes in the anatomical orientation of the gonad in relation to the body axis, the terms ventral and dorsal (in relation to the embryonic position) were used to identify different regions in the postnatal ovary (Figure 4.2, blue arrow)

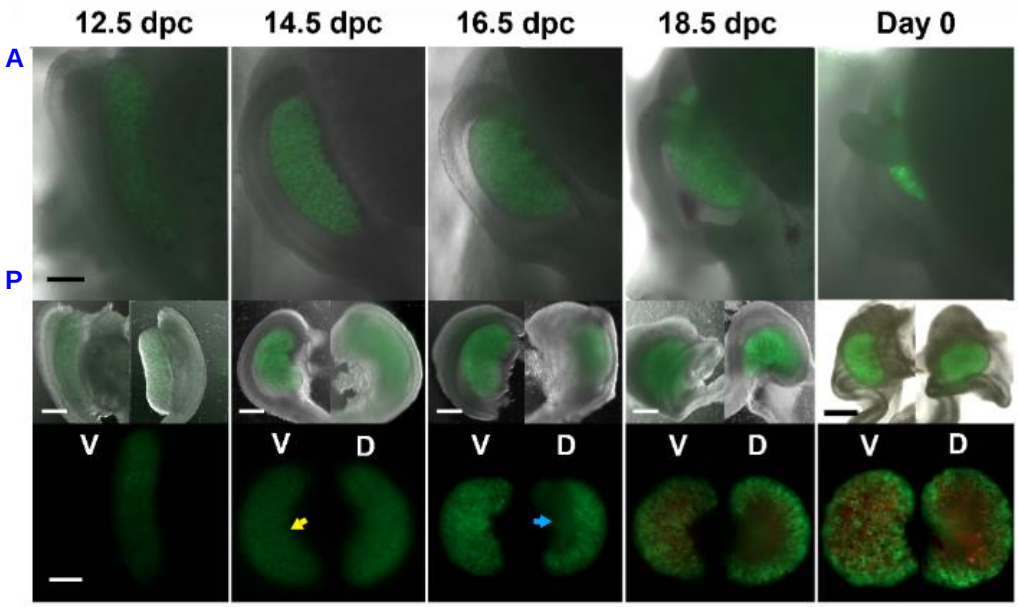

Figure 4.2 – Expression of fluorescent protein during the embryonic period and at birth (Day 0). Ovaries were imaged inside of the animal (top panel) and after rotation in the dish (middle panel). The expression of EGFP allowed observation of differences in the distribution of germ cells between the dorsal and ventral regions of the ovary. A – anterior, P – posterior, V – ventral, D – dorsal. More information about gonad orientation can be found in Figure 2.5-2.6.

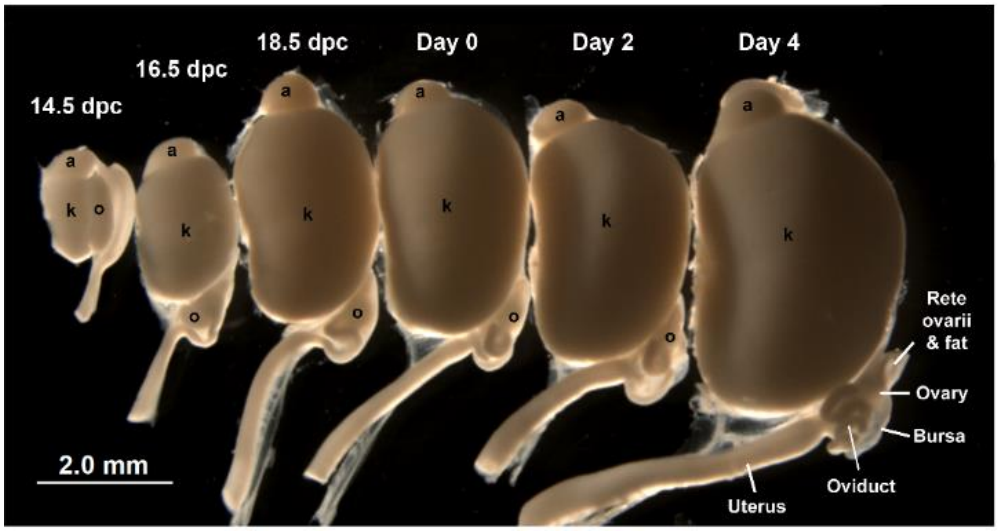

Figure 4.3 – Anatomic orientation of the ovary in relation to the body axis during embryonic and neonatal period (ventral view).

This anatomic study allowed concluding that the first activated follicles appear in the anterior-dorsal region of the mouse ovary (Figure 4.4).

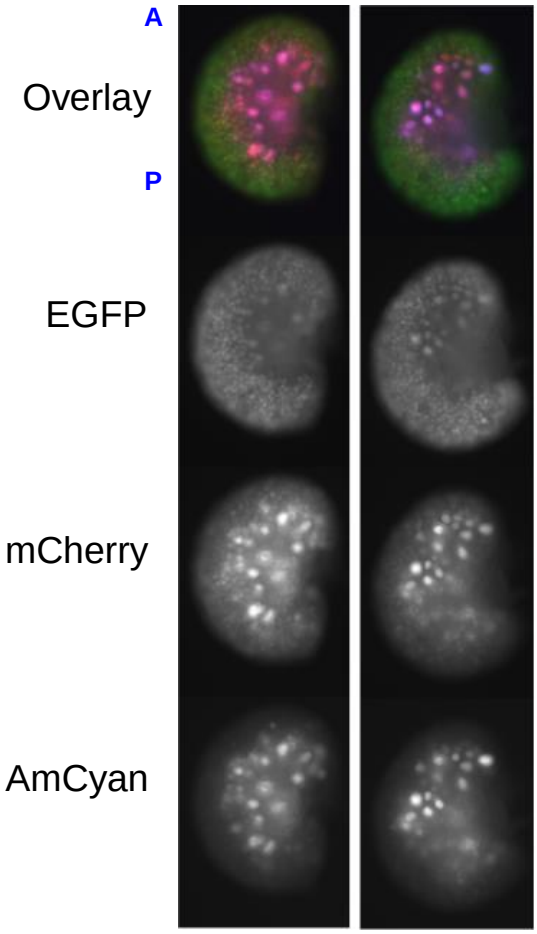

Figure 4.4 – First growing follicles appear in the anterior-dorsal area of the mouse ovary. Images represent the dorsal region of two independent ovaries. Although variability in the extent of the area containing activated follicles was observed between mice, the anterior region of the ovary always contained a higher percentage of growing follicles. Growing follicles were easily identified by expression of AmCyan (driven by *Zp3* promoter). The fluorescent signal is represented in separated channels. A-anterior, P-posterior

To study the relationship between the onset of meiosis, follicle formation and activation, taking into account ovarian anatomy, the expression and localization of OCT4, STRA8 and VASA were analyzed. These markers allowed the distinction of germ cells prior, during or independently of the meiotic entry, respectively [17, 99, 100]. As expected, at 12.5 dpc there was no evidence of meiotic progression, as OCT4 was uniformly distributed and STRA8 expression was absent (Figure 4.5). However, by 13.5 dpc an anterior to posterior gradient could be detected in the ventral region, with STRA8 expression in the anterior region of the ovary (Figure 4.5, arrow). Surprisingly, the dorsal region of the same 13.5 dpc ovary showed a pattern of expression of OCT4 and STRA8 similar to 12.5 dpc, suggesting that this ovarian region had a later onset of meiosis. In accordance with this observation, at 14.5 dpc the dorsal-posterior region contained a higher density of STRA8 positive germ cells, suggesting that also in this region the onset of meiosis followed an anterior to posterior gradient (Figure 4.5, arrow head).

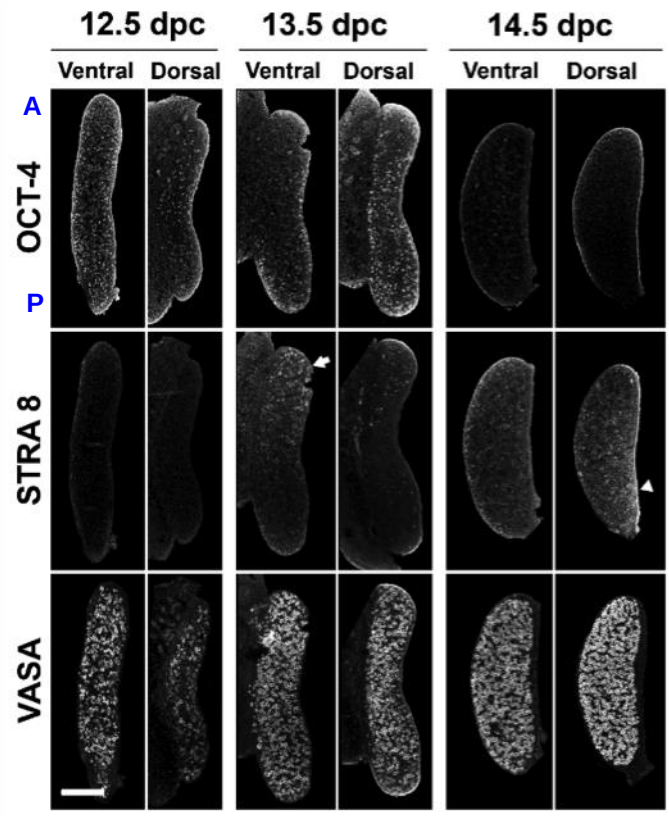

Figure 4.5 – Timing of meiosis entry differed between ventral and dorsal regions of the mouse ovary. Arrow indicates early onset of meiosis in the anterior-ventral region at 13.5 dpc. Arrowhead highlights enrichment of Stra8 positive cells in the posterior-dorsal region at 14.5 dpc. Scale bar = 200 µm. A- anterior, P- posterior.

Slight variation between meiosis extension into the dorsal region could be observed in different animals and litters (Appendix V). Altogether, this data shows for the first time that the onset of meiosis in the mouse ovary not only occurs differentially in the anterior-posterior regions of the ovary, but also in the dorsal-ventral regions.

In this study the first wave of follicle activation occurred in the dorsal region of the ovary, contrasting with the early meiosis entry occurring ventrally. To understand and conciliate these observations the localization of the first individual follicles formation was analyzed. In mouse, follicle formation through nest breakdown is well characterized in the neonatal period, however at birth individual follicles are already present in the medulla [39]. Thus, ovaries during late embryonic development were analyzed to explore the anatomical location of the first follicles formed, using VASA and Foxl2 as germ cell and granulosa cell lineage markers [99, 121], respectively. Consistent with Figure 4.2, the specification of cortex and medulla could be seen at 16.5 dpc with absence of germ cells (labeled with VASA) from the central area of the dorsal ovarian region (Figure 4.6A, arrow). Interestingly, even before the specification of the medulla, a higher density of cells expressing Foxl2 could be found in the dorsal region at 14.5 dpc (Figure 4.6A arrow head). Foxl2-labeled cells were not restricted

to ovarian medulla but also around the germ cells clusters in the ventral region (Figure 4.6, iii and iv) and by 18.5 dpc Foxl2-positive cells surrounded the first follicles formed in the dorsal region (Figure 4.6B iv). Furthermore, the basal lamina

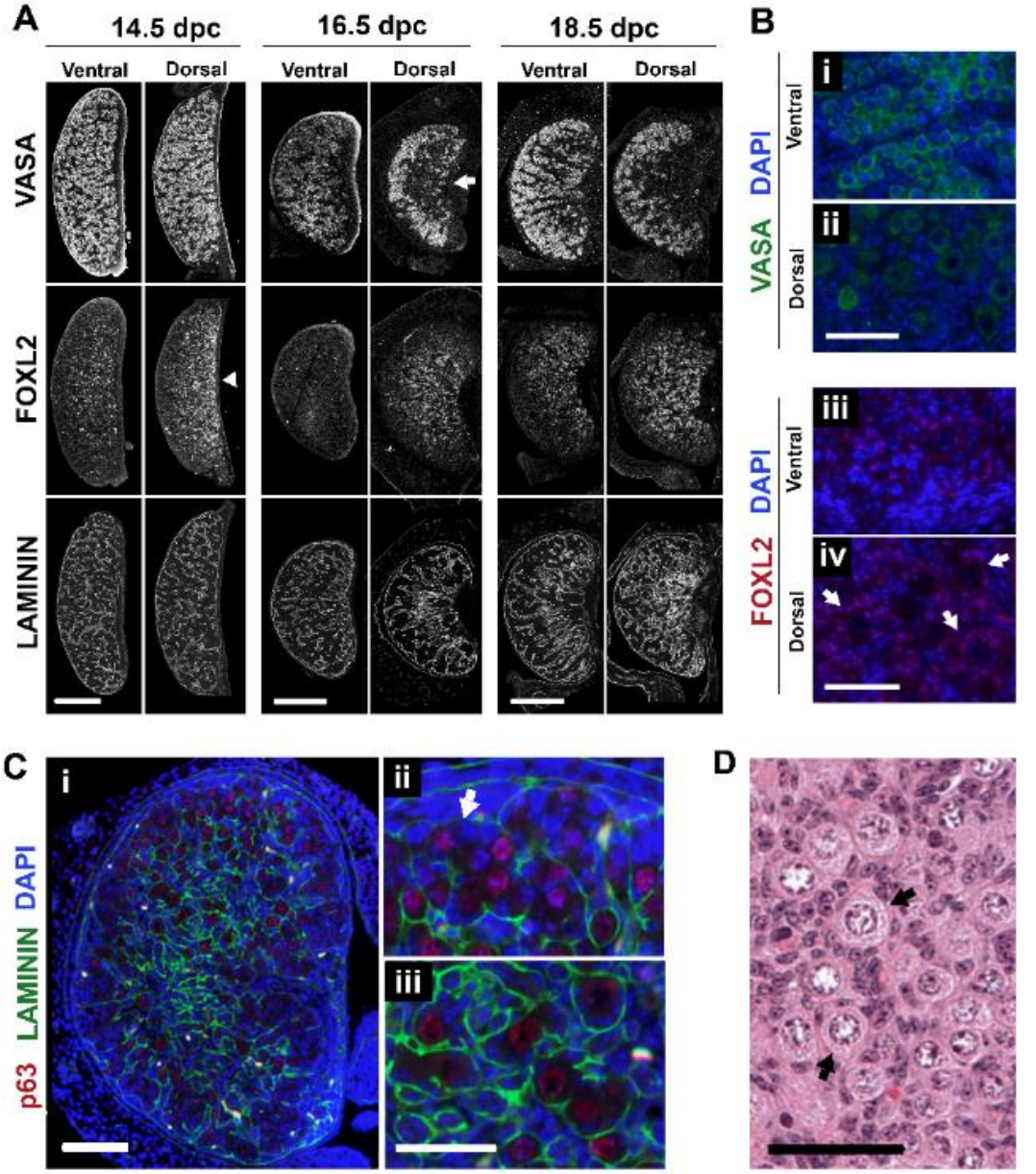

Figure 4.6 – Timing of individual follicle formation differed between ventral and dorsal regions of the mouse ovary. ***(A)*** Differences between dorsal and ventral ovarian regions identified by VASA (germ cell), Foxl2 (pregranulosa) and Laminin (basal lamina) immunofluorescence assay. Scale bars = 200 µm ***(B)*** Individual follicle formation at 18.5 dpc was restricted to the dorsal region of the ovary, visualized using VASA (i-ii) and Foxl2 antibody (iii-iv). ***(C)*** Spatial differences in development between the center and the periphery of the dorsal region at 18.5 dpc (i). Detail of the germ cell clusters at the periphery (ii) and individual follicles in the center (iii). Scale bar i = 100 µm; Scale bar ii and iii = 50 µm. Red, TAp63 (oocyte nucleus); green, laminin; blue, DNA. ***(D)*** Histology of the first individual follicles formed at 18.5 dpc. Scale bar = 50 µm.

protein Laminin, which delimitates germ cell cords or individual follicles [122, 123], also showed that follicle formation was restricted to the dorsal region at 18.5 dpc (Figure 4.6A and 4.6C).

Even within the dorsal region of the ovary, geographic differences in development could be identified between the center and the periphery of the gonad. Specifically, while germ cells towards the surface remained enclosed in clusters (Figure 4.6C ii, arrow), germ cells in the medulla were forming individual follicles, especially on the anterior region (Figure 4.6C iii). Interestingly, squamous granulosa cells, characteristic of primordial follicles formed postnatally, were rarely observed on the follicles that formed at 18.5 dpc (Figure 4.6D), as reported in rat ovary [107]. Altogether, we observed that the first individual follicles formed were located in the anterior-dorsal region of the 18.5 dpc ovary, the same region where first growing follicles were detected in the neonatal ovary (identified based on their fluorescent profile), indicating that the distribution of follicles in the prepubertal ovary is a consequence of embryonic development. To determine if the distinct timing of embryonic follicle formation translated into postnatal spatial differences in follicle growth, confocal microscopy was used to monitor the different follicle populations present in the surface of dorsal and ventral regions of the same ovary. Consistent with the observations at 18.5 dpc, growing follicles were observed on the dorsal region, predominantly, but not solely, in the anterior-dorsal region highlighted by the boxes (Figure 4.7A). In contrast, a higher number of primordial oocytes were visible on the ventral region (Figure 4.7A). Interestingly, many primordial follicles on the ovarian surface remain organized in cord-like structures even after individualization (Figure 4.7A, arrows). During the prepubertal period the gonad increases dramatically in size (Figure 4.7A and Figure 3.8) and, as a consequence of larger follicles growing underneath, a rearrangement of primordial follicles in the surface was observed, evidenced by the decreased density of primordial oocytes above secondary and antral follicles (Figure 4.67, 3.8 and 3.9) and an global increase of the

distance between primordial follicles (Figure 4.7A, i-iii). Despite the ovarian plasticity observed during this period, developmental differences between dorsal and ventral regions were always clear. Since confocal imaging restricted the detection of the transgenes to the ovarian surface, immunofluorescence assay with VASA antibody was performed to evaluate follicle organization at different ovarian depths. Most primordial follicles were localized in the ventral region of the ovarian cortex and were completely absent from the medulla, which only contained growing follicles (Figure 4.7B). Importantly, the first primary and secondary follicles were present in the interface between cortex and medulla, while some germ cells on the surface of the ovary were still organized in nests (Figure 4.7B, I and ii), reinforcing the concept that the initiation of follicle growth is not stochastic and that the trigger for follicle activation is related with geographic location in the ovary. Interestingly, as the mice advance in age (day 0 to 6) the number of activated follicles increased progressively, causing a gradual expansion of the area containing growing follicles (Figure 4.7C). This gradual recruitment suggested that follicular growth within the first wave of activation was not synchronized, as evidenced by differences in follicle size and the variable expression levels of HA (tagged to AmCyan, driven by ZP3). The existence of a gradient of activation from the medullar anterior-dorsal region into the periphery of the gonad raises the question of which follicles should be included as first wave and suggests that the concept needs to be specified. In summary, distinct follicle formation patterns between dorsal and ventral regions of the embryonic ovary resulted in spatial differences in the ability to initiate follicle growth throughout the prepubertal period.

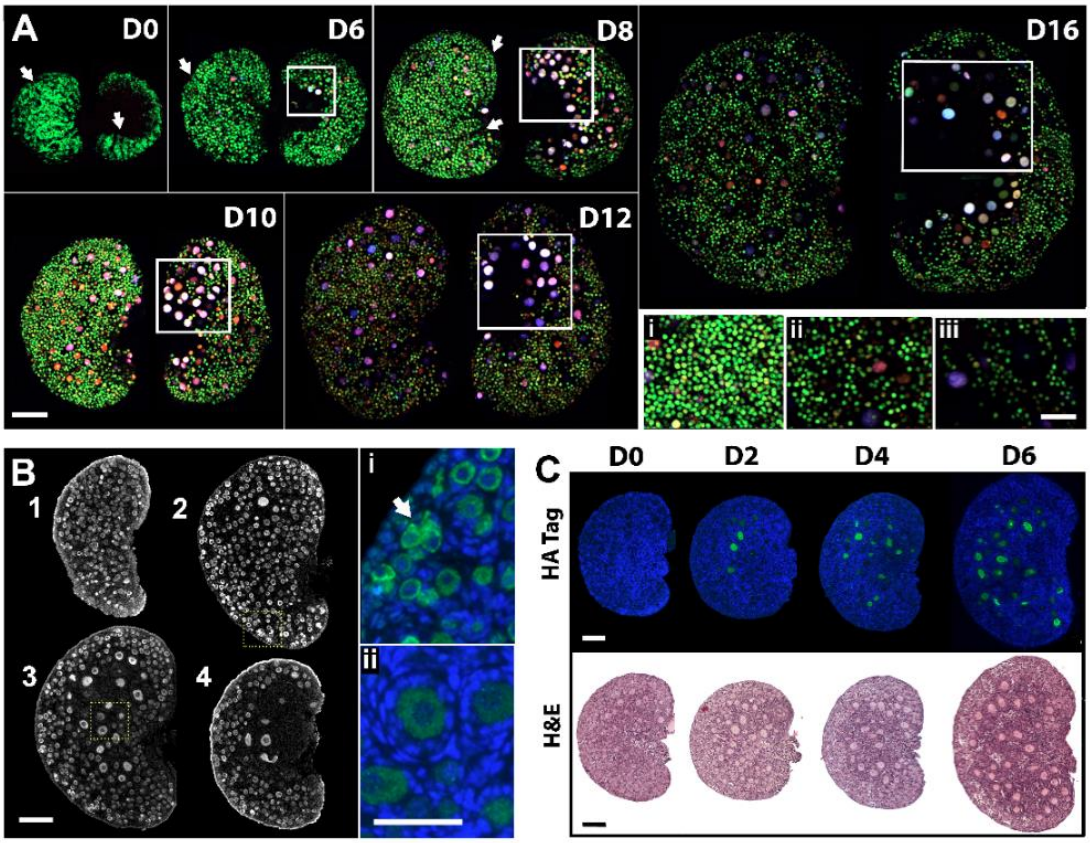

Figure 4.7 – Differential follicle development in ventral and dorsal ovarian regions is conserved throughout the prepubertal period. ***(A)*** Maximum projection of confocal z-stack images evidenced different oocyte populations on the surface of the two ovarian regions. Box highlights region with elevated number of growing follicles (anterior-dorsal). Arrows exemplify cord-like structures. Same imaging settings were used, except day 0, which required lower laser power for EGFP detection. *(i-iii)* Distance between primordial oocytes increased globally as the mouse advanced in age (ventral region). i, day 8; ii, day 16; iii, day 30. Scale bar ~200 µm. Scale bar of the insert ~100 µm. Scale bars are approximate because images are maximum projections ***(B)*** Geographic differences in follicle development in the same ovary. Immunofluorescence assay with VASA antibody in serial sections 45 µm apart. 1, ventral; 4, dorsal. Scale bar = 100 µm. Highlighted areas are expanded on i and ii, scale bar = 50 µm. Green, VASA; blue, DNA. Arrow shows region where ovarian nest remains. ***(C)*** Gradual expansion of the ovarian region containing growing follicles. Green, HA tag; blue, DNA; H&E, hematoxylin and eosin staining. Scale bars = 100 µm.

4.3. Discussion

Since differences in signal existed between primordial and growing follicles, the fluorescent profile of the oocyte could be used to visualize the first wave of activation, located in the anterior-dorsal region of the ovary. The localization of the first activated follicles in the anterior region of the mouse ovary, led to explore if it was related with the onset of meiosis, as described by the 'production line' hypothesis [56]. Thus, this study showed for the first time dorsal-ventral differences in the onset of meiosis with a late entry on the dorsal side of the ovary. Although this anatomical analysis did not account for germ cell rearrangements, it suggested that the timing of meiotic entry might not be the main factor to induce follicle formation, since the first formed and activated follicles were present in the dorsal region. Therefore, this study does not support the 'production line' hypothesis, although the influence of meiosis onset cannot be completely excluded. Interestingly, while germ cell meiosis in the mouse ovary occurs in an anterior to posterior wave, in the human ovary it starts in the medulla and spreads radially to the cortex [124, 125]. Importantly, despite the spatial differences in meiosis entry between species, the first individual follicles appear into the cortico-medullar interface in both mouse and human ovaries. This suggests a common mechanism determined by geographic clues that might include blood supply, specific somatic cell microenvironment or influence of the rete ovarii. The rete ovarii has been implicated in both meiosis and follicle formation, and although it is a remnant structure in the adult mouse ovary, at birth its network of cords and tubules occupies most of the central ovarian tissue [23, 126] In early studies this structure was appointed as the source of granulosa cells and/or secreted paracrine signals. However, it was shown recently that pregranulosa cells arise from the surface epithelium in two distinct waves, one before sexual differentiation contributing to the medullary located follicles, and other postnatally recruited contributing to primordial follicle formation in the neonatal period [121, 127].

Granulosa cells became mitotically arrested as they migrate and surround individual follicles, restarting proliferation around birth in medullary located follicles or remaining arrested for months or years in cortically located follicles. Thus, the origin of the granulosa cells may contribute to maintain primordial oocyte quiescence throughout reproductive life [112, 121]. These temporal differences in granulosa cell specifications suggest that follicle formation might differ during embryonic and postnatal period. Interestingly, squamous granulosa cells, an important feature of dormant primordial follicles, were rarely observed in the first individual follicles formed by 18.5 dpc, suggesting an immediate recruitment after formation or a different mechanism of primordial follicle individualization. Similar characteristics were found in the first individual follicles of the rat ovary [107]. Further studies are required to clarify the molecular mechanisms regulating follicle formation in the embryonic gonad and to explain why it occurs mainly in the anterior-dorsal region of the ovary.

These results suggest that the differentiation of cortical and medullar regions, rather than the onset of meiosis, might have a greater impact in defining the region where the first follicular activation wave occurs. The ability of the embryonic ovary to differentiate into cortex-medulla has been challenged by in vitro culture [128] and re-aggregation experiments [15], resulting in impaired development of early embryonic gonads (11 to 13 dpc). Interestingly, global recruitment to growth was associated with lack of specification into cortex and medulla in cultured ovaries [128]. On the other hand, it has been suggested that the specification in cortex and medulla occurs by accumulation of germ cells in the cortex, while the medullar oocytes die by apoptosis [6]. However a recent study suggested that the gradual invasion of mesonephros-derived somatic cells into the ovary is the driving force to form the medulla, ovarian cords and individual follicles [129], reinforcing the idea that the somatic cell microenvironment may be crucial for normal ovarian organogenesis. The

molecular mechanisms regulating the specification of the cortex and medulla are largely unexplored and should be investigated in future studies.

The gradual and unsynchronized expansion of the region containing growing follicles during the neonatal period, suggests that recruitment of the immediately adjacent follicles may occur as a consequence of differences in timing of follicle formation or influence of signals received during the embryonic period or growing follicles in close proximity. The follicles from the first wave of activation will then have a major impact in controlling the consecutive rounds of follicle activation through establishment of the hypothalamus-pituitay-ovary axis, responsible for reproductive cyclicity, and a hierarchy of activation by impacting the growth of neighbor follicles. The influence of substances produced by growing follicles on primordial oocyte dormancy has been proposed, including AMH (Anti-Müllerian Hormone) [50]. The spatial localization of the follicles in the ovary was used to conclude that primordial oocytes themselves could also produce an inhibitory substance [130], and although the hypothesis might be correct, the developmental changes of the ovary described in our study were not taken in account.

Altogether, this study indicates that the control of selective follicle activation is likely achieved by an asynchronous germ cell development in different regions of the ovary, allowing some follicles to initiate growth while others remain quiescent. Continuing to explore how the embryonic organization of the gonad and the inter-communication between follicles affects ovarian functionality will be essential to understand how the balance between quiescence, growth and germ cell loss is established and maintained in the ovary, which has implications for reproductive aging and premature ovarian failure in humans.

CHAPTER 5

Summary and Future Directions

In female mammals, a small number of ovarian primordial follicles are activated to grow in each cycle and produce mature oocytes capable of being fertilized. The balance between recruitment and dormancy is crucial to keep ovarian function throughout reproductive life; therefore, the molecular mechanisms controlling germ cell survival and loss at the time of primordial follicle formation and activation are vital to understand normal ovarian function. Thus, the propose of this thesis was to develop a new mouse line as a dynamic tool to study follicle activation and development *in vivo* and *in vitro*. In this mouse *Vasa*, *Gdf-9* and *Zp3* promoters drive distinct temporal expression of three reporter proteins EGFP, mCherry and AmCyan. The fluorescent profile of the oocytes from this mouse model revealed high heterogeneity (Figure 3.13-3.18), suggesting stratification of function, and the model was particularly important to determine that first wave of primordial follicle recruitment occurs in a conserved area of the mouse ovary, the anterior-dorsal region (Figure 3.8 and Figure 4.4). The study of the anatomical relationship between meiosis, follicle formation and activation, using molecular markers OCT4, STRA8, VASA, Foxl2 and Laminin, showed that the specification of cortex and medulla, rather than the onset of meiosis, impacts where the first follicular activation occurs, since the appearance of the first individual follicles always occurred on the interface between cortex and medulla (Figure 4.5-4.7). These new data do not support the 'production line' hypothesis, which pointed to an early entry in meiosis as the reason for initiation of follicular growth in the neonatal period. This study demonstrated that follicle formation and activation follow a predictable geographic pattern which reflects ovarian functionality throughout the prepubertal period and suggesting that the embryonic period represents a critical window to regulate the first wave of follicle activation. The asynchronous germ cell development in different regions of the ovary results in distinct ability to initiate growth and these first wave follicles can then induce the onset of puberty and potentially establish a hierarchy of activation to avoid a global follicular recruitment and early menopause (Figure 5.1).

Aditionally the gradual recruitment of the follicles from the anterior-dorsal region into the periphery suggests that follicle activation in the neonatal period occurs gradually from the medulla into the cortex rather than in a synchronized wave (Figure 4.7C). These data raises the question of which follicles should be included in the first wave of follicle activation and suggests that the concept needs to be specified. If this gradual follicle recruitment also results from differences in timing of follicles individualization or from the presence of a signals specifically located in this ovarian region is to be determined in future studies. Another possible explanation is that first growing follicles can influence the recruitment of primordial follicles in the proximity until larger follicles are present in the ovary. This idea is supported by the accelerated primordial follicle activation that occurs in advanced age, where a smaller number of antral follicles is present in each cycle [61]. Aditionally, the *in vitro* culture of several small follicles in groups has been shown to be beneficial to improve follicle survival and growth [131]. The data included on this thesis indicates that follicle activation on the first wave follows the embryonic order of follicle individualization but the scope of this study did not reach the adult period. If during the adult period follicle recruitment still occurs according to the time of individualization or if the complex communication between neighbor follicles determines the order of follicle activation, or both, remains to be determined. The use of the triple transgenic mouse line may be helpful to answer this particular question, although the development of new imaging systems may be required, due to the large size of the adult ovary.

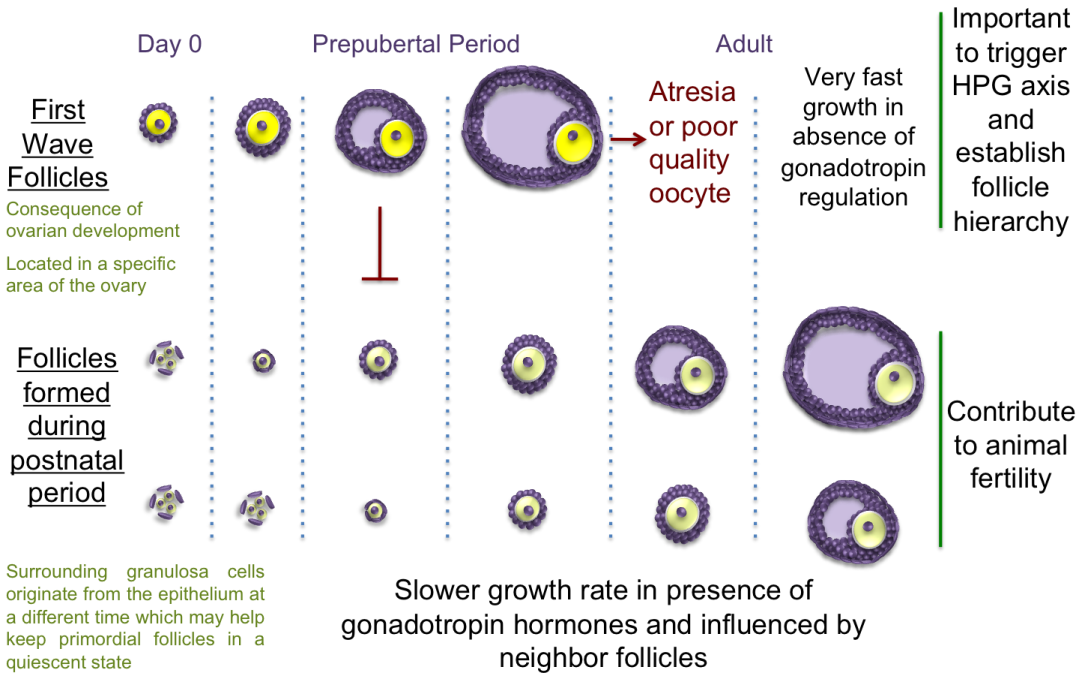

Figure 5.1 – Working model for the role of the first follicular wave in the establishment of the hierarchy of primordial follicle recruitment. The data obtained in this thesis suggests that selective primordial follicle activation can be explained by temporal differences in follicle formation, rather than meiosis onset, contradicting the 'production line' hypothesis. It was observed for the first time that individual follicle formation in the embryonic gonad occurs preferencially in the anterior-dorsal region of the ovary, a geographical area where the first growing follicles appear in the postnatal ovary. The importance of geographic microenviroments in the ovary is a new concept and the molecular mechanisms regulating the formation of the first primordial follicles should be explored in future studies. These first formed and activated follicles (represented on the first line on this scheme) have a higher expression level of fluorescent proteins, are surrounded by pregranulosa cells embryonically, growth faster and achieve antral stage before puberty. These follicles are potentially important to trigger the hypothalamus-pituitary-gonad (HPG) axis and induce puberty. Growing follicles can also produce substances that affect small follicles, for instance AMH. Many of the first growing follicles may be lost by atresia or originate oocytes of poor quality, while others may be ovulated and contribute to the fertility of the individual. In contrast, the primordial follicles in the ventral region of the ovary are formed postnatally and surrounded by pregranulosa cells that migrate from the surface epithelium during the neonatal period. The delayed timing of individualization of these primordial follicles causes their development in a complex ovarian environment containing other follicles in different stages and cyclic gonadotropins.

Furthermore, differences in fluorescent signal could be identified between follicular classes, including after nest breakdown (Figure 3.12) and follicle activation (Figure 3.16 and Figure 3.18), making this mouse line a powerful tool to visualize the process of selective primordial follicle recruitment under physiological conditions, explored on this thesis, but with incredible potential for future studies. The fluorescent signal can be used in the future to explore new signaling molecules

involved in primordial follicle activation as well as to assess the impact of environmental pollutants in toxicological studies. In addition, the fluorescent signal may be used to sort specific follicle populations and study the differences between follicular classes and ovarian regions. While this work was restricted to the female gonad, future studies may take advantage of the transgenic mice to study male germ cell development or use the reporter proteins for isolation of germ cells at a specific developmental stage.

In conclusion, the triple transgenic mice represent the first oocyte specific reporter lineage in which the signal of fluorescent proteins can be used to follow oocyte gene activity and follicle activation. The fluorescent profile of this mouse line was crucial to identify spatial differences in germ development and understand how it results in selective follicle recruitment. This transgenic mouse line has an enormous unexplored potential and promises to be an important tool for expand fundamental knowledge about the female gonad, including the mechanisms controlling follicle activation, selection and ovarian developmental dynamics, which are vital to understand normal ovarian function and allow the development of new therapies for infertility.

References

1. Hsueh, A.J., et al., *Intraovarian control of early folliculogenesis.* Endocr Rev, 2014: p. er20141020.
2. Anderson, R., et al., *The onset of germ cell migration in the mouse embryo.* Mech Dev, 2000. **91**(1-2): p. 61-8.
3. Molyneaux, K.A., et al., *Time-lapse analysis of living mouse germ cell migration.* Dev Biol, 2001. **240**(2): p. 488-98.
4. Koopman, P., et al., *Male development of chromosomally female mice transgenic for Sry.* Nature, 1991. **351**(6322): p. 117-21.
5. McElreavey, K., et al., *A regulatory cascade hypothesis for mammalian sex determination: SRY represses a negative regulator of male development.* Proc Natl Acad Sci U S A, 1993. **90**(8): p. 3368-72.
6. Maatouk, D.M. and B. Capel, *Sexual development of the soma in the mouse.* Curr Top Dev Biol, 2008. **83**: p. 151-83.
7. Sarraj, M.A. and A.E. Drummond, *Mammalian foetal ovarian development: consequences for health and disease.* Reproduction, 2012. **143**(2): p. 151-63.
8. Racki, W.J. and J.D. Richter, *CPEB controls oocyte growth and follicle development in the mouse.* Development, 2006. **133**(22): p. 4527-37.
9. Pepling, M.E., *From primordial germ cell to primordial follicle: mammalian female germ cell development.* Genesis, 2006. **44**(12): p. 622-32.
10. Maatouk, D.M., et al., *Disruption of mitotic arrest precedes precocious differentiation and transdifferentiation of pregranulosa cells in the perinatal Wnt4 mutant ovary.* Dev Biol, 2013. **383**(2): p. 295-306.
11. Jameson, S.A., et al., *Temporal transcriptional profiling of somatic and germ cells reveals biased lineage priming of sexual fate in the fetal mouse gonad.* PLoS Genet, 2012. **8**(3): p. e1002575.
12. Pepling, M.E. and A.C. Spradling, *Female mouse germ cells form synchronously dividing cysts.* Development, 1998. **125**(17): p. 3323-8.
13. Odor, D.L. and R.J. Blandau, *Ultrastructural studies on fetal and early postnatal mouse ovaries. I. Histogenesis and organogenesis.* Am J Anat, 1969. **124**(2): p. 163-86.
14. Konishi, I., et al., *Development of interstitial cells and ovigerous cords in the human fetal ovary: an ultrastructural study.* J Anat, 1986. **148**: p. 121-35.

15. Nicholas, C.R., K.M. Haston, and R.A. Pera, *Intact fetal ovarian cord formation promotes mouse oocyte survival and development.* BMC Dev Biol, 2010. **10**: p. 2.
16. Pepling, M.E. and A.C. Spradling, *Mouse ovarian germ cell cysts undergo programmed breakdown to form primordial follicles.* Dev Biol, 2001. **234**(2): p. 339-51.
17. Menke, D.B., J. Koubova, and D.C. Page, *Sexual differentiation of germ cells in XX mouse gonads occurs in an anterior-to-posterior wave.* Dev Biol, 2003. **262**(2): p. 303-12.
18. Bullejos, M. and P. Koopman, *Germ cells enter meiosis in a rostro-caudal wave during development of the mouse ovary.* Mol Reprod Dev, 2004. **68**(4): p. 422-8.
19. Bowles, J., et al., *Retinoid signaling determines germ cell fate in mice.* Science, 2006. **312**(5773): p. 596-600.
20. Koubova, J., et al., *Retinoic acid regulates sex-specific timing of meiotic initiation in mice.* Proc Natl Acad Sci U S A, 2006. **103**(8): p. 2474-9.
21. MacLean, G., et al., *Apoptotic extinction of germ cells in testes of Cyp26b1 knockout mice.* Endocrinology, 2007. **148**(10): p. 4560-7.
22. Kehler, J., et al., *Oct4 is required for primordial germ cell survival.* EMBO Rep, 2004. **5**(11): p. 1078-83.
23. Byskov, A.G., *Does the rete ovarii act as a trigger for the onset of meiosis?* Nature, 1974. **252**(5482): p. 396-7.
24. Mu, X., et al., *Retinoic acid derived from the fetal ovary initiates meiosis in mouse germ cells.* J Cell Physiol, 2013. **228**(3): p. 627-39.
25. Le Bouffant, R., et al., *Meiosis initiation in the human ovary requires intrinsic retinoic acid synthesis.* Hum Reprod, 2010. **25**(10): p. 2579-90.
26. McGee, E.A. and A.J. Hsueh, *Initial and cyclic recruitment of ovarian follicles.* Endocr Rev, 2000. **21**(2): p. 200-14.
27. de Cuevas, M., M.A. Lilly, and A.C. Spradling, *Germline cyst formation in Drosophila.* Annu Rev Genet, 1997. **31**: p. 405-28.
28. Greenbaum, M.P., et al., *Mouse TEX14 is required for embryonic germ cell intercellular bridges but not female fertility.* Biol Reprod, 2009. **80**(3): p. 449-57.
29. Ohno, S. and J.B. Smith, *Role of Fetal Follicular Cells in Meiosis of Mammalian Ooecytes.* Cytogenetics, 1964. **3**: p. 324-33.

30. Tingen, C., A. Kim, and T.K. Woodruff, *The primordial pool of follicles and nest breakdown in mammalian ovaries.* Mol Hum Reprod, 2009. **15**(12): p. 795-803.
31. Buccione, R., A.C. Schroeder, and J.J. Eppig, *Interactions between somatic cells and germ cells throughout mammalian oogenesis.* Biol Reprod, 1990. **43**(4): p. 543-7.
32. Eppig, J.J., K. Wigglesworth, and F.L. Pendola, *The mammalian oocyte orchestrates the rate of ovarian follicular development.* Proc Natl Acad Sci U S A, 2002. **99**(5): p. 2890-4.
33. Eppig, J.J., *Oocyte control of ovarian follicular development and function in mammals.* Reproduction, 2001. **122**(6): p. 829-38.
34. Peters, H., et al., *Follicular growth: the basic event in the mouse and human ovary.* J Reprod Fertil, 1975. **45**(3): p. 559-66.
35. Vanderhyden, B., *Molecular basis of ovarian development and function.* Front Biosci, 2002. **7**: p. d2006-22.
36. Woodruff, T.K., et al., *Inhibin A and inhibin B are inversely correlated to follicle-stimulating hormone, yet are discordant during the follicular phase of the rat estrous cycle, and inhibin A is expressed in a sexually dimorphic manner.* Endocrinology, 1996. **137**(12): p. 5463-7.
37. Makanji, Y., et al., *Inhibin at 90: from discovery to clinical application, a historical review.* Endocr Rev, 2014. **35**(5): p. 747-94.
38. Adhikari, D. and K. Liu, *Molecular mechanisms underlying the activation of mammalian primordial follicles.* Endocr Rev, 2009. **30**(5): p. 438-64.
39. Peters, H., *The development of the mouse ovary from birth to maturity.* Acta Endocrinol (Copenh), 1969. **62**(1): p. 98-116.
40. Tingen, C.M., et al., *Prepubertal primordial follicle loss in mice is not due to classical apoptotic pathways.* Biol Reprod, 2009. **81**(1): p. 16-25.
41. Kerr, J.B., M. Myers, and R.A. Anderson, *The dynamics of the primordial follicle reserve.* Reproduction, 2013. **146**(6): p. R205-15.
42. Rodrigues, P., et al., *Multiple mechanisms of germ cell loss in the perinatal mouse ovary.* Reproduction, 2009. **137**(4): p. 709-20.
43. Reddy, P., W. Zheng, and K. Liu, *Mechanisms maintaining the dormancy and survival of mammalian primordial follicles.* Trends Endocrinol Metab, 2010. **21**(2): p. 96-103.
44. Castrillon, D.H., et al., *Suppression of ovarian follicle activation in mice by the transcription factor Foxo3a.* Science, 2003. **301**(5630): p. 215-8.

45. Adhikari, D., et al., *Tsc/mTORC1 signaling in oocytes governs the quiescence and activation of primordial follicles.* Hum Mol Genet, 2010. **19**(3): p. 397-410.
46. Adhikari, D., et al., *Disruption of Tsc2 in oocytes leads to overactivation of the entire pool of primordial follicles.* Mol Hum Reprod, 2009. **15**(12): p. 765-70.
47. Reddy, P., et al., *Oocyte-specific deletion of Pten causes premature activation of the primordial follicle pool.* Science, 2008. **319**(5863): p. 611-3.
48. Rajareddy, S., et al., *p27kip1 (cyclin-dependent kinase inhibitor 1B) controls ovarian development by suppressing follicle endowment and activation and promoting follicle atresia in mice.* Mol Endocrinol, 2007. **21**(9): p. 2189-202.
49. Reddy, P., et al., *PDK1 signaling in oocytes controls reproductive aging and lifespan by manipulating the survival of primordial follicles.* Hum Mol Genet, 2009. **18**(15): p. 2813-24.
50. Durlinger, A.L., et al., *Control of primordial follicle recruitment by anti-Mullerian hormone in the mouse ovary.* Endocrinology, 1999. **140**(12): p. 5789-96.
51. Fortune, J.E., et al., *The primordial to primary follicle transition.* Mol Cell Endocrinol, 2000. **163**(1-2): p. 53-60.
52. Fortune, J.E., et al., *Activation of bovine and baboon primordial follicles in vitro.* Theriogenology, 1998. **49**(2): p. 441-9.
53. O'Brien, M.J., J.K. Pendola, and J.J. Eppig, *A revised protocol for in vitro development of mouse oocytes from primordial follicles dramatically improves their developmental competence.* Biol Reprod, 2003. **68**(5): p. 1682-6.
54. Wandji, S.A., et al., *Initiation in vitro of growth of bovine primordial follicles.* Biol Reprod, 1996. **55**(5): p. 942-8.
55. Wandji, S.A., et al., *Initiation of growth of baboon primordial follicles in vitro.* Hum Reprod, 1997. **12**(9): p. 1993-2001.
56. Henderson, S.A. and R.G. Edwards, *Chiasma frequency and maternal age in mammals.* Nature, 1968. **218**(5136): p. 22-8.
57. Bristol-Gould, S.K., et al., *Fate of the initial follicle pool: empirical and mathematical evidence supporting its sufficiency for adult fertility.* Dev Biol, 2006. **298**(1): p. 149-54.
58. Faddy, M.J. and R.G. Gosden, *A model conforming the decline in follicle numbers to the age of menopause in women.* Hum Reprod, 1996. **11**(7): p. 1484-6.
59. Hansen, K.R., et al., *A new model of reproductive aging: the decline in ovarian non-growing follicle number from birth to menopause.* Hum Reprod, 2008. **23**(3): p. 699-708.

60. Gilbert, S., *Developmental Biology. 6th edition*. 2000, Sunderland (MA): Sinauer Associates.
61. Baker, T.G., *Radiosensitivity of mammalian oocytes with particular reference to the human female.* Am J Obstet Gynecol, 1971. **110**(5): p. 746-61.
62. Goswami, D. and G.S. Conway, *Premature ovarian failure.* Hum Reprod Update, 2005. **11**(4): p. 391-410.
63. Coticchio, G., et al., *What criteria for the definition of oocyte quality?* Ann N Y Acad Sci, 2004. **1034**: p. 132-44.
64. Qiao, J., et al., *The root of reduced fertility in aged women and possible therapentic options: Current status and future perspects.* Mol Aspects Med, 2013.
65. Navot, D., et al., *Poor oocyte quality rather than implantation failure as a cause of age-related decline in female fertility.* Lancet, 1991. **337**(8754): p. 1375-7.
66. Wright, V.C., et al., *Assisted reproductive technology surveillance--United States, 2005.* MMWR Surveill Summ, 2008. **57**(5): p. 1-23.
67. Pan, H., et al., *Age-associated increase in aneuploidy and changes in gene expression in mouse eggs.* Dev Biol, 2008. **316**(2): p. 397-407.
68. Vogt, E., et al., *Spindle formation, chromosome segregation and the spindle checkpoint in mammalian oocytes and susceptibility to meiotic error.* Mutat Res, 2008. **651**(1-2): p. 14-29.
69. Hassold, T. and P. Hunt, *To err (meiotically) is human: the genesis of human aneuploidy.* Nat Rev Genet, 2001. **2**(4): p. 280-91.
70. Duncan, F.E., et al., *Chromosome cohesion decreases in human eggs with advanced maternal age.* Aging Cell, 2012. **11**(6): p. 1121-4.
71. de Bruin, J.P., et al., *Age-related changes in the ultrastructure of the resting follicle pool in human ovaries.* Biol Reprod, 2004. **70**(2): p. 419-24.
72. Titus, S., et al., *Impairment of BRCA1-related DNA double-strand break repair leads to ovarian aging in mice and humans.* Sci Transl Med, 2013. **5**(172): p. 172ra21.
73. Svoboda, P., *Cloning a transgene for transgenic RNAi in mouse oocytes.* Cold Spring Harb Protoc, 2009. **2009**(1): p. pdb prot5134.
74. Lan, Z.J., X. Xu, and A.J. Cooney, *Differential oocyte-specific expression of Cre recombinase activity in GDF-9-iCre, Zp3cre, and Msx2Cre transgenic mice.* Biol Reprod, 2004. **71**(5): p. 1469-74.
75. Gallardo, T., et al., *Generation of a germ cell-specific mouse transgenic Cre line, Vasa-Cre.* Genesis, 2007. **45**(6): p. 413-7.

76. Nagy A, G.M., Vintersten K, Behringer R *Manipulating the Mouse Embryo: A Laboratory Manual*. Third Edition ed. 2003: Cold Spring Harbor. 293-294.
77. McLean, A.C., et al., *Performing vaginal lavage, crystal violet staining, and vaginal cytological evaluation for mouse estrous cycle staging identification.* J Vis Exp, 2012(67): p. e4389.
78. Kurita, T., *Developmental origin of vaginal epithelium.* Differentiation, 2010. **80**(2-3): p. 99-105.
79. Pan, H., et al., *Transcript profiling during mouse oocyte development and the effect of gonadotropin priming and development in vitro.* Dev Biol, 2005. **286**(2): p. 493-506.
80. Stein, P., *Microinjection of plasmids into meiotically incompetent mouse oocytes.* Cold Spring Harb Protoc, 2009. **2009**(1): p. pdb prot5135.
81. Pedersen, T. and H. Peters, *Proposal for a classification of oocytes and follicles in the mouse ovary.* J Reprod Fertil, 1968. **17**(3): p. 555-7.
82. Griffin, J., et al., *Comparative analysis of follicle morphology and oocyte diameter in four mammalian species (mouse, hamster, pig, and human).* J Exp Clin Assist Reprod, 2006. **3**: p. 2.
83. Nakagata, N., *Cryopreservation of mouse spermatozoa and in vitro fertilization.* Methods Mol Biol, 2011. **693**: p. 57-73.
84. Shaner, N.C., P.A. Steinbach, and R.Y. Tsien, *A guide to choosing fluorescent proteins.* Nat Methods, 2005. **2**(12): p. 905-9.
85. Ikawa, M., et al., *A rapid and non-invasive selection of transgenic embryos before implantation using green fluorescent protein (GFP).* FEBS Lett, 1995. **375**(1-2): p. 125-8.
86. Villuendas, G., et al., *CMV-driven expression of green fluorescent protein (GFP) in male germ cells of transgenic mice and its effect on fertility.* Int J Androl, 2001. **24**(5): p. 300-5.
87. Anderson, R., et al., *Mouse primordial germ cells lacking beta1 integrins enter the germline but fail to migrate normally to the gonads.* Development, 1999. **126**(8): p. 1655-64.
88. Runyan, C., et al., *Steel factor controls midline cell death of primordial germ cells and is essential for their normal proliferation and migration.* Development, 2006. **133**(24): p. 4861-9.
89. Takeuchi, Y., et al., *The roles of FGF signaling in germ cell migration in the mouse.* Development, 2005. **132**(24): p. 5399-409.

90. Yoshida, S., M. Sukeno, and Y. Nabeshima, *A vasculature-associated niche for undifferentiated spermatogonia in the mouse testis.* Science, 2007. **317**(5845): p. 1722-6.
91. Nel-Themaat, L., et al., *Sertoli cell behaviors in developing testis cords and postnatal seminiferous tubules of the mouse.* Biol Reprod, 2011. **84**(2): p. 342-50.
92. Yan, C., et al., *Regulation of growth differentiation factor 9 expression in oocytes in vivo: a key role of the E-box.* Biol Reprod, 2006. **74**(6): p. 999-1006.
93. Baibakov, B., et al., *Sperm binding to the zona pellucida is not sufficient to induce acrosome exocytosis.* Development, 2007. **134**(5): p. 933-43.
94. Hoodbhoy, T., et al., *ZP2 and ZP3 traffic independently within oocytes prior to assembly into the extracellular zona pellucida.* Mol Cell Biol, 2006. **26**(21): p. 7991-8.
95. Suzuki, H., C.T. Dann, and A. Rajkovic, *Generation of a germ cell-specific mouse transgenic CHERRY reporter, Sohlh1-mCherryFlag.* Genesis, 2013. **51**(1): p. 50-8.
96. John, G.B., et al., *Foxo3 is a PI3K-dependent molecular switch controlling the initiation of oocyte growth.* Dev Biol, 2008. **321**(1): p. 197-204.
97. Jagarlamudi, K., et al., *Oocyte-specific deletion of Pten in mice reveals a stage-specific function of PTEN/PI3K signaling in oocytes in controlling follicular activation.* PLoS One, 2009. **4**(7): p. e6186.
98. de Vries, W.N., et al., *Expression of Cre recombinase in mouse oocytes: a means to study maternal effect genes.* Genesis, 2000. **26**(2): p. 110-2.
99. Noce, T., S. Okamoto-Ito, and N. Tsunekawa, *Vasa homolog genes in mammalian germ cell development.* Cell Struct Funct, 2001. **26**(3): p. 131-6.
100. Toyooka, Y., et al., *Expression and intracellular localization of mouse Vasa-homologue protein during germ cell development.* Mech Dev, 2000. **93**(1-2): p. 139-49.
101. McGrath, S.A., A.F. Esquela, and S.J. Lee, *Oocyte-specific expression of growth/differentiation factor-9.* Mol Endocrinol, 1995. **9**(1): p. 131-6.
102. Dong, J., et al., *Growth differentiation factor-9 is required during early ovarian folliculogenesis.* Nature, 1996. **383**(6600): p. 531-5.
103. Philpott, C.C., M.J. Ringuette, and J. Dean, *Oocyte-specific expression and developmental regulation of ZP3, the sperm receptor of the mouse zona pellucida.* Dev Biol, 1987. **121**(2): p. 568-75.

104. Wassarman, P.M., L. Jovine, and E.S. Litscher, *Mouse zona pellucida genes and glycoproteins.* Cytogenet Genome Res, 2004. **105**(2-4): p. 228-34.
105. Olenych, S.G., et al., *The fluorescent protein color palette.* Curr Protoc Cell Biol, 2007. **Chapter 21**: p. Unit 21 5.
106. Nicholls, P.K., et al., *Growth differentiation factor 9 is a germ cell regulator of Sertoli cell function.* Endocrinology, 2009. **150**(5): p. 2481-90.
107. Hirshfield, A.N. and A.M. DeSanti, *Patterns of ovarian cell proliferation in rats during the embryonic period and the first three weeks postpartum.* Biol Reprod, 1995. **53**(5): p. 1208-21.
108. Zheng, W., et al., *Two classes of ovarian primordial follicles exhibit distinct developmental dynamics and physiological functions.* Hum Mol Genet, 2014. **23**(4): p. 920-8.
109. Yoshida, S., et al., *The first round of mouse spermatogenesis is a distinctive program that lacks the self-renewing spermatogonia stage.* Development, 2006. **133**(8): p. 1495-505.
110. Bouniol-Baly, C., et al., *Differential transcriptional activity associated with chromatin configuration in fully grown mouse germinal vesicle oocytes.* Biol Reprod, 1999. **60**(3): p. 580-7.
111. Polani, P.E. and J.A. Crolla, *A test of the production line hypothesis of mammalian oogenesis.* Hum Genet, 1991. **88**(1): p. 64-70.
112. Hirshfield, A.N., *Heterogeneity of cell populations that contribute to the formation of primordial follicles in rats.* Biol Reprod, 1992. **47**(3): p. 466-72.
113. Tease, C. and G. Fisher, *Further examination of the production-line hypothesis in mouse foetal oocytes. I. Inversion heterozygotes.* Chromosoma, 1986. **93**(5): p. 447-52.
114. Speed, R.M. and A.C. Chandley, *Meiosis in the foetal mouse ovary. II. Oocyte development and age-related aneuploidy. Does a production line exist?* Chromosoma, 1983. **88**(3): p. 184-9.
115. Tease, C. and G. Fisher, *Further examination of the production-line hypothesis in mouse foetal oocytes. II. T(14; 15)6Ca heterozygotes.* Chromosoma, 1989. **97**(4): p. 315-20.
116. Meredith, S. and D. Doolin, *Timing of activation of primordial follicles in mature rats is only slightly affected by fetal stage at meiotic arrest.* Biol Reprod, 1997. **57**(1): p. 63-7.
117. Rowsey, R., et al., *Examining variation in recombination levels in the human female: a test of the production-line hypothesis.* Am J Hum Genet, 2014. **95**(1): p. 108-12.

118. Byskov, A.G., et al., *Influence of ovarian surface epithelium and rete ovarii on follicle formation.* J Anat, 1977. **123**(Pt 1): p. 77-86.
119. Sawyer, H.R., et al., *Formation of ovarian follicles during fetal development in sheep.* Biol Reprod, 2002. **66**(4): p. 1134-50.
120. McGee, E.A., et al., *Cell death and survival during ovarian follicle development.* Mol Cell Endocrinol, 1998. **140**(1-2): p. 15-8.
121. Mork, L., et al., *Temporal differences in granulosa cell specification in the ovary reflect distinct follicle fates in mice.* Biol Reprod, 2012. **86**(2): p. 37.
122. Lee, V.H., J.H. Britt, and B.S. Dunbar, *Localization of laminin proteins during early follicular development in pig and rabbit ovaries.* J Reprod Fertil, 1996. **108**(1): p. 115-22.
123. John, G.B., et al., *Specificity of the requirement for Foxo3 in primordial follicle activation.* Reproduction, 2007. **133**(5): p. 855-63.
124. Anderson, R.A., et al., *Conserved and divergent patterns of expression of DAZL, VASA and OCT4 in the germ cells of the human fetal ovary and testis.* BMC Dev Biol, 2007. **7**: p. 136.
125. Wilhelm, D., J.X. Yang, and P. Thomas, *Mammalian sex determination and gonad development.* Curr Top Dev Biol, 2013. **106**: p. 89-121.
126. Byskov, A.G. and S. Lintern-Moore, *Follicle formation in the immature mouse ovary: the role of the rete ovarii.* J Anat, 1973. **116**(Pt 2): p. 207-17.
127. Harikae, K., et al., *Heterogeneity in sexual bipotentiality and plasticity of granulosa cells in developing mouse ovaries.* J Cell Sci, 2013. **126**(Pt 13): p. 2834-44.
128. Byskov, A.G., X. Guoliang, and C.Y. Andersen, *The cortex-medulla oocyte growth pattern is organized during fetal life: an in-vitro study of the mouse ovary.* Mol Hum Reprod, 1997. **3**(9): p. 795-800.
129. Hummitzsch, K., et al., *A new model of development of the mammalian ovary and follicles.* PLoS One, 2013. **8**(2): p. e55578.
130. Da Silva-Buttkus, P., et al., *Inferring biological mechanisms from spatial analysis: prediction of a local inhibitor in the ovary.* Proc Natl Acad Sci U S A, 2009. **106**(2): p. 456-61.
131. Hornick, J.E., et al., *Multiple follicle culture supports primary follicle growth through paracrine-acting signals.* Reproduction, 2013. **145**(1): p. 19-32.

Appendix

Appendix I – Map and sequence of the plasmids

VASA-EGFP-T7

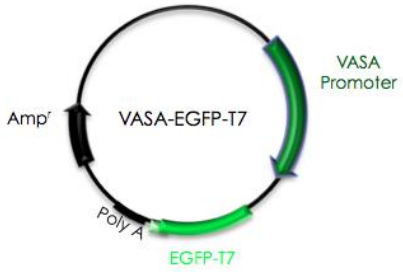

Plasmid DNA sequence: 1 to 8564

Linear DNA Sequence: 3 to 6689

```
                                   CACCATGC CTGGCCCAGT TTCTTGCTTT
                                   TAAGACTC TGGACCCACA CGTGTTTGAT
                                   TTTTTTCC CAGTAACATT TCCTGAATTT
 151 TGTATTTTAT TGTCTCTGCA TCTGTGCTGA GACATAACAA CTTCTGTTTC
 201 TTCTATTTGC CATGAACTGG GAGTTAAGTC TAAGAATTTG ATTAAAGCTG
 251 AAGTTGAGTT TGAAATCAAA CCTCTACATG TAGCGTTTTG TATTTCCCAC
 301 TGTGATACAT CAACCAGCAC ATGGTTCTTG GAGGTCTTTG CTTTGTGGTA
 351 TAAAGTTGGC CCAGTGTGTT TAAATGTTGT CCTCTTTAAG GAGGTAGCTA
 401 GGTAAGATCA CACGCCGGTT ACCTACCTCC CTACTGATGC ACTAACTGGT
 451 GTGCCTAGCC TAGCCTAAGG CCCTAGGGTA CCATGCATCC CATAATAGCT
 501 TATGTGAGGC CCAACACATT TGTAGATAAC AGCATCAGGT CATAGTGTCA
 551 TAAGGTTGGA CACCCCTGGC AGAGTTTCAT GCACCACACT ATCTTCAAAA
 601 GAGCTAAAGA AGTAAGGTGG AAAAAACAAA CATCATAGTG TTCTGGTTTT
 651 ACTGTGACAG GAAAAGACTC ACTGAAAAGG TGCCAAGGCC CAGATTTCCC
 701 CTCCCACAAT TCCAAGCTTC ATGGAGAATG ATACCTCCAC TTTGGGGATG
 751 GAGAAGGGAT TAAATCCTGA CCACAGACTT GAAGCAGTAA GAACTTATCA
 801 CCGTGATGTC AGTTCTGGGT GGAACCCTAT GCATCCCGTG GCCCAGTACC
 851 TGCAGATGCT GCTGCTGGAC CTGTGATAGA TGGCCAGTAC TACAGTTAGG
 901 AATCTTTCCG ACAACTGCAG CTTTTAGAAT GGAAAGCAAA ACTCCACCTA
 951 CTGGATGGCA CAACATGAAA GCAAGGGCTG TGCCTTGCAG CTCAGGGCCA
1001 GCCTTAGTAC TAGTCTCTGA GGGACCGTTG CTACCACCGG TTCCCAACCT
1051 GTAGCAGCAC AACTATCCTG GACCAGGGTT CACGGATGGA GCTCAAGACC
1101 TTGACATCTG TCACAGTTAT GCTCTGCACC ATGAGGAAGT TGTCTCAGTT
1151 TGCCTTACTG CCACAGCACC GGCTGTGGGC TCAGCATTGT GACACTCAGA
1201 GCCACAGGTC TGGAGCAGGA ACCAGGGCAG GCCCCTCTGG TGATTCTTTC
1251 TACAGTTCAC GACCAGAGGC TGTTGGCTTT GGAAGGCACC TGGAGGTCTG
1301 TGCAAGCCCC GGACAAAGGC TTGTGTAGAT GAAGGACCCT TTATAAAAAG
1351 CTCCCTAATT GAGTCTTGAA AAACTCACCC GCTGAGGATT TAGGAGAAAC
1401 CTAAGCTCGG ATCGCCTCCT AACACTGCCA CAGGTAACCT GAATTTTGGT
1451 GCCATATAGT GTTAGAAACT ATAGGCTGGG AGAGAGAAAA AAAAAACATT
1501 CTTTTTTCAA TTTCTGAAAA CAAACAAAAC CAAAACAAGC CATATTATGA
1551 AGACCGGAAT AAATACCTAA TCCTTTGTCC TCGAATGACA TCACGCATCA
1601 ATAAGAACCA AGGATGTTTA AGGAACTATG ACCTCATCTG ACAGTATAAA
1651 TATAAAATGC CAGAAACCGT CAAGATAGTA ACCAGTGTGG GTGGATGCTC
```

1701 ATATGTGTAC TGTATTAGTT ACTTTTTCAT TGTCGTGATA AAATACCACG
1751 ACTAAAGCCT GACTTATAGG AGAAGGAATT TGCCCTGTGT TTTCAGAGTG
1801 ATAAGACTCC ATCATGGCAG GGACGCATGG AAGCCAGCAA CAGGTATGAT
1851 GCTGGGGCAG CAAGCTGAGA GCTCACATCC GCCACTGAAG GCACAAAACA
1901 GCAAGTGTGA GCTGGAAGTG GTGTGAGGCT ATATACTAGC AAAGGCTGCC
1951 CTACTGATAC GCTGTCTCCA GGAGGACTGC GTTCCCCAAG CTTCTCTGAT
2001 CATCACAACC AACTGAGGAC TAAATGTTCA AATACCTGGG TCAGTGGGGA
2051 TCATTTCTCA TTCAAACTTC CACAGATAAT TAAAAGCAAA TAAATGAACC
2101 AGGCTTAAGG AAACTTACTG AATTCCAATA GAAAATATAG AAATAAATCA
2151 ATACTTTAGT AGATATAATT GACTGAGACA TGGGGGCAAA TTTTAAAAAG
2201 TCGAAATTCT TGATAATGAA GGTATACTAA ACAAAATAAA ATTGCATTAG
2251 GGAAGCATTG ATGTTAGAGT AAATCAAGCA GAAGAGAGAA TGAGTGAATT
2301 CCAAGATAGG CCATTTGAAA ATGCACAGAA GAGAAAAAGA ATTAAGAGGA
2351 AGAAATGTAC TCATGGTAAC CTTGGAGCAA CAGTGGAAGG GTAAGTAGGT
2401 TAGTGGGGAT ATGGACGGGA CTTGAGAACA CCAAAGGAGT TAATCGATGC
2451 AACTACGTTA TGATCAACCA CAGTCAGGTT CCAGGTTCTG CAGTAAACTG
2501 AATCTCCAGT TTTCACGCTA TGTAGATCCA TCTCCATGAA TCTGGCCTGG
2551 CCTTGTGACT TTCTGGTAAC TGATTAGTTG AAAGTTGCAA ATATAATTGT
2601 TTAACTTCTT ATGCTAGAAT TCAAGAAGCC TTGCAACTAT TACCCTGGTT
2651 TTGTTTTTCG GAGCGATGTC CCTGACAGGT GTGTCCAGTT GAAGTGCAGT
2751 ATCCTTACAG AGTCGGACTG GGATTGTCCA ACAACCTTCA GAGCCTAAGA
2701 CAGCCTCTTG GAAACTATTC AATTGTTCTG GCCATCCCAG CCCCTAGATG
2801 CCAGAGTAGA GAAGTCACCT TGGATGTTAA ACAAACTGGT ATTGGAGGTT
2851 GGGGATAAAC TCAGTAGTAC AGAGCTTGCC TGGCACGCTC AAGTACCTAG
2901 GTTCAAACTC TGGCAATGCC AAAAAAGAAA AAAGTTGATA GCAAACTCTC
2951 AGATGATTCA GGTTCTAGTT AGCGTTTGAA TGGAATTGTA TGAGATGGTC
3001 TCCTGAGCCC TCTCAATCCC TGAGAGAGAA TTTTTTTGTA AGTCAATATA
3051 TTATGCAATA ATTTGTTATA TAGTTGTACT GGCTAATTTG GGTCAAGCTG
3101 GAGTTATCAC AGAGAAAGGA GCTTCAGTTG GGGAAATGCC TCCATGAGAT
3151 CCAACTGTAA GGCATTTTCT CAATTAGTGA TCAAGGGGGA AAGGCCCCTT
3201 GTGGGTAGGG CCATCTCTGG GCTGGTAGTC TTGGTTCTAT AAGAGAGCAG
3251 GCTGAGCAAG CCAGGTGAGG CAAGCCAGTA AGGAACATCC CTCCATGGCC
3301 TCTGTATCAG CTCCTGCTCC TGACCTGCTT GAGTTCCAGT CCTGACTTCC
3351 TTTGGTGATG AACAGCAATG TGGAAAGTGT AAGCTGGATA AACCCTTTCC
3401 TCCCCAATTT GCTTAGTGGT CATGATGTTT TGTCCAGGAA TAGAAACCCT
3451 GACTAAGACA ATAGTAATAG GTAACAAGAA GAGAGCTGTG AACTCGTCAT
3501 GTAGTTAAGA TAAGTGTTTG CTAGATTTCC TATTGCATAG TTCCTATTTT
3551 CTCTTTATAT TTGGAAAAAA ATTGTGGTAA CATACCTTGG ACACTTATTG
3601 TTGTTCTCCC CCCTGACCTG CACTCAATGC TGAATTCTCA GCCAAACTCT
3651 AGTGATGTCC TCCCCATTCA AAAGCTTCAA CCTTCCAGTC TTTATTTAAA

3701 AAAAATGTTA TTATTACATT TACTTATTCT GTGGTGTGTG TGTGTGTGTG
3751 AGAGAGGATG GGAGCAGGTG TGTGCGTGTC GGTGTGTTTG TTAAATCAGA
3801 ACATGAGTGT GTGTGTAGGA CAGAGACGGG GTGAGTGTGT GTGTGTGTGT
3851 ATGGGAGCAG GTGTGTGTGT GTGTGGGTCA GTGGATAAGT TGTGGAAGTC
3901 AGTTCTTTCC TTCCCTTACT CGGATCTCAG GGATCAAACC CAAGTCCTCA
3951 GGTTGCCAGG TACATGTCAC CTGTCTTTGC TTTATTATTA TTTAGTCCTG
4001 GCTTTTGAG CCTAAGTGTTA TGTTACATAG GTTGACCTTG AATTAGCTAT
4051 GCACTGAGCT CCTGATCCTC CTGCCTATAT CTTCCAAGTA ATGGTTACAG
4101 GAATGGGCCA CTGGACCTAG CAAGTGAACC TACCTGGTCA CTCCAAAAAT
4151 GCACAGCAAA GAATATACGT TTAAAAATAG GTTCATTTTA GGAAGTTTGT
4201 CCACATTTTA AATGACAGTT CTGTTAAAGT ATACTGTGTT TTGTCCTTTG
4251 TTAAATGTGA CTTTTAAAAG CAATTCACCT TAATAGCCTG GGCGACTACA
4301 GTGCTCACTG TATAAATGCT AGTGTGTTTT TGGTGCTGAG ACAGAAAGGT
4351 GGCTCTAGAA AGCTGGAGTC CCTCATCTTT AAGTTCCAGA CTGAGATATC
4401 TAGAACTTCT TCAAAAATCC AGGGAAAGGA AAGCGATGGA AGTGAAAATA
4451 AAAACAAGAA CATGCTTTAC ATATATTTGA TTGTGATCCC TTTGGCGGGT
4501 ACTAGGAAAA CCACGGATGG AATTTTCCTT CTTGAAGGAA AGGAAAGCCG
4551 AGGAGCAGGC AGAATGTGAA CATCTACTTA ATGAGCTGAA CTGGCCGGTG
4601 CCCTCAGAAT TGTAAACAGG TTCACCACAA ATCCAGGCCT TGGCAAACGG
4651 ACCAAGTCTT CCTCTCTTCG GTTTTCTTTT TACAGACTGG CTTTCTTGAC
4701 AACTTCAAGA TGGAGTCTCA TCCTTGCCCT TTTTATGGAG AGGAGAAGCA
4751 TTGCTTCTAG TTGGTTTTAG TAGAGGAGTG AAGTGCATTT CTCAGATACA
4801 AAGAGAGCAC TTGAGACGTT CAGACTCAGA ATGGCCAAGC CTGGCACTTT
4851 GGGAGGTCAA GAGGAGGCTG GAACGGCTGG GAGAGAAAGC AATTAGATGT
4901 TCCGCCCCTT TGGTTTTTCT CCAGACAGGG TTTCTCTGTG TAGCCCTGAC
4951 TGTCCTGAAG TTTGCTCTGT AGACCAGGCT GGCCTCCACC CAGGGATTTG
5001 CCTGCCTCTG CCTCCCCGAG CCCCAGATTT TTATTTTTAT TTATATATAT
5051 ATTAACTTTT GAATGAACAC AATGGAATTG ATGAGCCCTT GGAGAGTGAA
5101 ACGGGATGTC GTGGGATGTC GTGCGTGGCA GCCCCGGGGA TCAGCTCACT
5151 CCCACAGGCC TCACAAGCCA TGGAGCCAAG AGGCCTCCCT GCCTCGGCCT
5201 CGGCCTCGGC CTCGGCCTCA ACAAAGGTGG AGAACGCGCA GGCCGTCCGT
5251 CCATGGGGCG GGAAGTCGCG CGCCGCGGCC GCTGATTGGC TGGCGGGCCC
5301 GGTCGCCTGA TGCTATTTGT TGTCCCCGCG CCAATGACGC AGTCGGCGTC
5351 CCGGCGTCCG CCCGCACGTG CAGCCGTTTA AGCCGCGTCG GCCGGCCGCG
5401 AGGAGCCCGG GGAGCCTGGA GCGGAGAGCG GCCGCTTAAT TAAGCGCTGC
5451 AGAAGTTGGT CGTGAGGCA CTGGGCAGGT AAGTACAAGG TTACAAGACA
5501 GGTTTAAGGA GACCAATAG AAACTGGGCT TGTCGGACAG AGAAGACTCT
5551 TGCGTTTCTG ATAGGCACCT ATTGGTCTTA CTGACATCCA CTTTGCCTTT
5601 CTCTCCACAG GTGTCCACTC CCAGTTCAAT TACAGCTCTT AAGGCTAGAG
5561 TACTTAATAC GACTCACTAT AGGGGCCCGG GCGCCACCAT GGTGAGCAAG

5701 GGCGAGGAGC TGTTCACCGG GGTGGTGCCC ATCCTGGTCG AGCTGGACGG
5751 CGACGTAAAC GGCCACAAGT TCAGCGTGTC CGGCGAGGGC GAGGGCGATG
5801 CCACCTACGG CAAGCTGACC CTGAAGTTCA TCTGCACCAC CGGCAAGCTG
5851 CCCGTGCCCT GGCCCACCCT CGTGACCACC CTGACCTACG GCGTGCAGTG
5901 CTTCAGCCGC TACCCCGACC ACATGAAGCA GCACGACTTC TTCAAGTCCG
5951 CCATGCCCGA AGGCTACGTC CAGGAGCGCA CCATCTTCTT CAAGGACGAC
6001 GGCAACTACA AGACCCGCGC CGAGGTGAAG TTCGAGGGCG ACACCCTGGT
6051 GAACCGCATC GAGCTGAAGG GCATCGACTT CAAGGAGGAC GGCAACATCC
6101 TGGGGCACAA GCTGGAGTAC AACTACAACA GCCACAACGT CTATATCATG
6151 GCCGACAAGC AGAAGAACGG CATCAAGGTG AACTTCAAGA TCCGCCACAA
6201 CATCGAGGA CGGCAGCGTG CAGCTCGCCG ACCACACCAG CAGAACACCC
6251 CCATCGGCGA CGGCCCCGTG CTGCTGCCCG ACAACCACTA CCTGAGCACC
6301 CAGTCCGCCC TGAGCAAAGA CCCCAACGAG AAGCGCGATC ACATGGTCCT
6351 GCTGGAGTTC GTGACCGCCG CCGGGATCAC TCTCGGCATG GACGAGCTGT
6401 ACAAGATGGC TAGCATGACT GGTGGACAGC AAATGGGTTA ATCTAGAGCG
6451 GCCGCTTCGA GCAGACATGA TAAGATACAT TGATGAGTTT GGACAAACCA
6501 CAACTAGAAT GCAGTGAAAA AAATGCTTTA TTTGTGAAAT TTGTGATGCT
6551 ATTGCTTTAT TTGTAACCAT TATAAGCTGC AATAAACAAG TTAACAACAA
6601 CAATTGCATT CATTTTATGT TTCAGGTTCA GGGGGAGGTG TGGGAGGTTT
6651 TTTAAAGCAA GTAAAACCTC TACAAATGTG GTAAAATCGA TAAGGATCCA
6701 GGTGGCACTT TTCGGGGAAA TGTGCGCGGA ACCCCTATTT GTTTATTTTT
6751 CTAAATACAT TCAAATATGT ATCCGCTCAT GAGACAATAA CCCTGATAAA
6801 TGCTTCAATA ATATTGAAAA AGGAAGAGTA TGAGTATTCA ACATTTCCGT
6851 GTCGCCCTTA TTCCCTTTTT TGCGGCATTT TGCCTTCCTG TTTTTGCTCA
6901 CCCAGAAACG CTGGTGAAAG TAAAAGATGC TGAAGATCAG TTGGGTGCAC
6951 GAGTGGGTTA CATCGAACTG GATCTCAACA GCGGTAAGAT CCTTGAGAGT
7001 TTTCGCCCCG AAGAACGTTT TCCAATGATG AGCACTTTTA AAGTTCTGCT
7051 ATGTGGCGCG GTATTATCCC GTATTGACGC CGGGCAAGAG CAACTCGGTC
7101 GCCGCATACA CTATTCTCAG AATGACTTGG TTGAGTACTC ACCAGTCACA
7151 GAAAAGCATC TTACGGATGG CATGACAGTA AGAGAATTAT GCAGTGCTGC
7201 CATAACCATG AGTGATAACA CTGCGGCCAA CTTACTTCTG ACAACGATCG
7251 GAGGACCGAA GGAGCTAACC GCTTTTTTGC ACAACATGGG GGATCATGTA
7301 ACTCGCCTTG ATCGTTGGGA ACCGGAGCTG AATGAAGCCA TACCAAACGA
7351 CGAGCGTGA CACCACGATG CCTGTGCAAT GGCAACAACG TTGCGCAAAC
7401 TATTAACTGG CGAACTACTT ACTCTAGCTT CCCGGCAACA ATTAATAGAC
7451 TGGATGGAGG CGGATAAAGT TGCAGGACCA CTTCTGCGCT CGGCCCTTCC
7501 GGCTGGCTGG TTTATTGCTG ATAAATCTGG AGCCGGTGAG CGTGGGTCTC
7551 GCGGTATCAT TGCAGCACTG GGGCCAGATG GTAAGCCCTC CCGTATCGTA
7601 GTTATCTACA CGACGGGGAG TCAGGCAACT ATGGATGAAC GAAATAGACA
7651 GATCGCTGAG ATAGGTGCCT CACTGATTAA GCATTGGTAA CTGTCAGACC

7701 AAGTTTACTC ATATATACTT TAGATTGATT TAAAACTTCA TTTTTAATTT
7751 AAAAGGATCT AGGTGAAGAT CCTTTTTGAT AATCTCATGA CCAAAATCCC
7801 TTAACGTGAG TTTTCGTTCC ACTGAGCGTC AGACCCCGTA GAAAAGATCA
7851 AAGGATCTTC TTGAGATCCT TTTTTTCTGC GCGTAATCTG CTGCTTGCAA
7901 ACAAAAAAAC CACCGCTACC AGCGGTGGTT TGTTTGCCGG ATCAAGAGCT
7951 ACCAACTCTT TTTCCGAAGG TAACTGGCTT CAGCAGACGG ATCAAGAGCT
8001 ACCAACTCTT TTTCCGAAGG TAACTGGCTT CAGCAGAGCG CAGATACCAA
8051 ATACTGTTCT TCTAGTGTAG CCGTAGTTAG GCCACCACTT CAAGAACTCT
8101 GTAGCACCGC CTACATACCT CGCTCTGCTA ATCCTGTTAC CAGTGGCTGC
8151 TGCCAGTGGC GATAAGTCGT GTCTTACCGG GTTGGACTCA AGACGATAGT
8201 TACCGGATAA GGCGCAGCGG TCGGGCTGAA CGGGGGGTTC GTGCACACAG
8251 CCCAGCTTGG AGCGAACGAC CTACACCGAA CTGAGATACC TACAGCGTGA
8301 GCTATGAGAA AGCGCCACGC TTCCCGAAGG GAGAAAGGCG GACAGGTATC
8351 CGGTAAGCGG CAGGGTCGGA ACAGGAGAGC GCACGAGGGA GCTTCCAGGG
8401 GGAAACGCCT GGTATCTTTA TAGTCCTGTC GGGTTTCGCC ACCTCTGACT
8451 TGAGCGTCGA TTTTTGTGAT GCTCGTCAGG GGGGCGGAGC CTATGGAAAA
8501 ACGCCAGCAA CGCGGCCTTT TTACGGTTCC TGGCCTTTTG CTGGCCTTTG
8551 CTCACATGGC TGAC

Appendix II – Map and sequence of the plasmids

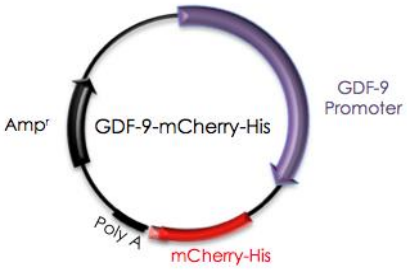

GDF-9-mCherry-His

Plasmid DNA sequence: 1 to 6351

Linear DNA Sequence: 3 to 4465

```
   1 AGATCTATAG GTACCGATAT CAGCCCAGGA AGATGTGGCC TTCGCTTTCC
  51 TAGTTAACAC CAAATTAAAA AAAAAAAAAT CACGGAATTT ACCTAACATA
 101 ATCTTCACCA TTTTAAAAAG TACTGTTGTG CTGGCGCATG CCTACAATTC
 151 CAGCCAACAG TCCCGAGGAG AGGGCAGTAA AATCTCAAGT TTAAGGCCAG
 201 CCTGGCTTCT ACAGCAAGAT CGGGCCTCAA CCTCTCCATC AAATTTAAGT
 251 GCACCTTCAC GGATATTCAC AATGCCATGA AACCGACAGC AAAATCGGCC
 301 GCACATCTAA CACAAGACAC TGATTGCATC AGCCTTTCAT CACAGATAGT
 351 GGCCAGCGAT GACCTCAGAG GGAGCCGTTG GAGTCACCCA AGTGACCTTA
 401 GGCCAGTCAT TTCGATATGA TAAGAACTCC TCCACGTCTG CCCCGCGAGG
 451 GCGTCGGAAG GAGAGGTGCG CGGCTGTACC CCGCCCGCCC CGCACTCACG
 501 CGGCGCCACG CGCAGGATGC GCTCGCGAGT GCGGCGCAGC ACGTTGGGGA
 551 TGCCTTTGCT GAAATAGCTT GGGAAGGCGC GCTGCTCAAA GGGCGACAAG
 601 CTGTAGGAGA TCACGTGCCG TATCCGCGCC AGGTTCCCAA ACTCGCGGCC
 651 CATGGTGACG GCGGCCCTGG GACAGAAGAT AGACGCGTGG CTCAGTCTCG
 701 CGAAAAACCT CCCACGGCCT AACACCGACC CCCAGGATCG GTCACCTCTA
 751 CCTCCAGAGC TCTGAGCCGG CTTTCGCCCG TCACTTCCGG GAGGAGCGGA
 801 AGCCGAGCCT AGAGAACGTG AAGTCATTTC CGGGAACTAC CATTTTCTTT
 851 CGATCTCAAG GGGGAGACTC AAAAAAAAAA TTGTCAGTTG ACCTGAGTGG
 901 GCGTGGCCTG ACCTTCGTGT AGCCGGAAAG GACCAGTACC AAGAGGGCTG
 951 GGCGGAGCTT AGAGGCGCTT CTAGCGACAC GTGGGTGGGG CTTATAGAGG
1001 TGCTTGTGGG CTTACGGTAA GTAGTGAACG CACGGGAGAG GTTGATGTTG
1051 CCAAGGGGCG GGGCTTGAAG AGGAATGGTG GCTTGGTGGG AGGGGTGCCA
1101 AGCAAGTGGG CGGGGCTTAT TAGCCACCCT GGGGATCTTA GGTGGATACG
1151 TCCGTAAGGT CCCCCGTCGA GAGGTGCACG GGGCGGGGCC TATAGGTGCA
1201 TGGGGCGCGG ATTAGGGTGA TGGGCGTGGC TTAGGAGCAC CTGGGTGTTC
1251 CAAGAGGCGG TCCTTTCCGC TCAGTACCAG GCCTTTGCAT AACAGCCGGC
1301 AGCTGCTCAA AAATTAAAAA GAAAAAACAA AAAGACTTGT TCTCCTCGTT
1351 CTTCTGCTGT CCCTTACTCT CCACCAGGTA TATGTGGTCC TCATAACCAA
1401 AAGGGCCTTC ACTGACCACA GTACAAAATT AAGGACACGG ATCTAGAGCT
1451 TTGGTACACA CTGCCTAGCA AGCCACTGGC AGGCTGTAGA CTTGTCCAAG
1501 ATGTGACATA AACGTTTCTC CCAGTTCAGC CACGAACGAG TGTGGCAGTT
```

1551 GTCAGACGCA CATAGTGGTG ATGGGAGCCA AGGAGAAAGT GGTGGGTTTG
1601 GGCTGAGTGT GTCATCAAAC CCAGACCCCA CTCTCTAAGG AACTGTTATG
1651 TTTTCTCTAA AGTGCATTCA TTCTCCTAGC TAATATTATC CTGTGGGACT
1701 CACCGCCCTT TCTCCTCCTC TCAGTGGCTG TAAATGGGTT AACTGGCTGT
1751 AAATAATCTG GCAATCAAAC TGGGGCAGTT TGGCGGTGAG CTTCAGTTTT
1801 GCAAGAGTAC TTCAGCCTTA TCTATCTGGT GCTGGGCAAA CTGATTTTTT
1851 TTTTATCCTG TGTCATTAGT GTGTTTTGAC TTTCTCCCAA GAGATAGTCT
1901 CCTTCCAAGG GGTGCTAGAT AGCCTTTCAT GGTGCACCTG CACATTCTCC
1951 CCCCCACCTC CACCCTGCCC CCATTTTCCT TAAACATTAT CTAGCTTGAT
2001 CTCACCTCCA AGGCCGGGAC ACAAATACTT TAATCAAGGA CTAAAACACT
2051 GTCCAGATTT CTGCCATCTG GGTGGTTGGT TAAAGAATAA ATACGATGTC
2101 TATTTAATTG CATTTGCTGA TGTCTCAAGA TTTTTCAACC AAAGTATAGT
2151 CAAGTGAATT GTAGACCAAA ACAAGGGCAT CAGGATATTG TACTGTCACT
2201 ACATTTTAAA ATATGTATTT GGTATGTAAG TGCTAGGGGT GTAGGTCAGA
2251 AGACGAGCTG TAGAAGTCTC TTCTCCCTTT TTCTCTGTGG ATCACAGGGG
2301 TTGAAGTTAG GCCTTTAGGA CTGGATGACT TTTGGTCGTT AGGCTTGGCG
2351 GCAAGTTGCT ATCTTGCCAT TCCAGCTAGA TATTGTGGCT TTTTTTTAAT
2401 TGTTTATTTT CATTTTATAA TGGGTGTTTT GTATTCCTAA GGATGCCCGA
2451 GAAAGGCATT GGCTCCCCTG GAAGTGGAGC TATAAATGGT TGTTCTAAGA
2501 AGAGCAACCA GTGCCCTTAA CTGCCAGGTC ATCCATCATC TTTCTGGCCC
2551 CAAGACATTG TATGTTTTAA TTGCTCAAAG TTAAAGGTGA TGTCCTCTTT
2601 TTATTTTGAG ATGGGGTCTC TCAAAATTAT GTAGCTCTGA CTGTCCTAGA
2651 ACTCTCTATA TAGACCAGGC TGGCTTGAAT CCACAGAGAT CCACCTGCCT
2701 GTGTCTCCTG AATGCTGGGA TTAAAGGCGT GAACCTCTAC ACCTGGGCCC
2751 TGATGTCCTT TTTCAAAGCA CATTGCAAGT AGCTGTTGTC TTGGGCCAAC
2801 TTTACAACCC CTCTACTAAG CCACCTGGAC AGGCTGAACA GCCTAACATC
2851 ACTGGAATTT CAGAACCCAT TGTGACTTTG TTTCTCTGAT TCACTGTGCA
2901 GTAAGCCATC AGTTATTCTA ACCACCTGGA CGTGGGAGCT GTGGAGATAG
2951 ACGATGAATC AAGAGGAAAA AATAAACCTA ATACTTCTGC AGTCACATCT
3001 CCAGCCCTAA GAGGTTTTGT TTTATAATTC CTTGGGTTTC TGTTGGGCTC
3051 TCACCTATAT AAGTAGTCCA CTAGGGTGAC GATACTTGGT GGGTTTGAAA
3101 TAAATGTCCA GGAGAAACAG GGAAAGAAAG CCAAATAAGT AGATAAATCT
3151 GTATCTAATG AGAACAAATT GGATAAAACC GTGTTGTCAG CTGACTGCTG
3201 TAGAGCTGAT AAGAAACAAT GTACAGCTAG GCAAGCTTGC GCTGCAGCTG
3251 CAGAAGTTGG TCGTGAGGCA CTGGGCAGGT AAGTATCAAG GTTACAAGAC
3301 AGGTTTAAGG AGACCAATAG AAACTGGGCT TGTCGAGACA GAGAAGACTC
3351 TTGCGTTTCT GATAGGCACC TATTGGTCTT ACTGACATCC ACTTTGCCTT
3401 TCTCTCCACA GGTGTCCACT CCCAGTTCAA TTACAGCTCT TAAGGCTAGA
3451 GTACTTAATA CGACTCACTA TAGGGGCCCG GGCGCCACCA TGGTGAGCAA
3501 GGGCGAGGAG GATAACATGG CCATCATCAA GGAGTTCATG CGCTTCAAGG

3551 TGCACATGGA GGGCTCCGTG AACGGCCACG AGTTCGAGAT CGAGGGCGAG
3601 GGCGAGGGCC GCCCCTACGA GGGCACCCAG ACCGCCAAGC TGAAGGTGAC
3651 CAAGGGTGGC CCCCTGCCCT TCGCCTGGGA CATCCTGTCC CCTCAGTTCA
3701 TGTACGGCTC CAAGGCCTAC GTGAAGCACC CCGCCGACAT CCCCGACTAC
3751 TTGAAGCTGT CCTTCCCCGA GGGCTTCAAG TGGGAGCGCG TGATGAACTT
3801 CGAGGACGGC GGCGTGGTGA CCGTGACCCA GGACTCCTCCC TGCAGGACG
3851 GCGAGTTCAT CTACAAGGTG AAGCTGCGCG GCACCAACTT CCCCTCCGAC
3901 GGCCCCGTAA TGCAGAAGAA GACCATGGGC TGGGAGGCCT CCTCCGAGCG
3951 GATGTACCCC GAGGACGGCG CCCTGAAGGG CGAGATCAAG CAGAGGCTGA
4001 AGCTGAAGGA CGGCGGCCAC TACGACGCT GAGGTCAAGAC CACCTACAAG
4051 GCCAAGAAGC CCGTGCAGCT GCCCGGCGCC TACAACGTCA ACATCAAGTT
4101 GGACATCACC TCCCACAACG AGGACTACAC CATCGTGGAA CAGTACGAAC
4151 GCGCCGAGGG CCGCCACTCC ACCGGCGGCA TGGACGAGCT GTACAAGTCC
4201 GGAAACCACC ATCACCACCA TCACTAGTCT AGAGCGGCCG CTTCGAGCAG
4251 ACATGATAAG ATACATTGAT GAGTTTGGAC AAACCACAAC TAGAATGCAG
4301 TGAAAAAAAT GCTTTATTTG TGAAATTTGT GATGCTATTG CTTTATTTGT
4351 AACCATTATA AGCTGCAATA AACAAGTTAA CAACAACAAT TGCATTCATT
4401 TTATGTTTCA GGTTCAGGGG GAGGTGTGGG AGGTTTTTTA AAGCAAGTAA
4451 AACCTCTACA AATGTGGTAA AATCGATAAG GATCCAGGTG GCACTTTTCG
4501 GGGAAATGTG CGCGGAACCC CTATTTGTTT ATTTTTCTAA ATACATTCAA
4551 ATATGTATCC GCTCATGAGA CAATAACCCT GATAAATGCT TCAATAATAT
4601 TGAAAAAGGA AGAGTATGAG TATTCAACAT TTCCGTGTCG CCCTTATTCC
4651 CTTTTTTGCG GCATTTTGCC TTCCTGTTTT TGCTCACCCA GAAACGCTGG
4701 TGAAAGTAAA AGATGCTGAA GATCAGTTGG GTGCACGAGT GGGTTACATC
4751 GAACTGGATC TCAACAGCGG TAAGATCCTT GAGAGTTTTC GCCCCGAAGA
4801 ACGTTTTCCA ATGATGAGCA CTTTTAAAGT TCTGCTATGT GGCGCGGTAT
4851 TATCCCGTAT TGACGCCGGG CAAGAGCAAC TCGGTCGCCG CATACACTAT
4901 TCTCAGAATG ACTTGGTTGA GTACTCACCA GTCACAGAAA AGCATCTTAC
4951 GGATGGCATG ACAGTAAGAG AATTATGCAG TGCTGCCATA ACCATGAGTG
5001 ATAACACTGC GGCCAACTTA CTTCTGACAA CGATCGGAGG ACCGAAGGAG
5051 CTAACCGCTT TTTTGCACAA CATGGGGGAT CATGTAACTC GCCTTGATCG
5101 TTGGGAACCG GAGCTGAATG AAGCCATACC AAACGACGAG CGTGACACCA
5151 CGATGCCTGT AGCAATGGCA ACAACGTTGC GCAAACTATT AACTGGCGAA
5201 CTACTTACTC TAGCTTCCCG GCAACAATTA ATAGACTGGA TGGAGGCGGA
5251 TAAAGTTGCA GGACCACTTC TGCGCTCGGC CCTTCCGGCT GGCTGGTTTA
5301 TTGCTGATAA ATCTGGAGCC GGTGAGCGTG GGTCTCGCGG TATCATTGCA
5351 GCACTGGGGC CAGATGGTAA GCCCTCCCGT ATCGTAGTTA TCTACACGAC
5401 GGGGAGTCAG GCAACTATGG ATGAACGAAA TAGACAGATC GCTGAGATAG
5451 GTGCCTCACT GATTAAGCAT TGGTAACTGT CAGACCAAGT TTACTCATAT
5501 ATACTTTAGA TTGATTTAAA ACTTCATTTT TAATTTAAAA GGATCTAGGT

5551 GAAGATCCTT TTTGATAATC TCATGACCAA AATCCCTTAA CGTGAGTTTT
5601 CGTTCCACTG AGCGTCAGAC CCCGTAGAAA AGATCAAAGG ATCTTCTTGA
5651 GATCCTTTTT TTCTGCGCGT AATCTGCTGC TTGCAAACAA AAAAACCACC
5701 GCTACCAGCG GTGTTTGTTT GCCGGATCAA GAGCTACCAA CTCTTTTTCC
5751 GAAGGTAACT GGCTTCAGCA GACGGATCAA GAGCTACCAA CTCTTTTTCC
5801 GAAGGTAACT GGCTTCAGCA GAGCGCAGAT ACCAAATACT GTTCTTCTAG
5851 TGTAGCCGTA GTTAGGCCAC CACTTCAAGA ACTCTGTAGC ACCGCCTACA
5901 TACCTCGCTC TGCTAATCCT GTTACCAGTG GCTGCTGCCA GTGGCGATAA
5951 GTCGTGTCTT ACCGGGTTGG ACTCAAGACG ATAGTTACCG GATAAGGCGC
6001 AGCGGTCGGG CTGAACGGGG GGTTCGTGCA CACAGCCCAG CTTGGAGCGA
6051 ACGACCTACA CCGAACTGAG ATACCTACAG CGTGAGCTAT GAGAAAGCGC
6101 CACGCTTCCC GAAGGGAGAA AGGCGGACAG GTATCCGGTA AGCGGCAGGG
6151 TCGGAACAGG AGAGCGCACG AGGGAGCTTC CAGGGGGAAA CGCCTGGTAT
6201 CTTTATAGTC CTGTCGGGTT TCGCCACCTC TGACTTGAGC GTCGATTTTT
6251 GTGATGCTCG TCAGGGGGGC GGAGCCTATG GAAAAACGCC AGCAACGCGG
6301 CCTTTTTACG GTTCCTGGCC TTTTGCTGGC CTTTTGCTCA CATGGCTCGA
6351 C

Appendix III – Map and sequence of the plasmids

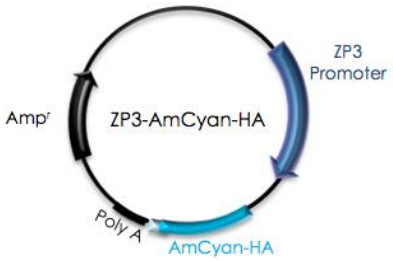

ZP3-AmCyan-HA

Plasmid DNA sequence: 1 to 4700

Linear DNA Sequence: 3 to 2822

```
   1 AGATCTCGAG CTCCACCGCG GTGGCGGCCG CTCTAGCTAG AACTAGTGGA
  51 TCTCTGGGAG TTCAAGGCCA GTCTGGTCCA TACAGTGAGT TCCAGAAATA
 101 CACACAGAGA AATCCTGTCT CAAAAAACAA ACAAAAAACA ATATACATAT
 151 ATATGTATAT GTATATATAT ATATATATAT ATTACATAAA ATAGACAAAT
 201 TAACTTAATT TGCTTTTGCC TGGCAGGGGT TGCTCATAAC TGAGGAGTTT
 251 ACCCCAAGGG ACAAGCTGTT GAATAGGTCC CAGGCACATA TATTTTCTCT
 301 TGACACCTAA TTAATGGCTC TTTAGTCTTC ACTTGCCAGG AGTCCTCCAG
 351 CTGATTCTAA GAAAACCCCT GTGTCTTCCT AAGTCTCTCT CCAGGGTCCC
 401 CTCCCAGGCC CATGATGACA CCTGGAGAGA AGCCTGGAGC TTTGAGCTTC
 451 CAACATCCAA CCATACAGCT CTGAGCACAC CGGGTGGGGA TGGGGAGAAA
 501 GTGAAAAACT ATGGCCCACC AGGCTTTAAC GTGCAAAGTC CAGCCTCCAT
 551 GGCCAGGCCT TTCATCACAG CTACTTGAGA GATTGAGGCC AGAAGACTCA
 601 GAAGACTGTG AAGTTCAGGC TTCCCAAGCC ACAGAGTGAG TCCAAGGCCA
 651 AGAGGAGCAA CTTAATAAAA CTATCTTGAA AGAGAGAGAG AGAAAGAAAG
 701 AGAGGGTGGG GAAGAGAGGG AGAGAGAAAG AGCAAAAGAA AGGAAAGGAA
 751 AGGAAAGGAA AAAGCTGGGG TTAAAGCTTA GAGCACCTGC CTAGAGTACC
 801 CCTGTAAAGG GCTGGGGGCA TGGCTCAGTG GTAGAGTCCC TGCCTAGAAT
 851 CCCCCAGGGA GGGGTTGGGG GCGTGGCTCA GGGGTAGAGC CCCTGCCTAG
 901 AATCCTCCAG TGAGGGGCTG GGGGCGTGGC TCAGGGGTAG AGCCCCTGCC
 951 TAGAATCCTC CAGTGAGGGG CTGGGGCATG GCTCAGGGGT AGAGCCCCTG
1001 CCTAGAATCC CCCATTGAGG GGCTGGAGGC GTGGCTCAGT AGCAGAGCCC
1051 CTGCCTAAAA TGCCCCAGGG AGGGGGTGGG TGCCTCACTA GAGCACTTGG
1101 CTTATATTCA GGAAAAGAAT TAAAATTTGA ATAGGATCCT GGTGTGGTGA
1151 CATAGGCCTT TCATCCCAGC ATAGGCTTTT AATCTCTGGA GGCAGAGGTA
1201 GGCAGATTGC TGAATTCGAA GGCAGCCTAG TCTACGAATG CAGCCAGTTC
1251 CTCGACAGCC AGAGTTACAC TGAGAAATCC TGCCCTGAAA AACAGAAATA
1301 AAACAAAACC CAACAACAGC AAAACCCCCA AAACCCAAAA CAAAACAAAA
1351 ACAAAAACCT AAGTAAACAA AATAATAACA GAAACCCCAA CCAACCGAAG
1401 AAATAAAAAC CTTGAATAGG AATCACGTGG AGTGTCTTTA CAACTATAAC
1451 CCAGATTCTG ATCGTTGGTT CAGATGAGGT TTGAGGCCAC AGGTCTAATA
1501 ATGTGTTGAT AATGGGCTCC ACCCGAGATT GAGGGAAGCA GAGGGAATTC
1551 AGGTGGGAGG GTGGGCCATC GGTGATATAA GAACAGTGGT GTCAGCCTCT
```

1601 CATTAAGCTT CGAATTCTGC AGAAGTTGGT CGTGAGGCAC TGGGCAGGTA
1651 AGTATCAAGG TTACAAGACA GGTTTAAGGA GACCAATAGA AACTGGGCTT
1701 GTCGAGACAG AGAAGACTCT TGCGTTTCTG ATAGGCACCT ATTGGTCTTA
1751 CTGACATCCA CTTTGCCTTT CTCTCCACAG GTGTCCACTC CCAGTTCAAT
1801 TACAGCTCTT AAGGCTAGAG TACTTAATAC GACTCACTAT AGGGGCCCGG
1851 GCGCCACCAT GGCCCTGTCC AACAAGTTCA TCGGCGACGA CATGAAGATG
1901 ACCTACCACA TGGACGGCTG CGTGAACGGC CACTACTTCA CCGTGAAGGG
1951 CGAGGGCAGC GGCAAGCCCT ACGAGGGCAC CCAGACCTCC ACCTTCAAGG
2001 TGACCATGGC CAACGGCGGC CCCCTGGCCT TCTCCTTCGA CATCCTGTCC
2051 ACCGTGTTCA TGTACGGCAA CCGCTGCTTC ACCGCCTACC CCACCAGCAT
2101 GCCCGACTAC TTCAAGCAGG CCTTCCCCGA CGGCATGTCC TACGAGAGAA
2151 CCTTCACCTA CGAGGACGGC GGCGTGGCCA CCGCCAGCTG GGAGATCAGC
2201 CTGAAGGGCA ACTGCTTCGA GCACAAGTCC ACCTTCCACG GCGTGAACTT
2251 CCCCGCCGAC GGCCCCGTGA TGGCCAAGAA GACCACCGGC TGGGACCCCT
2301 CCTTCGAGAA GATGACCGTG TGCGACGGCA TCTTGAAGGG CGACGTGACC
2351 GCCTTCCTGA TGCTGCAGGG CGGCGGCAAC TACAGATGCC AGTTCCACAC
2401 CTCCTACAAG ACCAAGAAGC CCGTGACCAT GCCCCCCAAC CACGTGGTGG
2451 AGCACCGCAT CGCCAGAACC GACCTGGACA AGGGCGGCAA CAGCGTGCAG
2501 CTGACCGAGC ACGCCGTGGC CCACATCACC TCCGTGGTGC CCTTCTACCC
2551 ATACGATGTT CCAGATTACG CTTGATCTAG AGCGGCCGCT TCGAGCAGAC
2601 ATGATAAGAT ACATTGATGA GTTTGGACAA ACCACAACTA GAATGCAGTG
2651 AAAAAAATGC TTTATTTGTG AAATTTGTGA TGCTATTGCT TTATTTGTAA
2701 CCATTATAAG CTGCAATAAA CAAGTTAACA ACAACAATTG CATTCATTTT
2751 ATGTTTCAGG TTCAGGGGGA GGTGTGGGAG GTTTTTTAAA GCAAGTAAAA
2801 CCTCTACAAA TGTGGTAAAA TCGATAAGGA TCCAGGTGGC ACTTTTCGGG
2851 GAAATGTGCG CGGAACCCCT ATTTGTTTAT TTTTCTAAAT ACATTCAAAT
2901 ATGTATCCGC TCATGAGACA ATAACCCTGA TAAATGCTTC AATAATATTG
2951 AAAAAGGAAG AGTATGAGTA TTCAACATTT CCGTGTCGCC CTTATTCCCT
3001 TTTTTGCGGC ATTTTGCCTT CCTGTTTTTG CTCACCCAGA AACGCTGGTG
3051 AAAGTAAAAG ATGCTGAAGA TCAGTTGGGT GCACGAGTGG GTTACATCGA
3101 ACTGGATCTC AACAGCGGTA AGATCCTTGA GAGTTTTCGC CCCGAAGAAC
3151 GTTTTCCAAT GATGAGCACT TTTAAAGTTC TGCTATGTGG CGCGGTATTA
3201 TCCCGTATTG ACGCCGGGCA AGAGCAACTC GGTCGCCGCA TACACTATTC
3251 TCAGAATGAC TTGGTTGAGT ACTCACCAGT CACAGAAAAG CATCTTACGG
3301 ATGGCATGAC AGTAAGAGAA TTATGCAGTG CTGCCATAAC CATGAGTGAT
3351 AACACTGCGG CCAACTTACT TCTGACAACG ATCGGAGGAC CGAAGGAGCT
3401 AACCGCTTTT TTGCACAACA TGGGGGATCA TGTAACTCGC CTTGATCGTT
3451 GGGAACCGGA GCTGAATGAA GCCATACCAA ACGACGAGCG TGACACCACG
3501 ATGCCTGTAG CAATGGCAAC AACGTTGCGC AAACTATTAA CTGGCGAACT
3551 ACTTACTCTA GCTTCCCGGC AACAATTAAT AGACTGGATG GAGGCGGATA

3601 AAGTTGCAGG ACCACTTCTG CGCTCGGCCC TTCCGGCTGG CTGGTTTATT
3651 GCTGATAAAT CTGGAGCCGG TGAGCGTGGG TCTCGCGGTA TCATTGCAGC
3701 ACTGGGGCCA GATGGTAAGC CCTCCCGTAT CGTAGTTATC TACACGACGG
3751 GGAGTCAGGC AACTATGGAT GAACGAAATA GACAGATCGC TGAGATAGGT
3801 GCCTCACTGA TTAAGCATTG GTAACTGTCA GACCAAGTTT ACTCATATAT
3851 ACTTTAGATT GATTTAAAAC TTCATTTTTA ATTTAAAAGG ATCTAGGTGA
3901 AGATCCTTTT TGATAATCTC ATGACCAAAA TCCCTTAACG TGAGTTTTCG
3951 TTCCACTGAG CGTCAGACCC CGTAGAAAAG ATCAAAGGAT CTTCTTGAGA
4001 TCCTTTTTTT CTGCGCGTAA TCTGCTGCTT GCAAACAAAA AAACCACCGC
4051 TACCAGCGGT GGTTTGTTTG CCGGATCAAG AGCTACCAAC TCTTTTTCCG
4101 AAGGTAACTG GCTTCAGCAG ACGGATCAAG AGCTACCAAC TCTTTTTCCG
4151 AAGGTAACTG GCTTCAGCAG AGCGCAGATA CCAAATACTG TTCTTCTAGT
4201 GTAGCCGTAG TTAGGCCACC ACTTCAAGAA CTCTGTAGCA CCGCCTACAT
4251 ACCTCGCTCT GCTAATCCTG TTACCAGTGG CTGCTGCCAG TGGCGATAAG
4301 TCGTGTCTTA CCGGGTTGGA CTCAAGACGA TAGTTACCGG ATAAGGCGCA
4351 GCGGTCGGGC TGAACGGGGG GTTCGTGCAC ACAGCCCAGC TTGGAGCGAA
4401 CGACCTACAC CGAACTGAGA TACCTACAGC GTGAGCTATG AGAAAGCGCC
4451 ACGCTTCCCG AAGGGAGAAA GGCGGACAGG TATCCGGTAA GCGGCAGGGT
4501 CGGAACAGGA GAGCGCACGA GGGAGCTTCC AGGGGGAAAC GCCTGGTATC
4551 TTTATAGTCC TGTCGGGTTT CGCCACCTCT GACTTGAGCG TCGATTTTTG
4601 TGATGCTCGT CAGGGGGGCG GAGCCTATGG AAAAACGCCA GCAACGCGGC
4651 CTTTTTACGG TTCCTGGCCT TTTGCTGGCC TTTTGCTCAC ATGGCTCGAC

Appendix IV– Fluorescent Protein Expression in Separated Channels

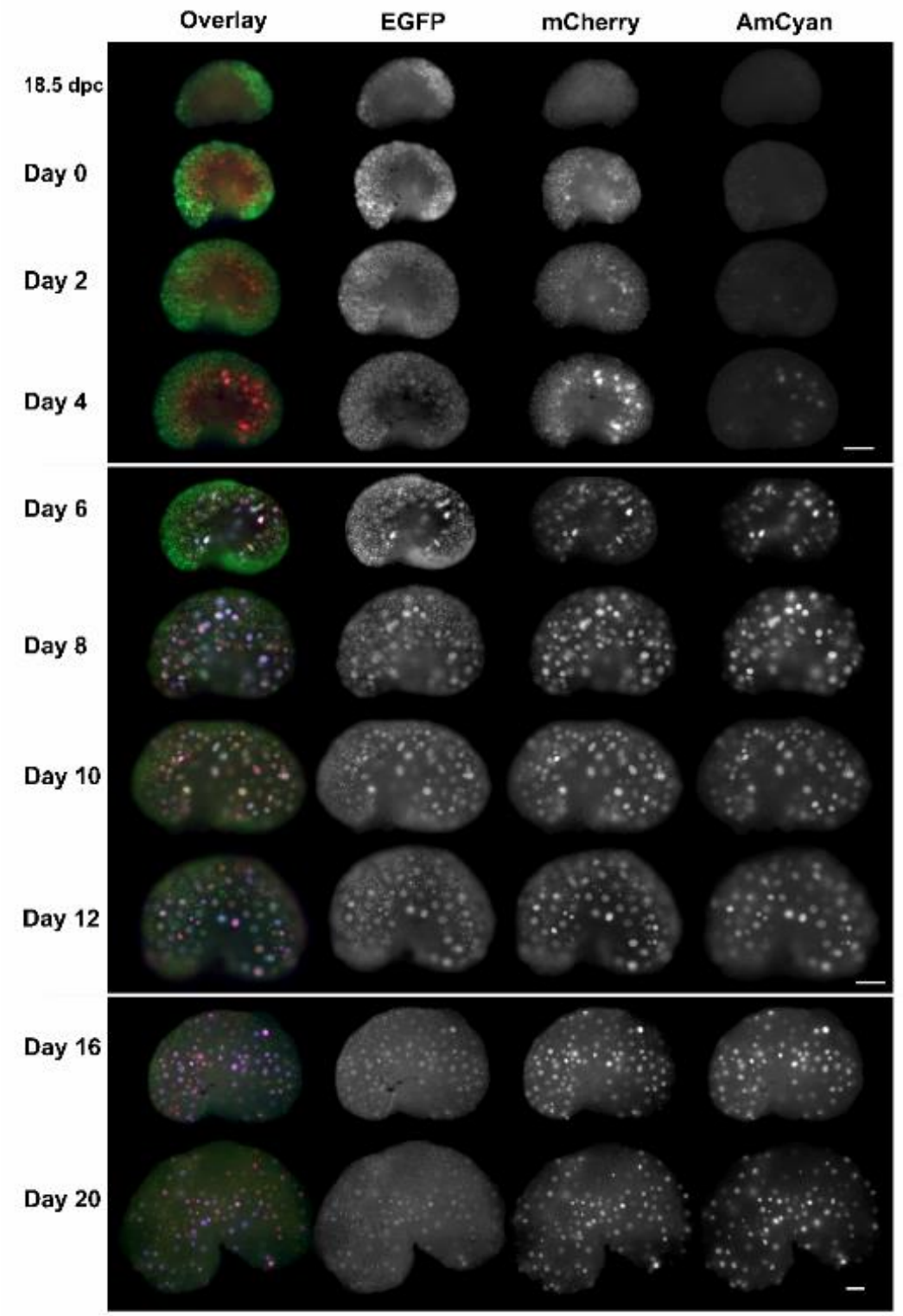

Figure A1 – Different settings were used between 18.5 dpc-Day4 and Day6-Day 12. A higher EGFP and lower AmCyan and mCherry exposure times were used on the Day6-Day12 to avoid saturation of the images. The images from Day 16-Day 20 were captured using a smaller amplification objective, 4x. Scale bar = 200 µm.

Appendix V – Variability on the onset of meiosis in different 13.5 dpc ovaries

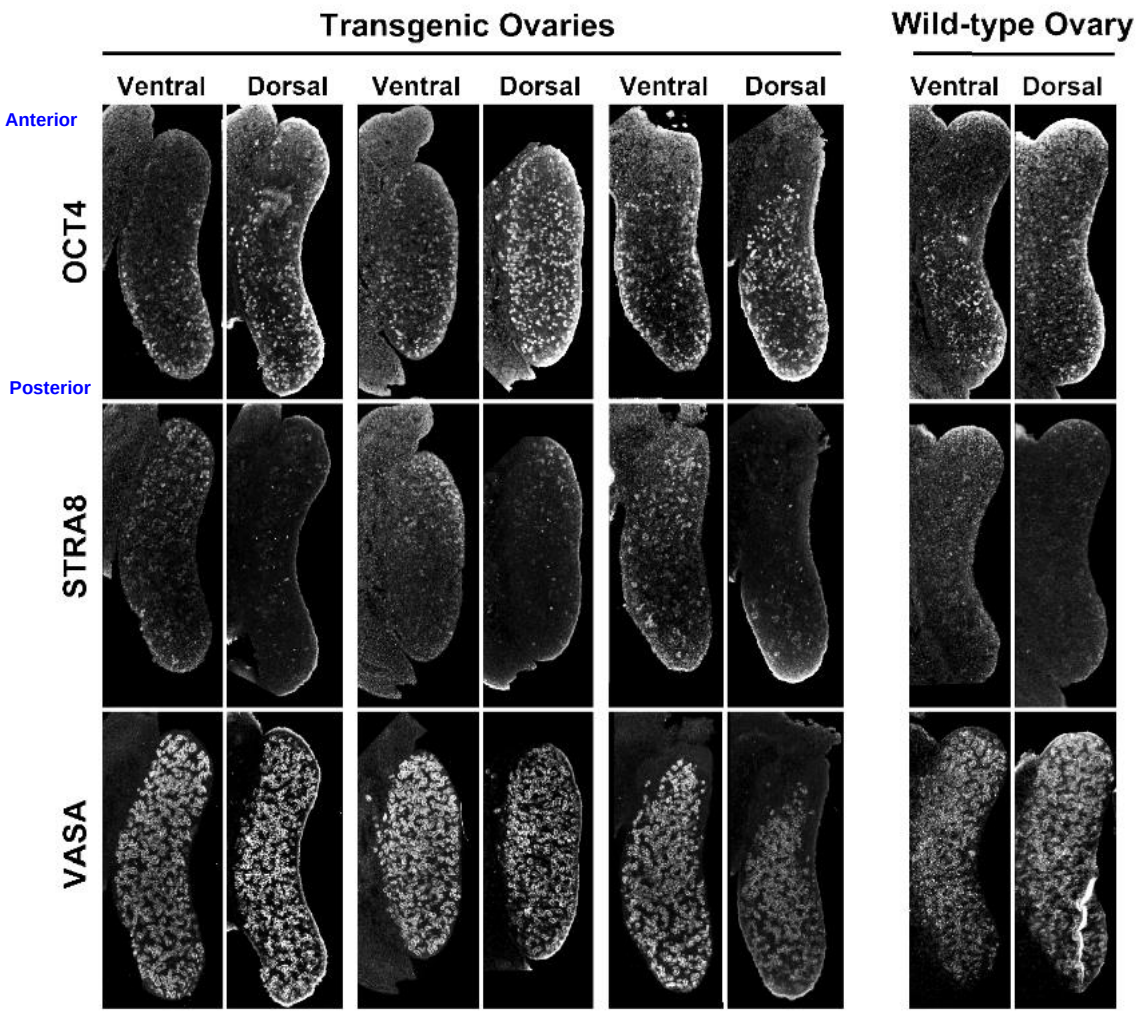

Figure A2 – At 13.5 dpc slight differences on the extent of meiotic entry were observed between different individuals and litters. However, in all the gonads analyzed an early onset of meiosis was observed in the ventral area, as detected by the expression of Stra8 on the anterior region of the gonad. For more information see Figure 4.5.